



HAL
open science

Study for the improvement of low frequencies in Seltech speaker enclosures

Frédéric Fallais

► **To cite this version:**

Frédéric Fallais. Study for the improvement of low frequencies in Seltech speaker enclosures. Acoustics [physics.class-ph]. 2021. dumas-03609253

HAL Id: dumas-03609253

<https://dumas.ccsd.cnrs.fr/dumas-03609253v1>

Submitted on 15 Mar 2022

HAL is a multi-disciplinary open access archive for the deposit and dissemination of scientific research documents, whether they are published or not. The documents may come from teaching and research institutions in France or abroad, or from public or private research centers.

L'archive ouverte pluridisciplinaire **HAL**, est destinée au dépôt et à la diffusion de documents scientifiques de niveau recherche, publiés ou non, émanant des établissements d'enseignement et de recherche français ou étrangers, des laboratoires publics ou privés.

**CONSERVATOIRE NATIONAL DES ARTS ET MÉTIERS
PARIS**

MEMOIRE

**présenté en vue d'obtenir
le DIPLOME D'INGENIEUR CNAM
SPECIALITE : Mécanique
PARCOURS : Acoustique**

par

Frédéric Fallais

**Study for the improvement of low
frequencies in Seltech speaker enclosures**

Soutenu le 17 décembre 2021

JURY

PRESIDENT : Alexandre Garcia (Cnam)

MEMBRES : Eric Bavu (Cnam)

Jean-Baptiste Doc (Cnam)

Thomas Dromer (Devialet)

Alexandre Fenieres (Harman)

Jin Leng (Seltech)

Remerciements

Conclusion d'un parcours de vie initié en septembre 2013, ce mémoire traitant d'électroacoustique me permet non sans émotion de revenir à mes toutes premières passions.

Nourri par la richesse des diverses rencontres faites tout au long de cette période, je garderai une admiration pour Eric Bavu, qui fut à mon égard un enseignant transmettant la connaissance de manière captivante, avant d'être le tuteur académique pour ce mémoire. Comment pourrais-je ne pas citer Manuel Melon, de qui j'ai reçu mes premiers enseignements d'électroacoustique, et qui m'a à plusieurs reprises soutenu dans les recherches autour de ce document.

Intégrant la société Seltech et ses marchés de l'audio en 2018, je remercie très chaleureusement Giulio Di Capua qui en m'accordant sa confiance, aura donné carte blanche quant au développement du pôle acoustique de la société, permettant ainsi de donner lieu avec l'appui indispensable de Jin Leng, à des sujets d'investigations tels que celui-ci.

A Lionel François et Christine Caubel qui auront permis aux conceptions de ce mémoire de voir le jour. Lionel, Christine, je sais combien les idées fantasques d'un acousticien peuvent être terrifiantes à concevoir tant sur le volet mécanique qu'industriel. Pour ça ainsi que pour votre patience, merci énormément.

La liste des personnes à remercier pour m'avoir soutenu de près ou de loin dans cette épreuve serait beaucoup trop longue, mais je tiens à citer ici Carole Sautereau, Raphael Azria, Winnie Chan, Victoria Bacigalupo, Mariem Filali, Valentin Minter, Nicolas Delabaere, Alain Szadel et Nicolas Rollin, pour avoir accepté de participer à ces tests subjectifs, dont je reconnais les conditions parfois difficiles.

Enfin, avec un entourage familial ancré dans la musique depuis des générations, comment penser un seul instant que ma passion pour ce domaine n'a pas vu ses sources depuis tout jeune dans les moments familiaux. Merci à mes parents, mes frères, ma sœur, pour tout ce que vous m'avez et continuerez à m'apporter.

Glossary

Abbreviations

SPL: Sound Pressure Level to:

- a swept sine signal, when coming from acoustic measurements
- a music signal, when coming from listening tests

LF: Low frequency region of an acoustic spectrum

HF: High frequency region of an acoustic spectrum

LFRO: Low Frequency Roll-Off. Defined as the -3 dB point from the nominal level over an acoustic spectrum

BR: Bass-Reflex design

PR: Passive Radiator design

PE: Passive Element in a Passive Radiator design

HPF: High-Pass Filter in an audio chain upstream to a speaker enclosure.

EQ: Equalization / Equalizer

Terms (1/2)

ρ_0 , air density, fixed = 1.205 kg/m³

μ_0 , dynamic air viscosity, fixed = 1.850e-5 Pa/s

c , sound velocity in the air, fixed = 343.318 m/s

P_0 , acoustic reference pressure = 2e-5 Pa

q , acoustic flow rate, in m³/s

Z , acoustical impedance for a plane wave = $\rho_0 c$

f_S , fundamental resonance of an electro-dynamic speaker. Detected as the first maximum over the electric input impedance of the speaker, in Hz

f_B , fundamental resonance of a speaker enclosure. Detected as the first maximum over the electric input impedance of the enclosure system, in Hz

M_{MD} , mass of the moving part in an electro-dynamic speaker, in kg

$M_{MS} = M_{MD} +$ mass of air particles around a speaker diaphragm, in kg

R_{MS} , mechanical resistance of suspensions in an electro-dynamic speaker, in N.s/m

C_{MS} , mechanical compliance of suspensions in an electro-dynamic speaker, in m/N

S_D , projected area of a speaker diaphragm, including half of the outer suspension, in m²

Terms (2/2)

$M_{AS} = M_{MS}/S_D^2$, acoustic mass equivalent to M_{MS} , in kg/m^4

$C_{AS} = C_{MS} * S_D^2$, acoustic compliance equivalent to C_{MS} , in m^5/N

$R_{AS} = R_{MS}/S_D^2$, acoustic resistance equivalent to R_{MS} , in N.s/m^3

$C_{AB} = \frac{V_b}{\rho_0 c^2}$, acoustic compliance for a closed air volume, in m^5/N

R_{AP} , acoustic losses created in a Bass-Reflex port, in N.s/m^3

M_{AP} , equivalent moving mass (air particles) into a Bass-Reflex port, in kg/m^4

f_L , LFRO either of a Bass-Reflex or Passive Radiator design, in Hz

f_M , Helmholtz resonance (assuming a lossless behavior) either of a Bass-Reflex or Passive Radiator design, in Hz

R_{AR} , acoustic resistance of a passive element in a Passive Radiator design, in N.s/m^3

M_{AR} , acoustic mass of a passive element in a Passive Radiator design, in kg/m^4

C_{AR} , acoustic compliance of a passive element in a Passive Radiator design, in m^5/N

x_{max} , maximum possible peak displacement/excursion for a speaker diaphragm, often in mm

I_{max} , maximum possible peak current in the voice coil of a speaker, in A

f_{HPF} , High-Pass Filter center frequency, in Hz

Q , High-Pass or Parametric filter quality factor at the center frequency, ratio

Contents

- I. Introduction 1
 - I.I. Global context 1
 - I.II. Audio electronics market trends 3
 - I.III. Objectives of the study and presentation of the Seltech company 5
- II. Scope of the investigations 6
 - II.I. Speakers of interest and their sealed enclosure..... 6
 - II.II. Studied methods for the improvement 11
 - II.III. Approach used for prediction 14
 - II.IV. Protocol for the perceptual evaluation of each of the improvement 24
- III. Investigations around the speaker enclosure N ° 1 27
 - III.I. Improvement method N ° 1 (Bass-Reflex)..... 27
 - III.II. Improvement method N ° 2 (Passive Radiator) 42
 - III.III. Improvement method N ° 3 (Active Equalization) 53
 - III.IV. Perceptual evaluation of each of the improvement 62
- IV. Investigations around the speaker enclosure N ° 2 71
 - IV.I. Improvement method N ° 1 (Bass-Reflex)..... 71
 - IV.II. Improvement method N ° 2 (Passive Radiator) 78
 - IV.III. Improvement method N ° 3 (Active Equalization) 86
 - IV.IV. Perceptual evaluation of each of the improvement 91
- V. Summary of the investigations and conclusion..... 98
 - V.I. Synthesis 98
 - V.II. Industrial feasibility and cost point of view 99
 - V.III. Future work proposals 100

I. Introduction

I.I. Global context

In an electronic market where multimedia devices are increasingly versatile, recent statistics published on the Voicebot.ai website and reported in Figure 1 highlight that wireless speaker systems are widely used for streaming music, in front of functions such as asking questions or checking the weather. Also, although the camera performance of a smartphone is often a predominant criterion for the choice of model, recent measurements from the Dxomark.com website (Figure 2) illustrate that consumers of smartphones actually use their device more for listening to music than for recording videos. It is so within this context that we understand the low frequency (LF) sound reproduction of devices, which remain compact in size, to be a noticeable interest for designers in this market.

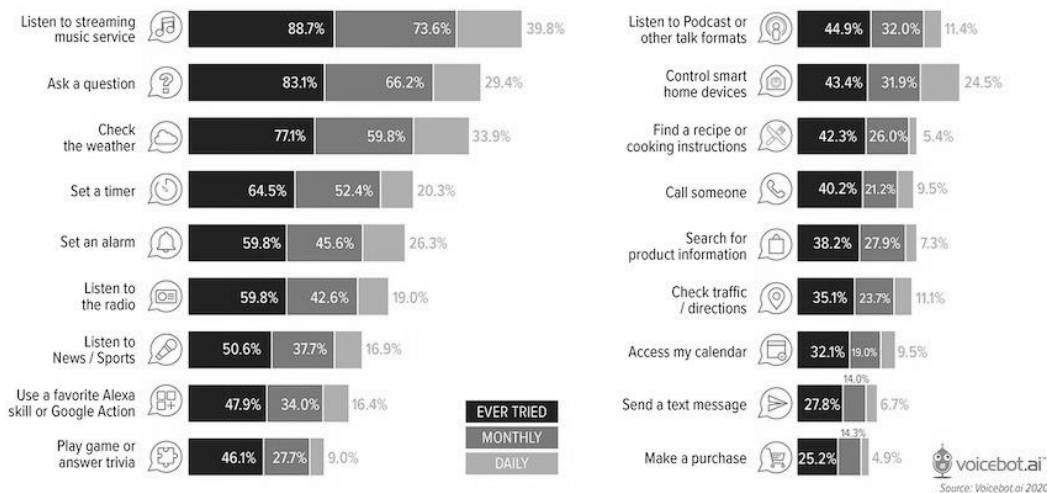


Figure 1 – “Smart speaker use case frequency. January 2020” [1]

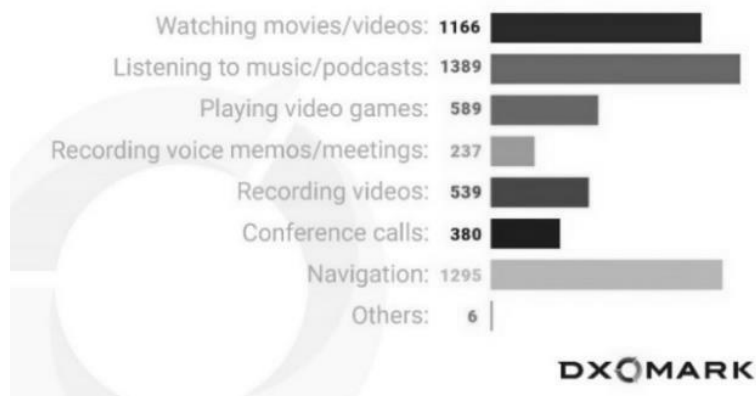


Figure 2 - “What do you use your smartphone for?” September 2020 [2]

In example, considering smartphone companies as popular as Nokia and Xiaomi, Figure 3 illustrates the LF performance gap between two different generations of devices: the Nokia N95 (released in 2006) and the Xiaomi Black Shark 4 Pro (released in 2021). From this graphic, which show normalized sound pressure levels (SPL) from the mid-range, we observe that the Black Shark 4 Pro extends the nominal level from about 700 Hz to 480 Hz, subsequently with a smoother SPL decay slope.

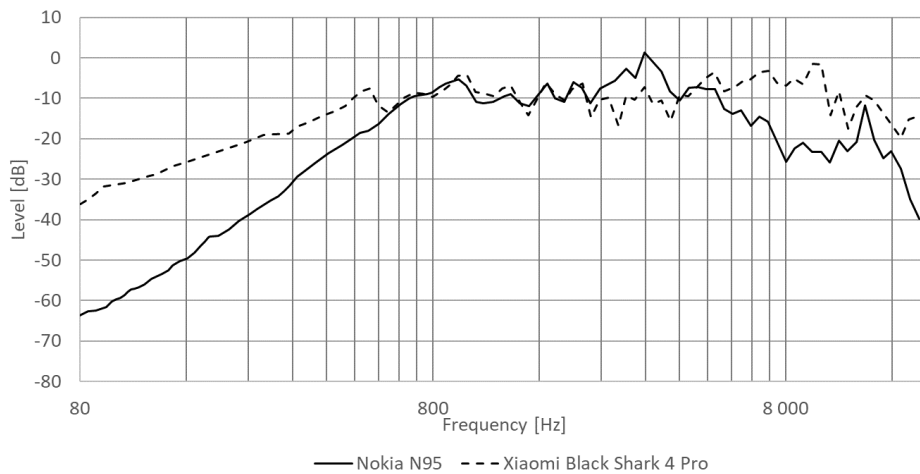


Figure 3 - SPL comparison: Nokia N95 / Xiaomi Black Shark 4.
Graph recreated from [3]

Also, from the Bluetooth speaker market, the example in Figure 4 illustrates how JBL improved the LF region of its Go version 3 (released in 2020) compared to its Go version 2 (released in 2018). The graphic illustrates normalized SPLs from 1000 Hz. In addition of having a flatter sound signature, the Go version 3 bring a flat extension of about 60 Hz.

From the above two examples as well as from the previously reported statistics, we therefore understand the interest for the audio industry to continuously improve the low frequency sound reproduction of multimedia devices which remain compact as they evolve on other aspects.

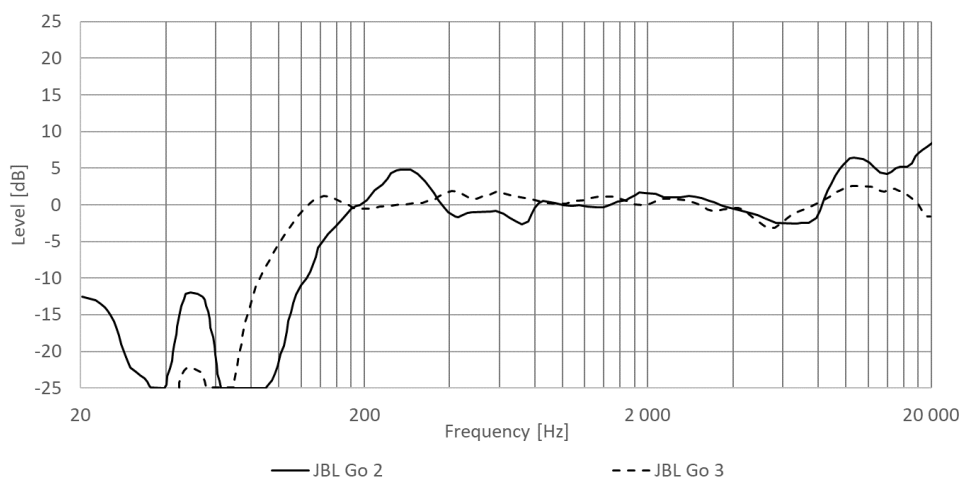


Figure 4 - SPL comparison: JBL Go 2 / JBL Go 3. Graph recreated from [4] and [5]

I.II. Audio electronics market trends

By looking at recent developments in the Bluetooth and Smart speaker market, we observe that when a LF improvement is achieved, it most often relies on the Passive Radiator principle [6] [7] [8], so that only a few of the largest devices use Bass-Reflex conceptions [9] [10] [11]. The operating principle of these two systems being described a little later in part II.II, Figures 5 and 6 respectively illustrate a market example for each of the two solutions.

However, in 2015 a Bass-Reflex design had been found in the small JBL Go Bluetooth speaker [12], but it was then replaced by a Passive Radiator system in both the version 2 and 3, maybe both for reasons of mechanical simplicity and waterproof requirements.



Figure 5 – Apple HomePod mini split view [8]



Figure 6 – Anker Rave split view [10]

Also, in the domain of speakers designed for tablets and smartphones the work from Jiang et al. (illustrated on Figure 7) is an example that show the interest in Passive Radiators for improving the LF response of such a small system [13].

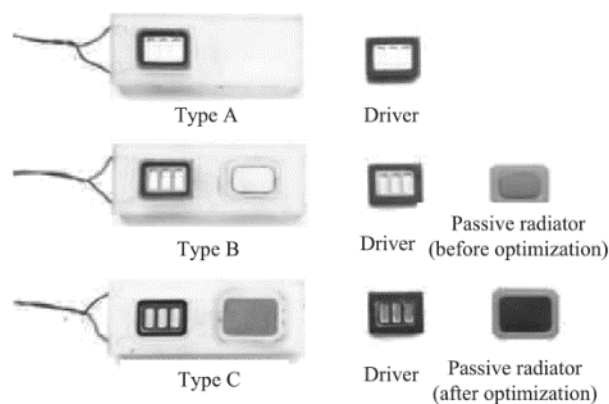


Figure 7 – Micro Passive Radiator prototypes [6]

But overall, we understand that most of these speaker systems rely on audio processors, often used to reshape the sound signature [14] [15] [16] [17]

In 2006-2007, Samsung researchers published two articles [18] [19] on the so-called "missing fundamental" technique, adapted for small transducers in portable multimedia devices. A brief description of this technique consists in creating the illusion of a fundamental frequency which cannot be physically generated by a speaker, by regenerating particular harmonics, as illustrated in Figure 8. An example of application on the market was seen in 2016 with the MaxxBass algorithm from the Waves company integrated into the SHARKK Wave Bluetooth speaker. But this device does not seem to be manufactured anymore, and it is possible that today most of the popular designers on the market developed their own algorithms to improve the bass response of their systems.

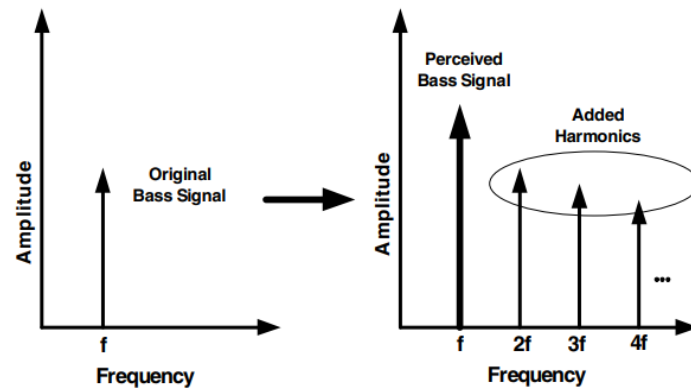


Figure 8 - Pitch perception of a complex tone (Missing fundamental effect) [15]

I.III. Objectives of the study and presentation of the Seltech company

The scope of this document is to investigate three well-known methods from the audio industry for the low frequency improvement of relatively small speaker enclosures designed by the company Seltech (www.seltech-international.com). Also, as the word "improvement" can lead to many different subjective interpretations, another objective of this study is to acquire knowledge about the perceptual evaluation of the improved enclosures, and thus, to relate the subjective criteria to the measurement of each of these enclosures.

Seltech is a medium-sized company (about 50 salaries), with a worldwide presence on diverse markets of the audio electronics, such as mobiles phones, Internet of Things (IoT), home automation, wearables, multimedia, telecom, toys, and others. Created in 1989, Figure 9 illustrates at today the different offices over the world, the headquarters being in Paris.

As Field Application Engineer in Acoustics for the company, my function is to support Seltech customers in the development of their application, everywhere where electroacoustics components are needed. My work is mainly founded on 3D and prototypes reviews, acoustics calculations, predictions, and measurements. Another part of my function is to continuously support and train the Seltech sales team into the challenges of the acoustics domain, as well as around the new technologies from the electroacoustics market.



Figure 9 – Geographical distribution of Seltech offices

II. Scope of the investigations

II.I. Speakers of interest and their sealed enclosure

The investigations intend to focus on two electro-dynamic speakers from the Seltech portfolio:

- one round shaped speaker of 40 mm outer diameter and of 18 mm height. The reason for this choice is that this type of speaker is commonly used when looking at the compact Bluetooth / Smart speaker system market.
- one rectangular shaped speaker of (L x w) 15 x 11 mm dimensions and of 3.5 mm height. Although too thick to remain of interest in modern smartphones, this speaker is historically popular in the mobile phone market and is still a high runner in many Seltech customer applications.

Description of the speaker N ° 1 and its enclosure

Composed as per illustrated on Figure 10, its main characteristics are summarized in the Table I. The typical electric impedance as well as the SPL at 0.1 m for the baffled speaker are illustrated in Appendix A.

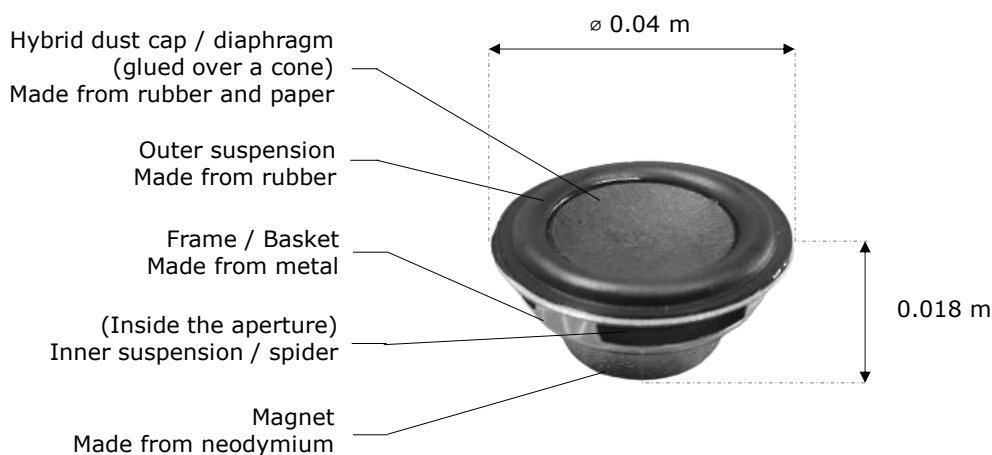


Figure 10 – Speaker N ° 1 - Detailed composition

Table I – Speaker N° 1 - Main characteristics

Nominal Impedance [Ohms]	4 +/- 15 %
Maximum input pink noise power [Watts]	4
Fundamental resonance (f_S) [Hz]	160 +/- 25 %
Sensitivity [dB SPL / W / m]	77 +/- 3 averaged at 0.4, 0.6, 0.8, 1.0 kHz

The enclosure designed for this speaker is presented and detailed on Figures 11 and 12. It is made from 3D printed ABS plastic, with a fixed thickness for the walls = 2 mm. Being rectangular, this enclosure brings a rear acoustic volume (the volume seen by the rear side of the speaker diaphragm) = $165e-6 \text{ m}^3$. The electric impedance as well as the SPL for the sealed enclosure at 0.3 m are respectively illustrated on Figures 14 and 15, and the setup for this measurement is detailed on Figure 13. The reason for this measurement distance is that we want the microphone to measure both the speaker diaphragm and any additional source (coming from the improvement) as a unique acoustic source.

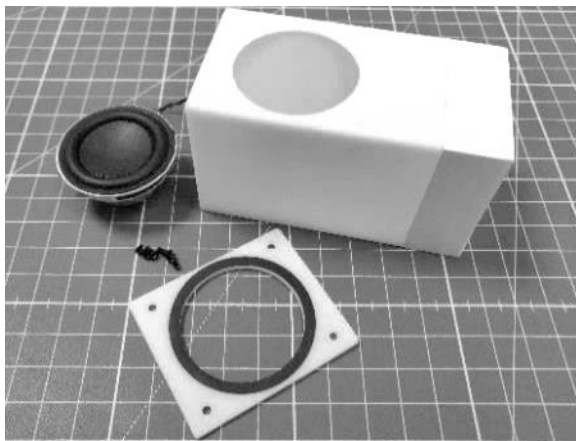


Figure 11 – Sealed enclosure N° 1 - Assembly elements

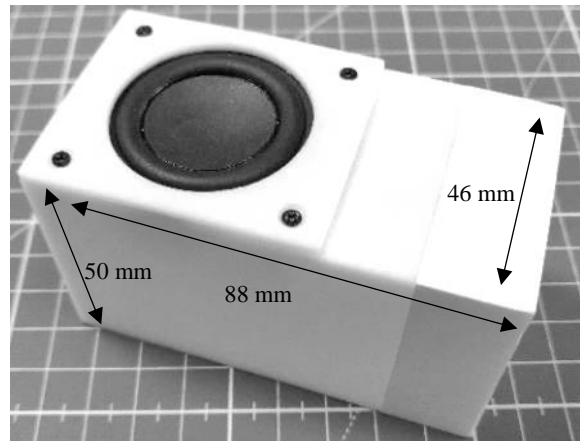


Figure 12 - Sealed enclosure N° 1 - Assembled system

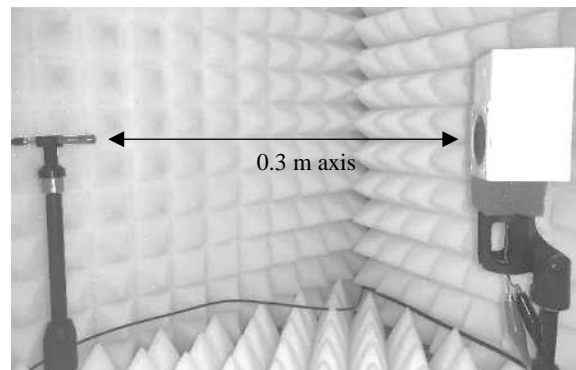


Figure 13 – Sealed enclosure N° 1 - Measurement setup

Part II - Scope of the investigations: Speakers of interest and their enclosure

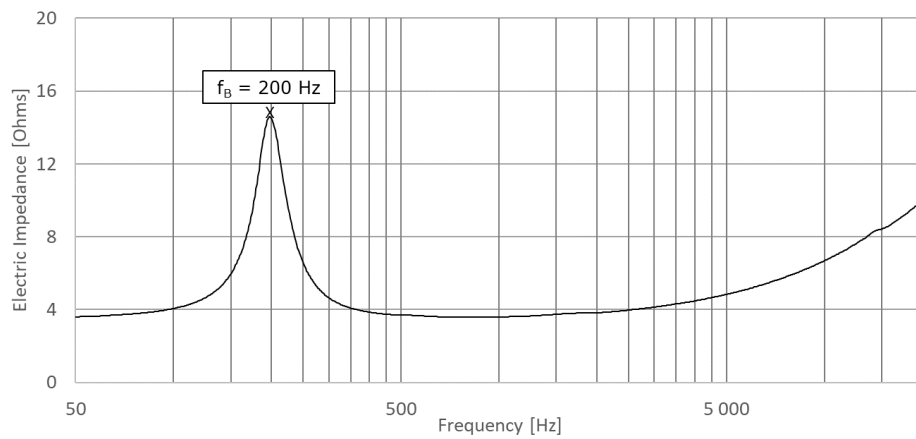


Figure 14 – Sealed enclosure N ° 1 - Typical electric impedance

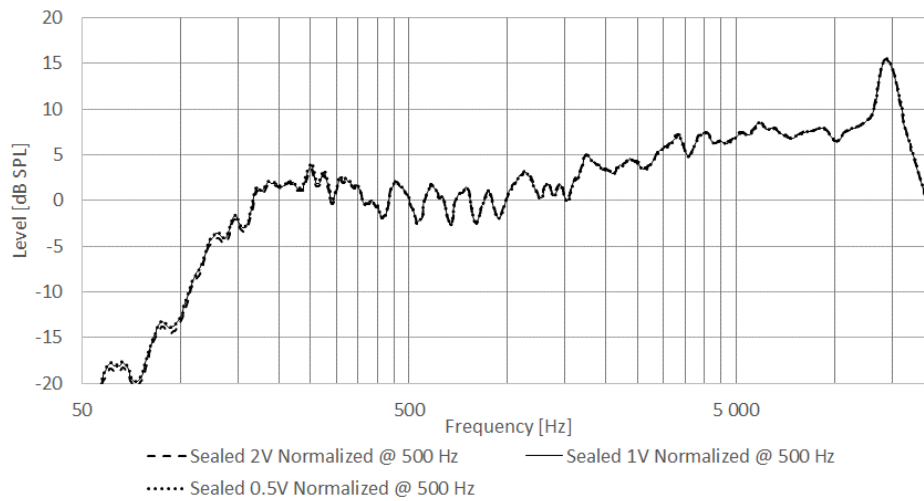


Figure 15 – Sealed enclosure N ° 1 - Typical SPL at 0.3 m, normalized at 500 Hz

Description of the Speaker N ° 2 and its enclosure

Composed as per illustrated on Figure 16, its main characteristics are summarized in the Table II.

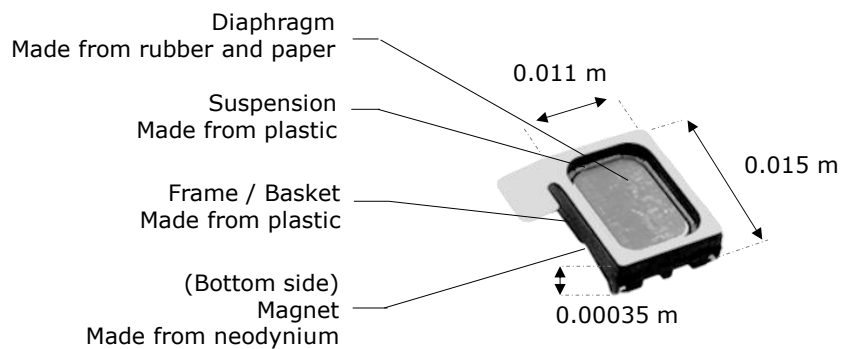


Figure 16 – Speaker N ° 2 - Detailed description

Table II – Speaker N ° 2 – Main characteristics

Nominal Impedance [Ohms]	8 +/- 15 %
Maximum input pink noise power [Watts]	0.7
Fundamental resonance (f_s) [Hz]	550 +/- 20%
Sensitivity [dB SPL / 0.1 W / m]	62 +/- 3 at 2 kHz

The typical electric impedance as well as the SPL at 0.1 m for the baffled speaker are illustrated in Appendix A.

Illustrated on Figures 17 and 18, the 3D printed enclosure for this speaker is made in two parts, and the thickness of its walls is = 1.5 mm. The rear acoustic volume so created is = $2e-6 \text{ m}^3$. The electric impedance as well as the SPL at 0.1 m for this sealed enclosure are respectively illustrated on Figures 20 and 21. The setup for this measurement is detailed on Figure 19.



Figure 17 – Sealed enclosure N ° 2 - Assembly elements

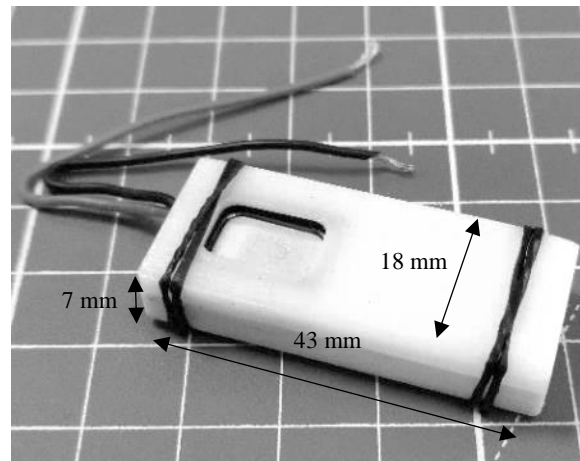


Figure 18 – Sealed enclosure N ° 2 - Assembled system

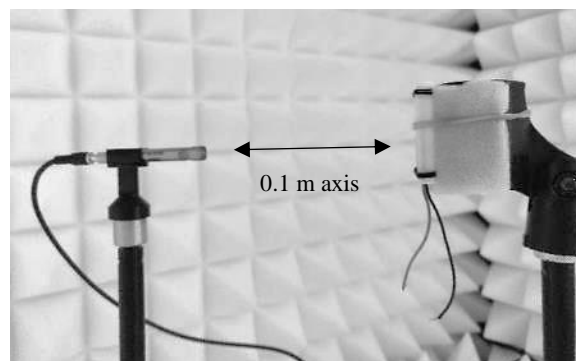


Figure 19 – Sealed enclosure N ° 2 - Measurement setup

Part II - Scope of the investigations: Speakers of interest and their enclosure

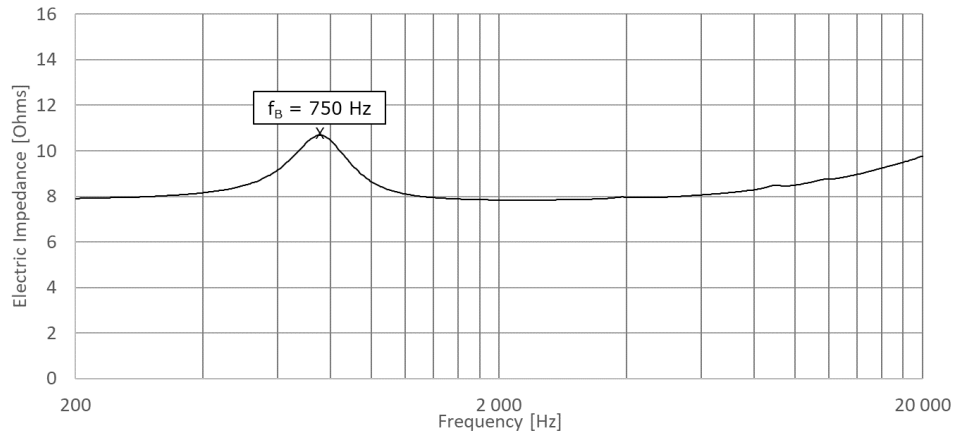


Figure 20 – Sealed enclosure N ° 2 - Typical electric impedance

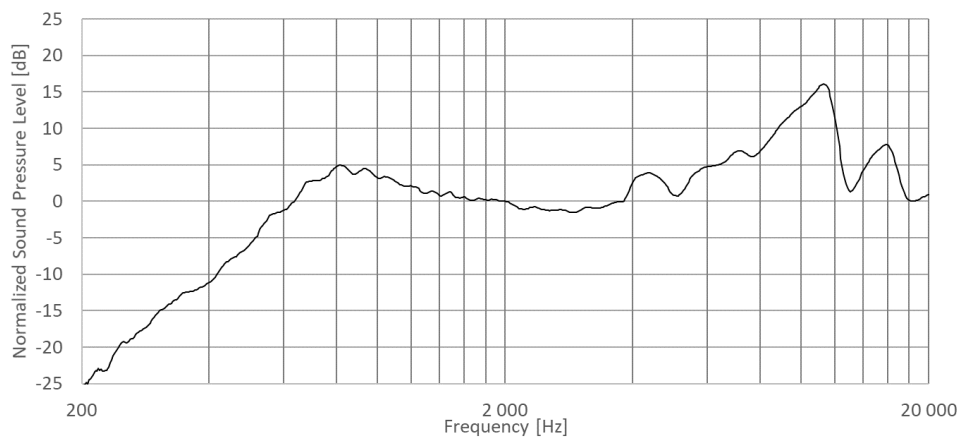


Figure 21 – Sealed enclosure N ° 2 - Typical SPL at 0.1 m, normalized at 2000 H

II.II. Studied methods for the improvement

As briefly discussed into the introduction section, this document focuses on three improvement methods well-known from the industry. This part of the document intends to describe the working principle of each of the three methods.

Improvement method N ° 1: Bass Reflex

Invented by Albert L. Thuras in 1932 [20], a Bass-Reflex system is described as a speaker enclosure into which an opening has been made, to insert a tube (also called “vent” or “port”), as per illustrated on Figure 22. This port, in combination with the residual volume of air inside the enclosure, will so form a resonator (Helmholtz type), which once its fundamental resonance well-adjusted, will contribute to extend the LF response when compared to the original sealed enclosure design (Figure 23)

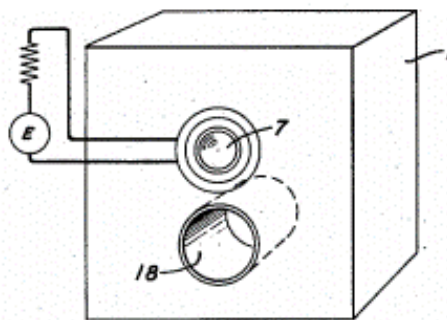


Figure 22 – Bass-Reflex principle drawing [20]

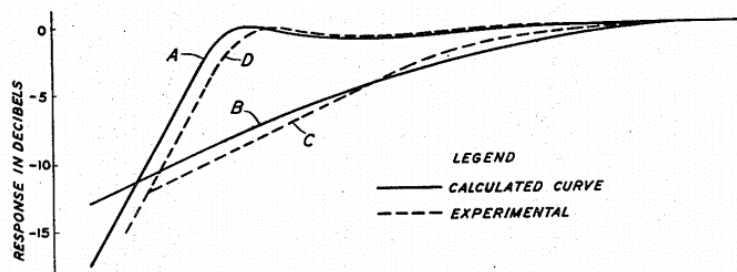


Figure 23 – Bass-Reflex response against sealed enclosure response [20]

Improvement method N ° 2: Passive Radiator

Harry Olson is the inventor of the Passive Radiator system. Patented in 1935 [21], this system is composed of an enclosure both containing a speaker and at least one diaphragm. This last element being often called “passive radiator” itself by confusion. Acting in a similar way than a Bass-Reflex system, the diaphragm, in combination with the residual volume of air inside the enclosure, will also form a resonator which will contribute to extend the LF response when compared to the original sealed design (Figure 25)

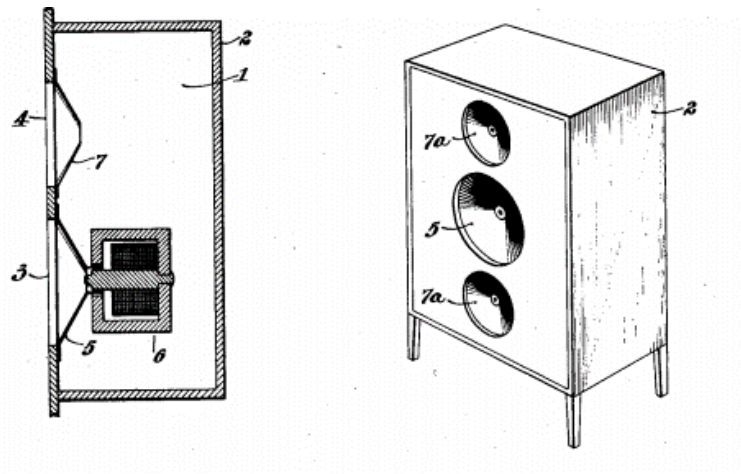


Figure 24 – Passive Radiator principle drawing [21]

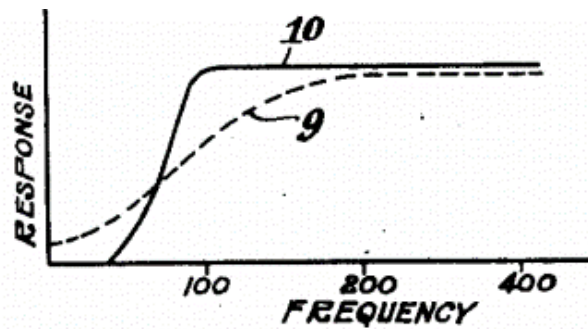


Figure 25 – Passive Radiator response against sealed enclosure response [21]

Improvement method N ° 3: Active Equalization

Unlike for the two previously described methods, the audio equalization does not really have a particular inventor but is more inspired from the acoustic telegraph and telecom domains [22]. An example of persons having used the equalization to extend the LF response of a sealed enclosure is W. Marshall Leach, JR. into his article *Active Equalization of Closed-Box Loudspeaker Systems* [23]. From this work, a particular assembly of 2nd order active high-pass filters (as per illustrated on Figure 26) is used to transform the sealed enclosure response “a” from Figure 27 into the response “b” from this same Figure. A basic functional description of this filtering network is that it receives a voltage signal constant in frequencies at its input and transform it into a signal having the shape of the curve “c” of Figure 27. The increase of energy we can see on this curve (at around 0.6, from the x-axis) will so lead the speaker to radiate more sound in this same frequency region.

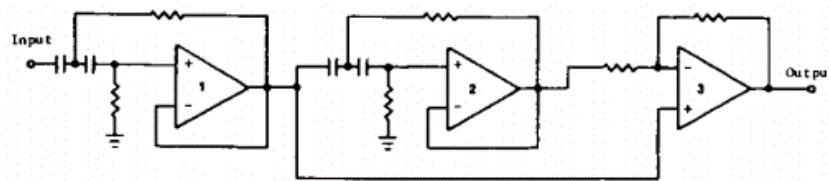


Figure 26 – “ Possible three-operational-amplifier realization of the active equalizer” [23]

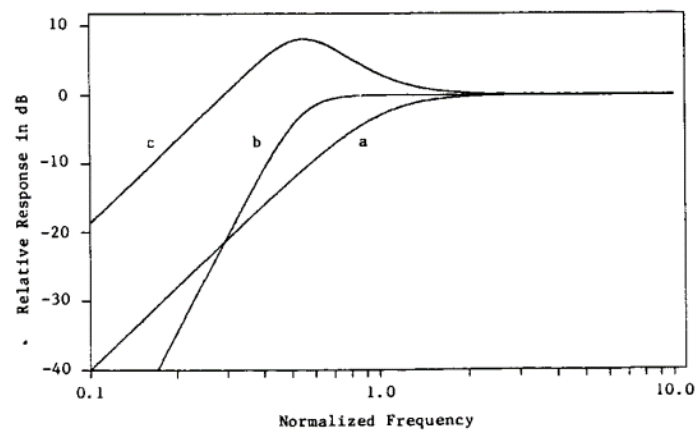


Figure 27 – (a) system before equalization; (b) system after equalization; (c) equalizer [23]

II.III. Approach used for prediction

A way to predict the LF behavior of the previously introduced speaker enclosures, is the use of the electro-mechano-acoustical circuits. The first persons to have opened strong interests for electro-dynamic loudspeakers are Chester W. Rice and Edward W. Kellogg, in 1925 with their publication *Notes on the development of a new type of hornless loudspeaker* [24]. But later in 1954, Leo L. Beranek published *Acoustics*, a book which summarizes the electroacoustics of the era [25] [26]. In the chapter “Direct-Radiator loudspeakers” of his book, Leo Beranek formulated a list of parameters from which six of them are considered for our study:

- R_e , the electrical resistive part of the voice coil, in ohms.
- $B.l$, the product of magnet field strength in the voice coil gap and the length of wire in the magnetic field, in tesla-meters
- M_{MD} , the mass of the assembly “diaphragm / voice coil” and the mass of half of the outer suspension, in kilograms.
- R_{MS} , the mechanical resistance of suspensions, in Newton-second per meters
- C_{MS} , the total mechanical compliance of suspensions, in meter per Newton
- S_D (mentioned in the form of the radius “a” in the Beranek’s book), the projected area of the speaker diaphragm

Based on these parameters, Leo Beranek then illustrated in the chapter “Loudspeaker enclosures” of his book, an acoustical analogous circuit for a sealed enclosure system (Figure 28). From this circuit, the current is considered analogous to an acoustic flow rate.

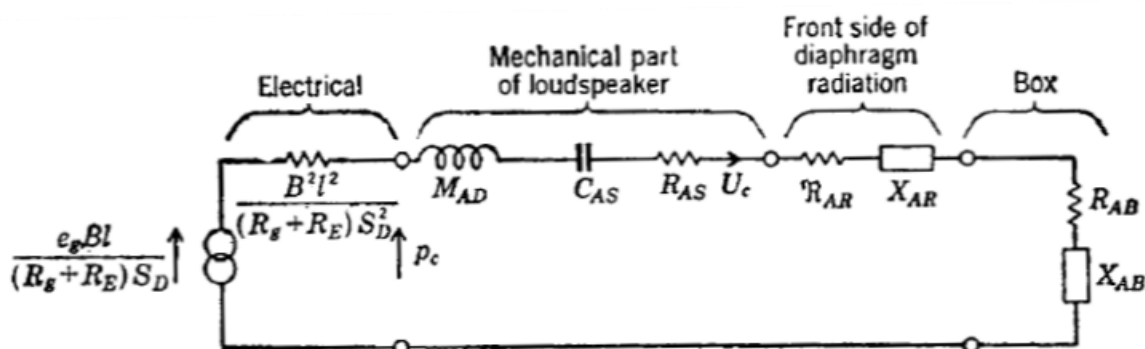


Figure 28 - Acoustical analogous circuit for a sealed enclosure system [25]

The different components for this circuit are defined as below:

- R_g , the output resistance of the electric source (ignored in the scope of this document)
- $M_{AD} = M_{MD}/S_D^2$, the acoustic mass of the diaphragm assembly
- $C_{AS} = C_{MS} * S_D^2$, the acoustic compliance of suspensions
- $R_{AS} = R_{MS}/S_D^2$, the acoustic resistance of suspensions
- R_{AR} and X_{AR} , represent the acoustic radiation impedance from the front side of the diaphragm. Theoretically, this radiation impedance varies accordingly to the acoustic environment around the speaker. *Within the scope of this document, we decide to not consider those terms, since a part of this impedance is contained, by measurement, into the other mass and resistance terms.*
- R_{AB} and X_{AB} , represent the acoustic load for the enclosure, at the rear side of the diaphragm. It is assumed that $X_{AB} = \omega M_{AB} - \frac{1}{\omega C_{AB}}$, where:

M_{AB} , is the acoustic mass given by the enclosure dimensions and geometry. For both previously described sealed enclosures, this term is entirely assumed negligible when compared to M_{AD} ,

$C_{AB} = \frac{V_b}{\rho_0 c^2}$, is the acoustic compliance of the air volume into the enclosure

For the enclosure designed around the speaker N ° 1: $C_{AB} = 1.16e-09 \text{ m}^5/\text{N}$

For the enclosure designed around the speaker N ° 2: $C_{AB} = 1.41e-11 \text{ m}^5/\text{N}$

Also, regarding the size of the considered systems, it is assumed that the damping behavior of the air trapped inside the box is quite low, or non-existing. This leads us to neglect the term R_{AB} from the circuit as well. Therefore, the analogous circuit for the sealed enclosure becomes as per illustrated on Figure 29.

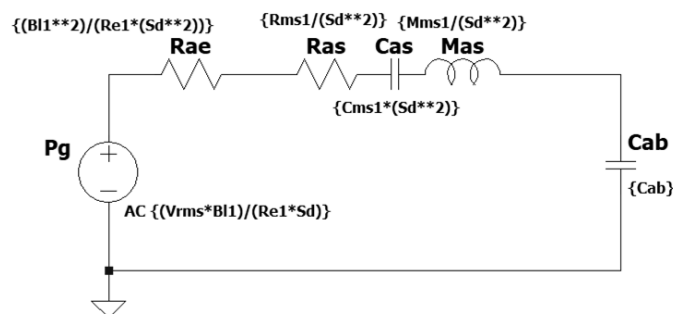


Figure 29 – Simplified analogous circuit for a sealed enclosure

To measure the previously listed parameters, we can use a method called “Known Volume” as per described by R. Elliott into his web article [27]. This method consists of two measurements of the speaker electric impedance, when mounted into a baffle: one without any acoustic load around it, and one with a known and sealed volume often added to the front side of it. The parameters are then calculated from the two recorded impedance curves, into the measurement software Audiomatica Clio, and using a procedure described by A. N. Thiele in one of its seminal papers [28] [29]

But since the measurement of these parameters cannot be performed in vacuum, we observe the value of M_{MD} to be affected by the mass of air particles located around the speaker diaphragm. This phenomenon therefore defines a new parameter named $M_{MS} = M_{MD} + \text{air load}$

A theoretical formula to estimate the value of this load term can be $2[\frac{8}{3}\rho_0r^3]$ where r is the projected radius of the speaker diaphragm.

Measurement of the parameters for the speaker N ° 1

The parameter S_D reflecting the area of the speaker which pushes the air particles, it is often admitted that half of the outer suspension also contribute together with the diaphragm to generate the acoustic wave. Therefore, considering the diameter illustrated on Figure 30, we calculate the value of $S_D = 1.02e-3 \text{ m}^2$.

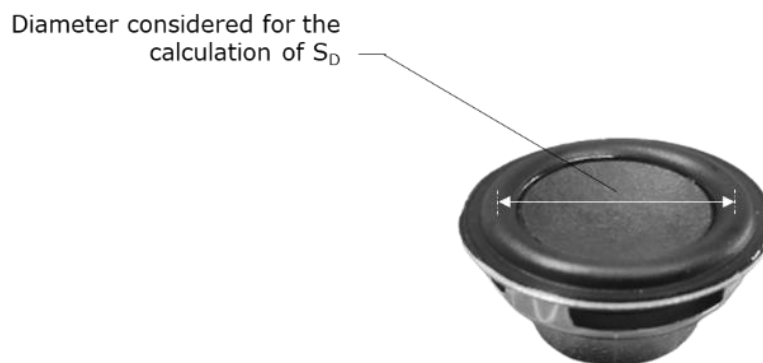


Figure 30 – Speaker N ° 1 – Diameter considered for the calculation of S_D

Figures 31 and 32 illustrate the test setup for the measurement of the rest of the parameters, and the Table III summarizes the measured values. Five measurements have been consecutively made to verify the stability of the speaker.

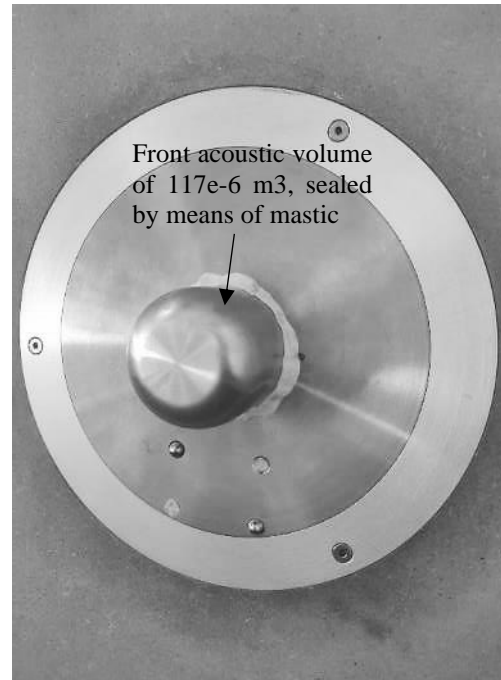
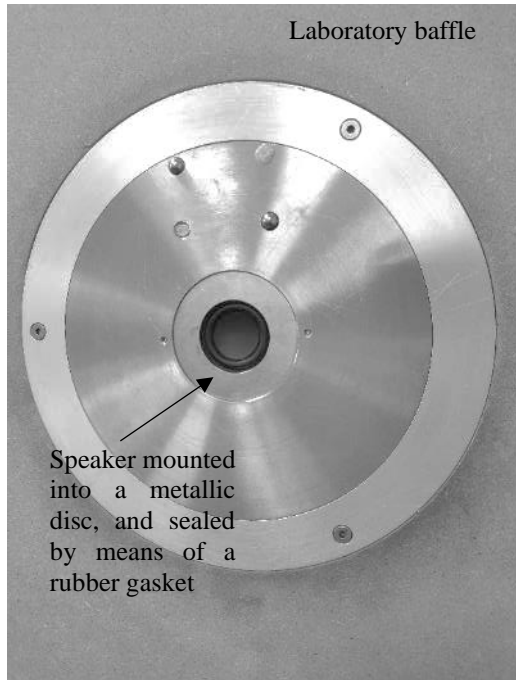


Figure 31 – Speaker N ° 1 – Parameters measurements 1/2 Figure 32 - Speaker N ° 1 – Parameters measurements 2/2

Table III – Speaker N ° 1 – Measurements of the fundamental parameters

Parameter	#1	#2	#3	#4	#5	Average	Standard Deviation	Coefficient Of Variation [%]
R_e [Oms]*	3.62	3.62	3.62	3.62	3.62	/	/	/
R_{MS} [N.s/m]	5.37e-01	5.30e-01	5.54e-01	5.31e-01	5.44e-01	5.39e-01	9.78e-03	1.81
C_{MS} [m/N]	5.35e-04	5.45e-04	5.21e-04	5.29e-04	5.21e-04	5.30e-04	1.00e-05	1.89
M_{MS} [kg]	1.78e-03	1.75e-03	1.83e-03	1.78e-03	1.82e-03	1.79e-03	3.22e-05	1.79
B.l [T.m]	2.23	2.22	2.27	2.22	2.26	2.24	2.36e-02	1.06

*Measured from the impedance curve without the volume

From this table, we can observe the value of R_e to remain the same within the available measurement accuracy. On the other hand, as we observe the rest of parameters to change over the measurements, the coefficient of variation is calculated (both from the average and from the standard deviation) to briefly status on the importance of these variations from the each of average. Despite the calculated percentages are all reasonably low (the parameter C_{MS} showing the highest variation with 1.89 %), we decide to consider the averaged values for the construction of the acoustic model.

Measurement of the parameters for the speaker N ° 2

Considering the small dimensions for the diaphragm of this speaker, Figure 33 illustrates the two lengths which are considered to approximate S_D into a rectangular area of $1e-04 \text{ m}^2$.

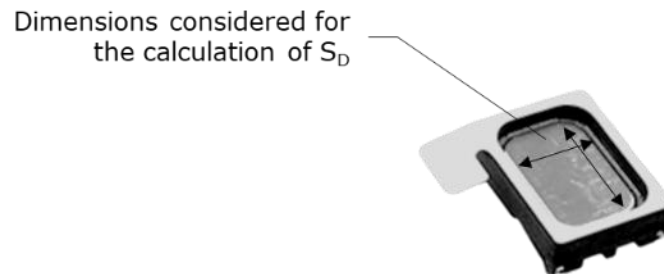


Figure 33 - Speaker N ° 2 – Dimensions considered for the calculation of S_D

Figures 34 and 35 illustrate the test setup for this measurement, while the Table IV summarizes the measured values. Here also, five measurements have been consecutively made to verify the stability of the speaker.

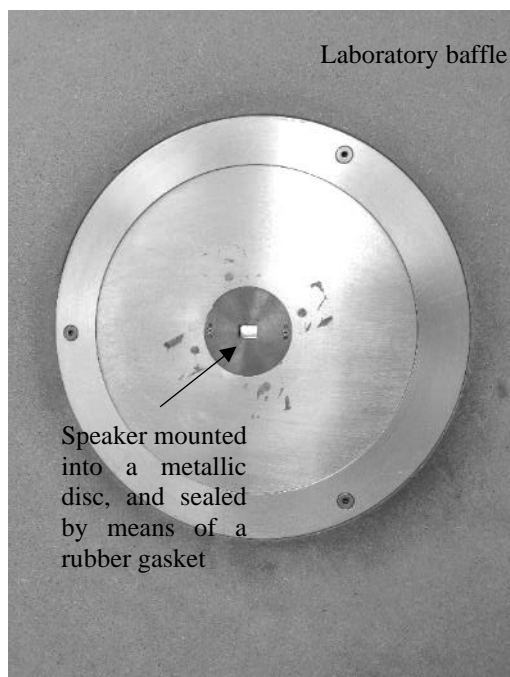


Figure 34 - Speaker N ° 2 – Parameters measurements 1/2

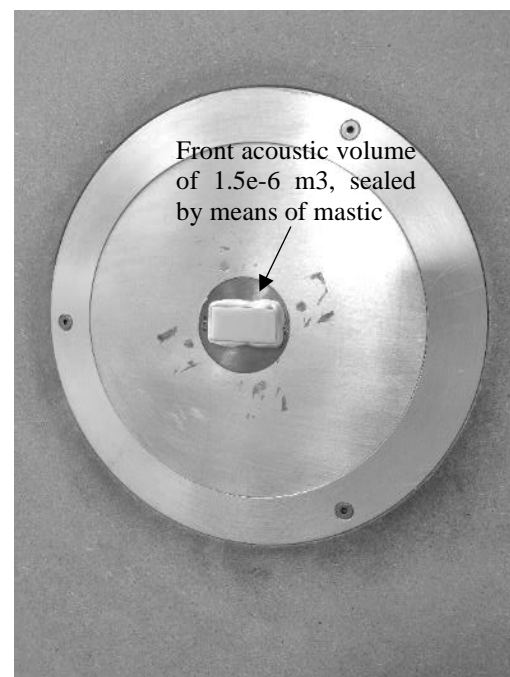


Figure 35 - Speaker N ° 2 – Parameters measurements 2/2

Table IV – Speaker N ° 2 - Measurements of the fundamental parameters

Parameter	#1	#2	#3	#4	#5	Average	Standard Deviation	Coefficient Of Variation [%]
R_e [Oms]*	7.93	7.93	7.93	7.93	7.93	/	/	/
R_{MS} [N.s/m]	1.46e-01	1.40e-01	1.45e-01	1.45e-01	1.45e-01	1.44e-01	2.25e-03	1.56
C_{MS} [m/N]	8.85e-04	9.21e-04	8.64e-04	8.55e-04	8.92e-04	8.83e-04	2.60e-05	2.94
M_{MS} [kg]	8.07e-05	7.75e-05	8.15e-05	8.24e-05	8.00e-05	8.04e-05	1.86e-06	2.32
B.l [T.m]	0.61	0.60	0.61	0.61	0.61	0.61	5.02e-03	0.83

*Measured from the impedance curve without the volume

As for the speaker N ° 1, the value of R_e remains the same within the available measurement accuracy. From the calculation of the coefficients of variation, we see the parameter C_{MS} to show the highest variation with 2.94 %. This value being a little higher than for the speaker N ° 1, we might understand that this speaker heats a bit more the air trapped inside the volume used for the measurement. This phenomenon would so start to significantly affect the correct quantification of C_{MS} . As for the speaker N ° 1, we decide to consider the averaged values for the construction of the acoustic model.

Once all the parameters measured, we can build the acoustical circuit for each of the sealed enclosure and compare predictions against measurements, to verify the validity of our models. As previously stated, the electric current of the circuit being equivalent to an acoustic flow rate, a separated network is built to transform the final output voltage into a quantity analogous to an acoustic pressure from a monopole type source.

Illustrated on Figure 36, this additional circuit consists of:

- A current source, reflecting the measured acoustic flow rate (q) at the diaphragm point
- An inductor, being equal to $\frac{Z}{4\pi r c} * \frac{1}{P_0} = \frac{\rho_0}{4\pi r} * \frac{1}{2e-5}$, where r is the distance from the source

When computed, the output voltage is frequency dependent and takes the following form:

$$u(f) = \frac{1}{2e-5} * \frac{\rho_0}{4\pi r} * 2\pi f * q(f)$$

By finally calculating $20 * \log [u(f)]$ we so obtain a quantity representative of the SPL at a certain distance from the sealed enclosure, in a free field.

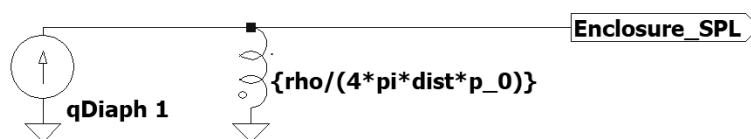


Figure 36 – Additional electric network for the SPL calculation

Sealed enclosure N ° 1: comparison of predictions against measurements

This paragraph compares the output of the previously described model against the measurement illustrated in part II.I.

Also, both because the models we use are linear and because this type of small speaker can rapidly behave in a non-linear way, we intend to verify that the SPL behavior of the enclosure remains the same for three arbitrary defined input voltages: $0.5 u_{RMS}$, $1 u_{RMS}$ and $2 u_{RMS}$.

Figure 37 exposes the comparison for the electric impedance. This comparison gives a good correlation for most of the frequency band, until 2000 Hz, where the inductive behavior of the speaker voice coil starts to dominate the shape of the curve. This discrepancy can be explained by the fact that our acoustic model does not contain any inductance term for the voice coil. But this is by far acceptable since our investigations focus on the LF part of the spectrum. Within this range, we can observe the resonance peak as well as the damping for this peak to well be reproduced by the model.

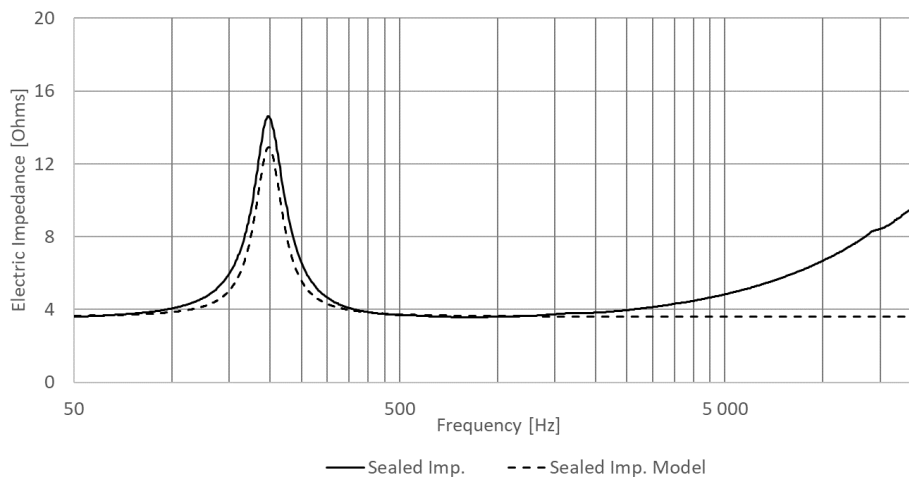


Figure 37 - Sealed enclosure N ° 1 – Model / Measurement electric impedance comparison

On the next page, Figure 38 compares predicted and measured SPLs together for $1 u_{RMS}$. From this graph, we observe a good correlation of the curves until 1500-2000 Hz. But on the rest of the bandwidth, the gap we see between predictions and measurements might find two explanations:

- The first aspect to verify is the frequency limit for the model we use, which only assumes a piston motion of the diaphragm. This frequency can be approached by stating that its quarter-wavelength should be equal to the diameter of the diaphragm. Considering a diaphragm diameter of 36 mm, this frequency should be $= \frac{c}{(0.036*4)} = 2384 \text{ Hz}$. This

result signifies that above this frequency the motion of the diaphragm will break up in resonances and will so not move as a rigid piston anymore. The calculated value being close to the correlation limit we found; it might be a good explanation for the difference we see from 1500-2000 Hz.

- Another cause for this discrepancy, might be that at 0.3 m of distance from the enclosure, the microphone sees additional acoustic sources coming from the diffraction of the generated waves at the edges of the enclosure.

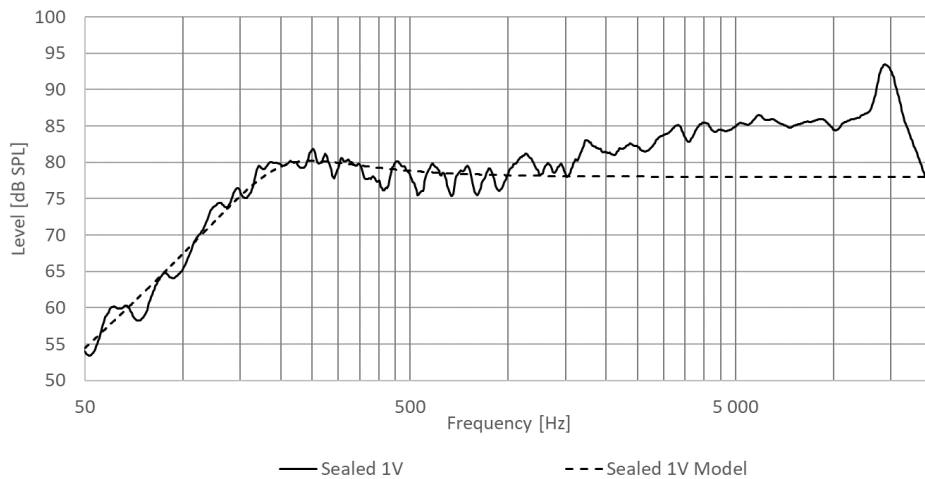


Figure 38 - Sealed enclosure N ° 1 – Model / Measurement SPL comparison

Finally, comparing in Figure 39 the normalized SPL from the enclosure for the three previously defined voltages, we confirm that its behavior remains linear for all the voltages applied. In conclusion, we can rule on the validity of our model from 50 Hz to 2000 Hz, and for input voltages between $0.5 u_{RMS}$ and $2 u_{RMS}$.

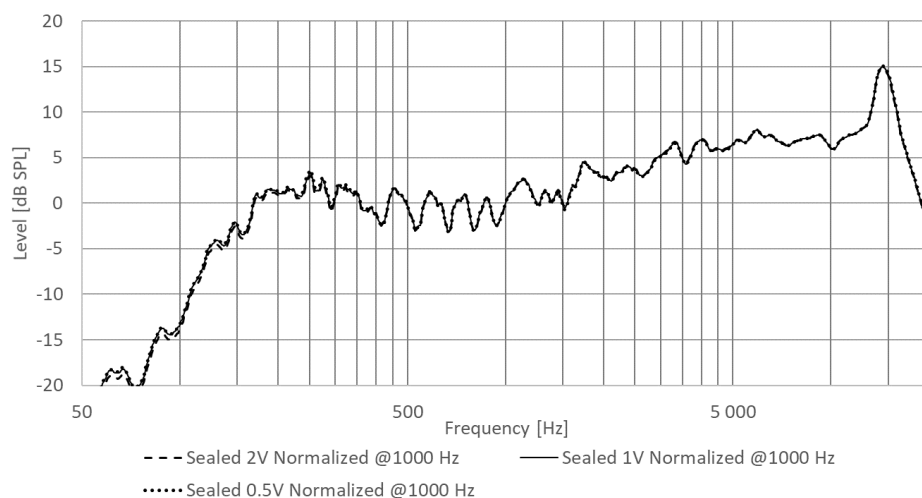


Figure 39 – Sealed enclosure N ° 1 – SPL behavior over the voltage

Sealed enclosure N ° 2: comparison of predictions against measurements

As for the enclosure N ° 1, a comparison is performed for both the electric impedance and the SPL, and we intend to verify the linear behavior of the enclosure at the three following voltages: $0.1 u_{RMS}$, $0.5 u_{RMS}$ and $1 u_{RMS}$.

Figure 40 compares the electric impedance. In this second design where the inductive contribution of the voice coil starts higher in frequencies, we observe an almost perfect correlation of the curves until 6000 Hz. The resonance peak recreated by the model is a bit shifted (few Hz higher), but the damping for this peak is perfectly reproduced.

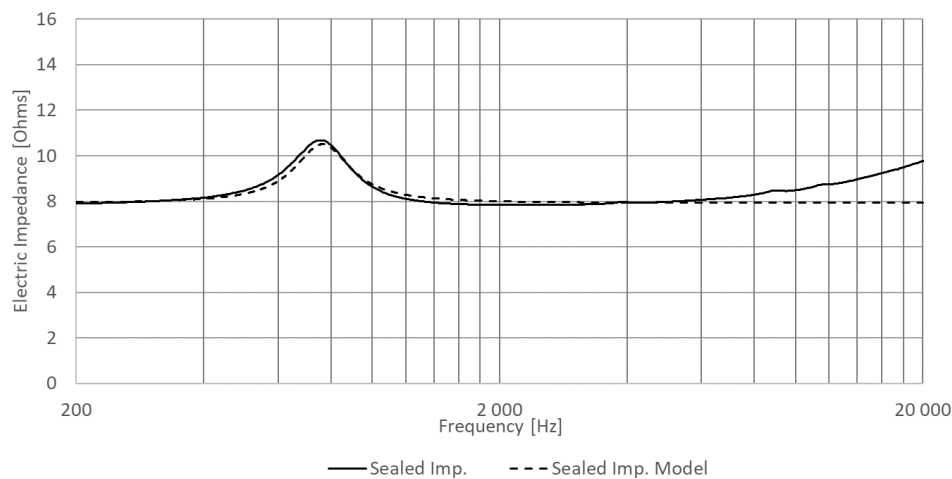


Figure 40 - Sealed enclosure N ° 2 – Model / Measurement electric impedance comparison

Figure 41 compares predicted and measured SPLs together, at 0.1 m and for $0.5 u_{RMS}$. From the observation, the model perfectly recreates the behavior of the system until 4000 Hz. The frequency limit for this model can be approached considering the biggest dimension for the rectangular diaphragm of this speaker. With a length of about 11.5 mm and a width of about 7.5 mm, if we consider the diagonal dimension for the calculation of the limit, its value is $= \frac{c}{(0.014*4)} = 6131 \text{ Hz}$. As for the sealed enclosure N ° 1, the theoretical estimation of the frequency limit for this model gives a value a bit higher than what observed.

Part II - Scope of the investigations: Approach used for prediction

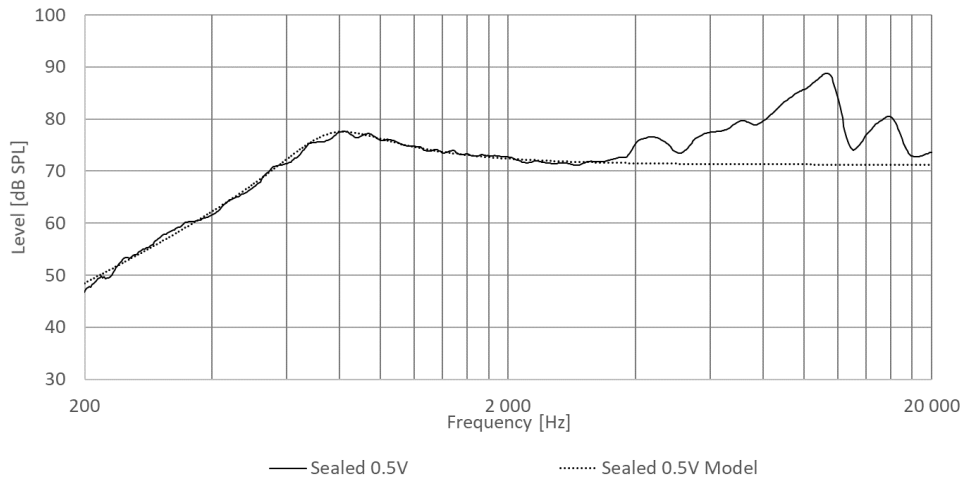


Figure 41 - Sealed enclosure N ° 2 – Model / Measurement SPL comparison

Comparing in Figure 42 the normalized SPL from the enclosure for the three previously defined voltages, we find a perfect match of the curves for all the voltages applied. In conclusion, we can rule on the validity of our model from 200 Hz to 4000 Hz, and for input voltages between $0.1 u_{RMS}$ and $1 u_{RMS}$.

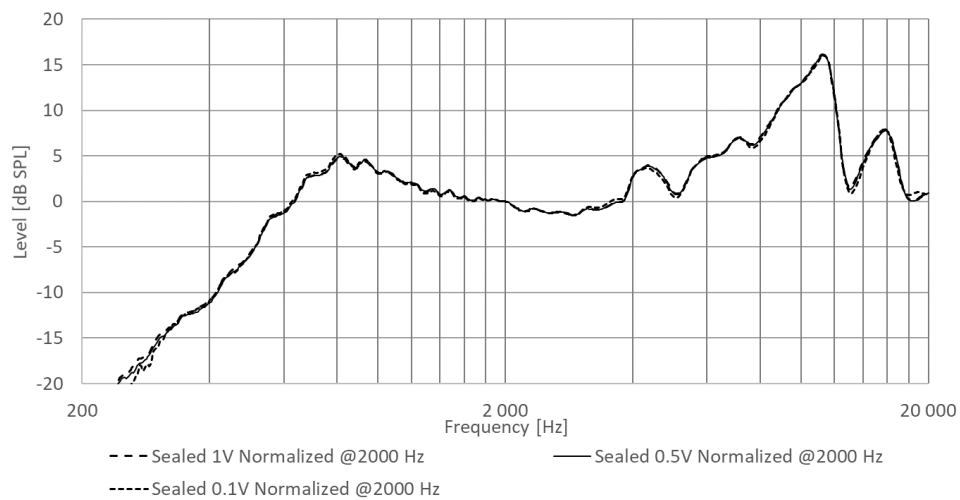


Figure 42 - Sealed enclosure N ° 2 – SPL behavior over the voltage

II.IV. Protocol for the perceptual evaluation of each of the improvement

As introduced within the scope of the study, a listening test is intended to be carried out on the prototypes resulting from the various improvements. This type of test allows the objective performance to be linked to the subjective performance, and thus, to decide on the relevance of each of these improvements. The protocol established for this test is inspired from two articles by E. Parizet et al. [30] [31], from an article by G. Lorho [32] and from an article by G. Liu et al. [33].

Subjects number and description

The four introduced articles respectively describe a number of 72, 64, 16, and 9 subjects. Even if we understand a small number to only give a tendency for the results, our experience can only rely on 10 subjects (5 men and 5 women), for which the age repartition is from 20 up to 55 years old.

Setup of the listening test

The test is based on paired comparisons, and similarly to the protocol described in [30], a square matrix is built with each of the improvement to test as inputs. From this matrix, the diagonal is removed, and a further analysis is performed to determine the relevant pairs to submit for the test. Among the improvements, a Bluetooth speaker JBL Go 3 is intended to be considered for the comparisons around the speaker N ° 1, and a smartphone Oneplus 6 will also be considered for the comparisons around the speaker N ° 2. A brief description of these devices as well as their acoustic signature (measured from our acquisition software) are reported in appendix B. For each subject, the pairs order is randomly set by means of a combination generator tool available on the website *generatormix.com*.

Figure 43 describes the listening test environment. Each subject seats at about 70 cm from the pairs to listen to. The solutions are installed on a stand, over a decoupling foam pad, and are hidden to the subject by means of an acoustically transparent tissue. A microphone is installed on the side to record all comments and answers from the subject to different questions asked between each pair listened.

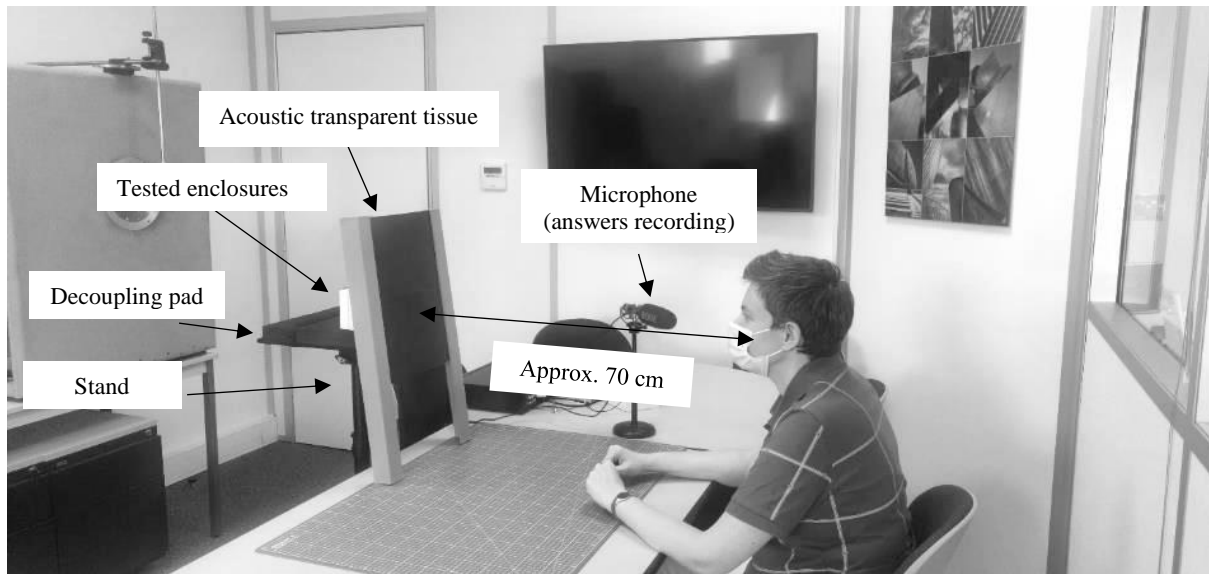


Figure 43 – Listening tests environment

Questions asked between each pair listened to

Inspired from [30], the first task requested to the subject is to freely speak and comment about what he just listened to. This open talk allows to collect some words (also called “descriptors”), which once put in common from all the subjects, may help to explain a tendency or a discrepancy between the subjective and the objective performance. This task is then followed by two closed questions:

- “Which of the two systems brings more low frequencies to the sound?”
- “Which of the two systems do you prefer?”

This type of forced choice procedure is directly inspired from the “Test 3” described in [31], but with the possibility here to answer: “I don’t see the difference” or “I don’t have any preference”. This additional possibility avoids blocking the test or looping into many listening repeats. It therefore ensures to keep the test duration reasonably short.

Audio signals used for the test

Music songs are used in both [32] and [33], but only this last article deals with short extracts of about 20 – 30 seconds. Using extracts instead of entire songs is a predominant criterion for our test since we cannot retain each subject more than 30 minutes.

As a compromise between the time and the number of extracts to be played, it was decided to submit two extracts of 15 seconds each, the first of which is played on a first half of combinations, before playing the other on the second half of combinations.

The selected music styles for improvements around the speaker N ° 1, are pop and jazz, both chosen loud in bass. The selected styles for improvements around the speaker N ° 2, are rock and jazz, both soft in bass, as the distortion for this type of transducer can increase rapidly when used out of its typical range.

Results exploitation

From the analysis of the results, the objectives will be:

- To correlate the subjective attribution of LF to the measurements and explain any discrepancy with the help of collected words from the open talks.
- To compare the preferences to the LF attribution, and to also rely on the collected words to justify on the preference attribution when not due to the extended presence of LF.

III. Investigations around the speaker enclosure N ° 1

III.I. Improvement method N ° 1 (Bass-Reflex)

Although early Bass-Reflex (BR) systems were described in [20] and [25], the investigations carried out in this chapter mainly rely on the articles from A. N. Thiele [28] and R. H. Small [34]. According to this last author, the acoustical analogous circuit of a BR system has the form of the one illustrated on Figure 44.

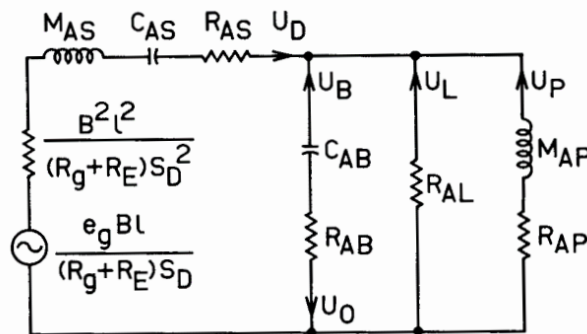


Figure 44 – Acoustical analogous circuit of a BR system [34]

From this circuit:

- R_{AP} represents the losses created into the port. We choose to neglect this term at a first design step,
- $M_{AP} = \frac{\rho_0 \cdot \text{port length}}{\text{port area}}$ is the equivalent moving mass for the air particles into the port. The value for the port length containing some end corrections,
- R_{AL} represents leakages caused by the port into the enclosure. This last parameter being difficult to estimate, it is decided to not consider it within the scope of our investigations.

Estimation of the shape for the extension

A proposed starting point for the design of a BR system, is to estimate the shape (also called “alignment”) that can be reached for the extended portion of the response curve. At a time when IT was not as developed as it is today, A. Thiele released a full table of values ([28]: part V), where the ratio $\frac{C_{AS}}{C_{AB}}$ called “system compliance ratio” appears as a predominant criterion for the calculation of the alignment. From this ratio, we understand the alignment to be both dependent of the speaker compliance property and of the enclosure size. Based on Table from

A. Thiele, three alignments qualified of “popular” by R. Small are reported on Table V and illustrated through an example on Figure 45. The values are then compared to our design. Figure 45 illustrates, with the ratio $\frac{f}{f_s}$ defined for the x-axis, typical response curves for the three alignments, using the same speaker but different sizes for the enclosure. Depending on the alignment, we observe a noticeable difference in the SPL shape for the extension, the C₄ type giving the most irregular shape, but also a difference in the frequency amount, the QB₃ type showing the smallest extension.

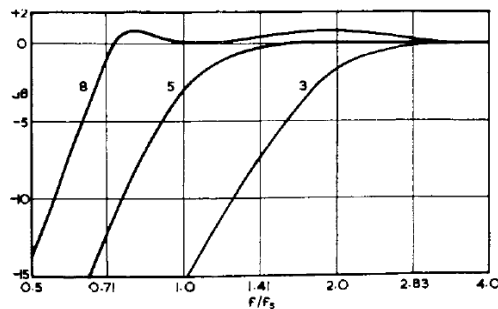


Figure 45 – Illustration of alignments C₄, B₄, and QB₃ (n ° 8, 5, and 3) [28]

Table V - BR alignments: corresponding compliance ratios [28]

Alignment reference	System compliance ratio (C _{AS} /C _{AB})	Alignment name
Alignment N ° 8 from Figure 45	0.56	C ₄
Alignment N ° 5 from Figure 45	1.41	B ₄
Alignment N ° 3 from Figure 45	4.46	QB ₃

From the page 15₂ we calculated $C_{AB} = 1.16e-09 \text{ m}^5/\text{N}$ and listed the formula for the calculation of C_{AS} . Considering the measured value for C_{MS} and S_D , we calculate $C_{AS} = 5.51e-10 \text{ m}^5/\text{N}$ and the ratio $\frac{C_{AS}}{C_{AB}} = 0.48$. This value reports an alignment close to the shape of the C₄ one. We therefore expect to get a considerable amount of extension in our design but with an irregular shape for the SPL in this region.

Design of the port

Once this first step reviewed, we need to estimate more accurately the quantity of LF we can bring in our design. In their respective articles [28] [34], A. Thiele and R. Small explained that the key frequencies for a BR system can fully be studied from the electric impedance curve of the speaker. The typical shape of such a curve is illustrated on Figure 46.

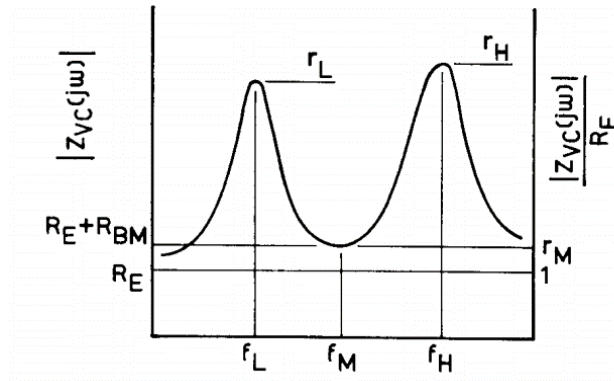


Figure 46 – Typical electric impedance of a BR system [34]

From this Figure:

- f_H is often understood as the shifted resonance of the original sealed enclosure,
- f_L is the low frequency roll-off (LFRO) for the extension. Defined as the -3 dB point from the nominal SPL (considered at 1000 Hz in this section),
- f_M is the Helmholtz resonance, assuming a lossless system. Its value corresponds to the minimum of impedance in between f_L and f_H .

Although f_L is the frequency that interests us for the calculation of the extension, the design approach is made by determining f_M , the three frequencies being intimately linked and possible to compute through our acoustic model thereafter [28] [34].

From the Helmholtz resonator principle, we find the link between f_M and the port dimensions

in the following formula: $f_M = \frac{c}{2\pi} \sqrt{\frac{A}{Vl}}$, where:

- V , is the inner volume of the enclosure
- l , is the length of the port (including end corrections)
- A , is the area of the port

But when designing BR systems, this formula is not the only one to consider for the dimensions of the port. To avoid the generation of noise caused by aerodynamic turbulences at the ends of the port, R. Small [34] recommends adjusting the port area so that the velocity of air particles inside will not exceed 5% of the sound velocity.

This condition can be satisfied with the following formula: $A \geq 0.8f_M S_D x_{max}$ (x_{max} being the peak linear displacement of the speaker diaphragm, equal to 3.5 mm in our case)

Considering the resonance of the sealed enclosure (f_B) to be = 200 Hz and a small target for f_M fixed = 150 Hz, the above condition would require:

- A port area $A \geq 4.28 \text{ cm}^2$
- A port length $l = 34 \text{ cm}$ (end corrections included)

By far, this port is too long and so not technically feasible in regards with the dimensions of our system. Moreover, in our estimations, we do not consider that the port goes inside the enclosure.

Resulting both from mechanical constraints and acoustical targets, the design proposed on Figure 47 illustrates a curved port with an area A fixed = 0.5 cm^2 (8 mm diameter), a total length of 8 cm and a theoretical resonance f_M calculated = 106 Hz, considering the ends correction term = $0.614 * \text{Port Diameter}$

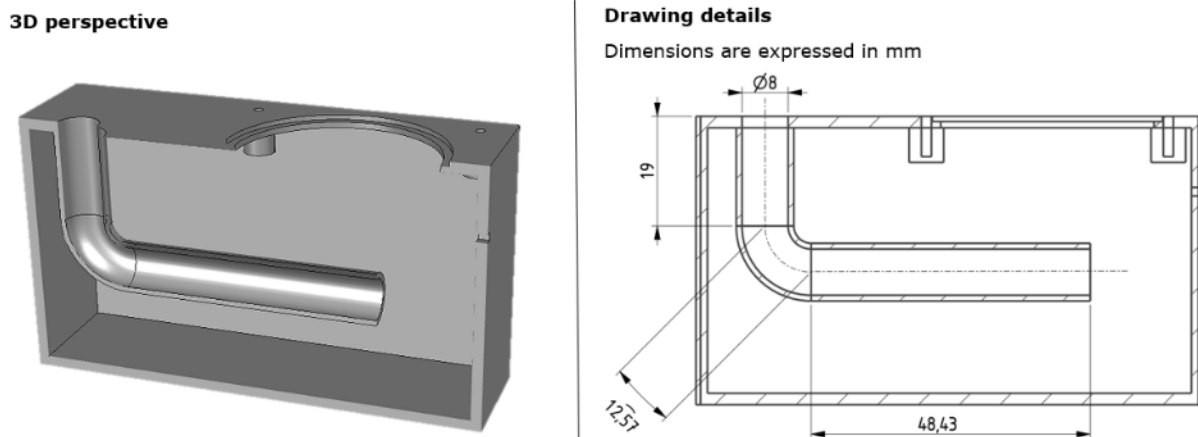
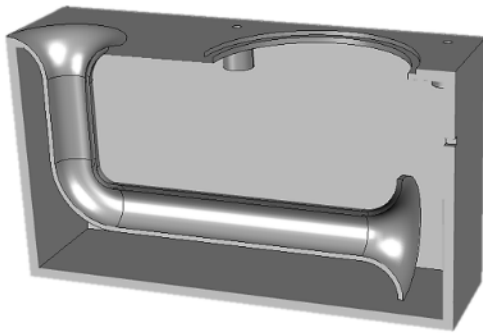


Figure 47 – BR system N° 1 – Prototype drawings

As this design does not respect the above condition for the minimum area, it becomes relevant to study the noise added by the turbulences at the ends of the port. To quantify this phenomenon, we propose to design an alternative BR system relying on the article from N. Roozen et al. [35] In this publication the authors summarize different terminations for the port of a BR system, from which the proposed design called “Port C” appears as a good compromise between mechanics and acoustics for being considered in our system. The curvature radius for the ends of this port is related to the port inner radius by a factor 2. This leads us to design the alternative

system illustrated on Figure 48 featuring horn shaped ends. In this design, the port length is adjusted considering its effective value at half of the horns.

3D perspective



Drawing details

Dimensions are expressed in mm

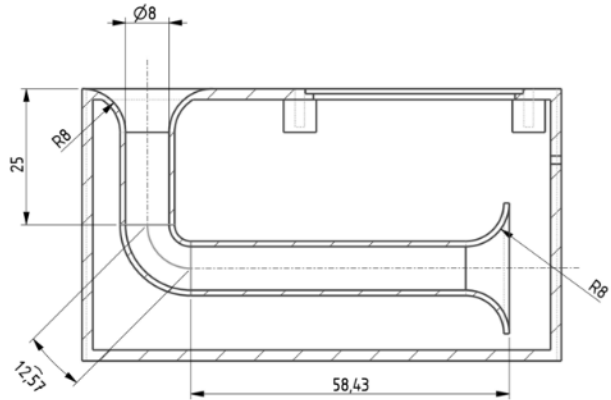


Figure 48 – BR system N ° 1 – Horn port prototype drawings

Acoustic prediction

The below section reports only about the expected electric impedance and SPL for both the original and horn port design. The impact of turbulences for the original port design will be quantified by measuring the prototypes.

The analogous circuit for the BR system is built as per illustrated on Figure 49, with M_{AP} , the added moving mass term for the air particles into the port and calculated according to the formula listed in page 27. Also, the value for the term C_{AB} is reduced from the volume taken by the port into the enclosure.

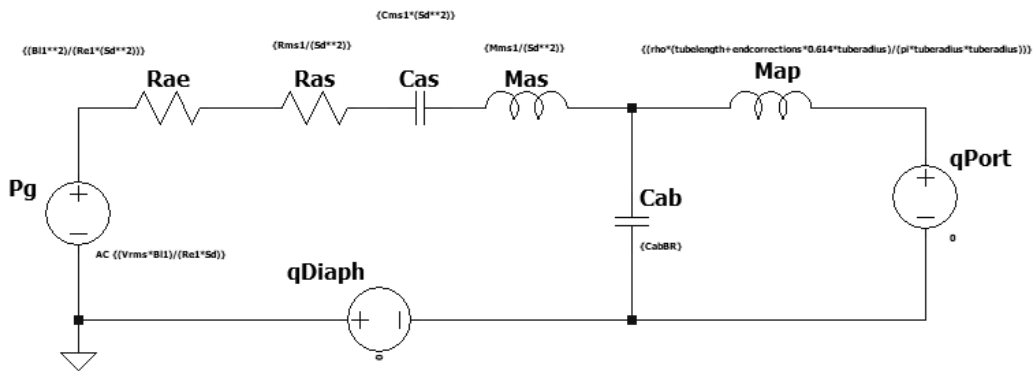


Figure 49 – Simplified acoustical circuit of a BR system (lossless)

To compute the global SPL of the system, the acoustic flow rate for the port section is measured similarly to the one for the diaphragm section, and then, the two flows are simply mixed into the additional circuit illustrated on Figure 50.

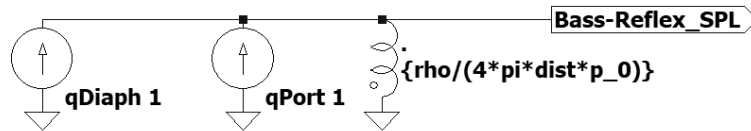


Figure 50 – Electric network for the SPL calculation of a BR system

Figure 51 illustrates the computed electric impedance for the system. From this simulation, we will reproduce the previously calculated value of 106 Hz for f_M . The frequency f_H is found = 210 Hz, and f_L is found = 82 Hz. We so understand that the designed system should extend the enclosure response down to about 80 Hz.

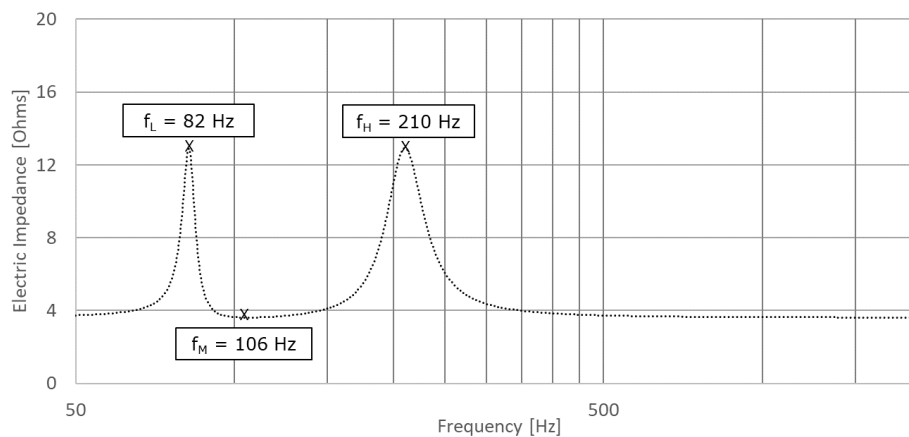


Figure 51 – BR system N ° 1 – Simulated electric impedance

Figure 52 compares simulated SPLs of the BR system against the sealed response, at $1 u_{RMS}$. From this comparison, we first confirm the shape for the extension to be close to a C4 alignment, as per studied in the beginning of this section. Then, with a LFRO around 80 Hz we confirm the expected extension. The sharp drop observed below this frequency, and well described in [20] [25] [28] [34], is often attributed to destructive interferences between the speaker and the port. Finally, according to the prediction we conclude that we should improve the LF of our enclosure with a slightly fluctuating SPL (± 3 dB) until 80 Hz.

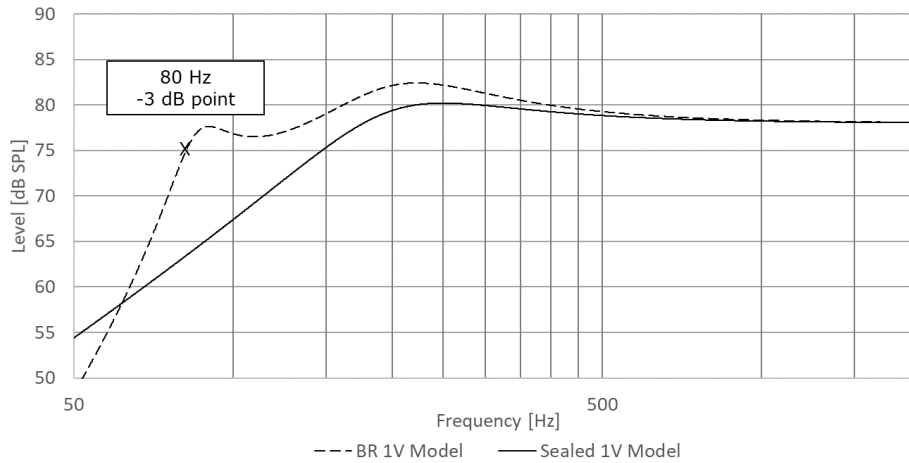


Figure 52 - BR system N ° 1 – Simulated SPL comparison: BR / Sealed

Prototypes realization and qualification

Based on the previous drawings, Figures 53, 54, and 55 illustrate the 3D printed prototypes of both the original and horn BR design. The thickness for the walls remains the same as for the sealed enclosure (2 mm). Prior to compare measurements against predictions, we decide to quantify the improvement realized by the proposed design. The setup for the measurement is detailed on Figure 56.

On the next page, Figure 57 compares the SPL for the original BR against the sealed enclosure at $1 u_{RMS}$. Looking at some points on this graph, we observe that the BR amplifies the SPL by about 3-4 dB at 150 Hz, and by about 5 dB at 100 Hz. However, we observe a LF extension that drops quickly in frequencies, far above the predicted LFRO of 80 Hz. Indeed, this point is seen at around 110 Hz, or 30 Hz above the predicted value. An explanation for this might be that the system brings some losses while our model is lossless.

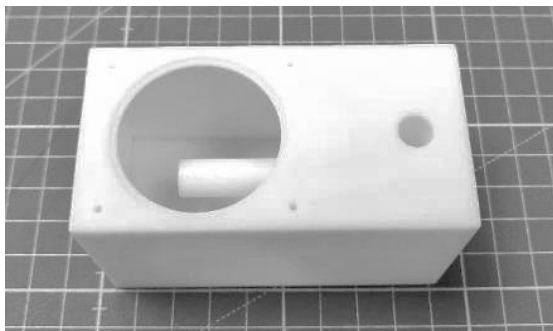


Figure 53 - BR system N ° 1 – Original prototype

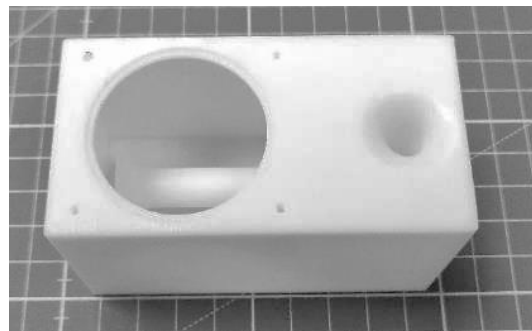


Figure 54 - BR system N ° 1 – Horn port prototype

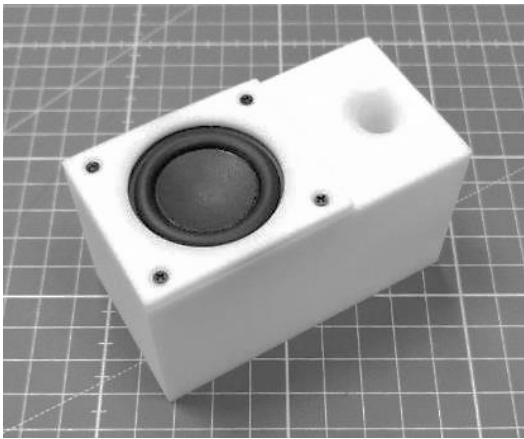


Figure 55 - BR system N ° 1 – Assembled prototype

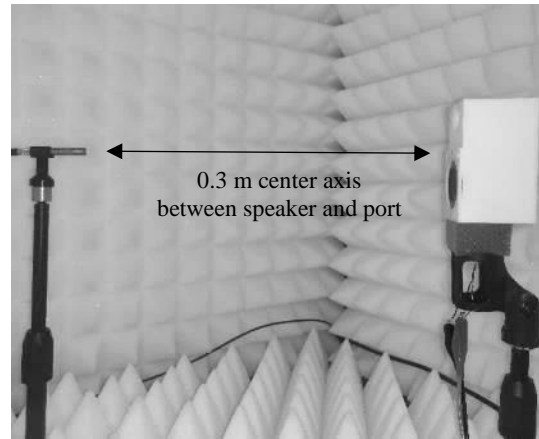


Figure 56 - BR system N ° 1 – Measurement setup

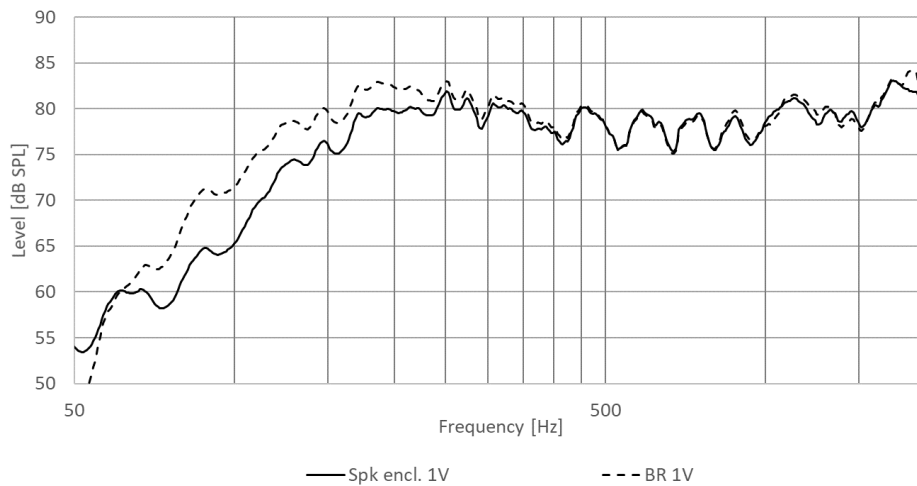


Figure 57 - BR system N ° 1 – Measured SPL comparison: BR / Sealed

Figure 58 compares the normalized SPL from the BR design at the three considered voltages. From this comparison, we can observe few dBs of difference between the curves in the LF region below 100 Hz. Since the strongest attenuation is shown from the curve obtained for 2 u_{RMS} , we might understand a phenomenon related to non-linearities in the port when it receives strong energy. But considering this small difference of SPL, we simply conclude that this attenuation should not really be perceived when listening to this design within the voltage range considered in this study. As an aside, it might be interesting to analyze this non-linearity at higher voltages. But it would also be necessary to verify that the speaker itself remains linear in this range.

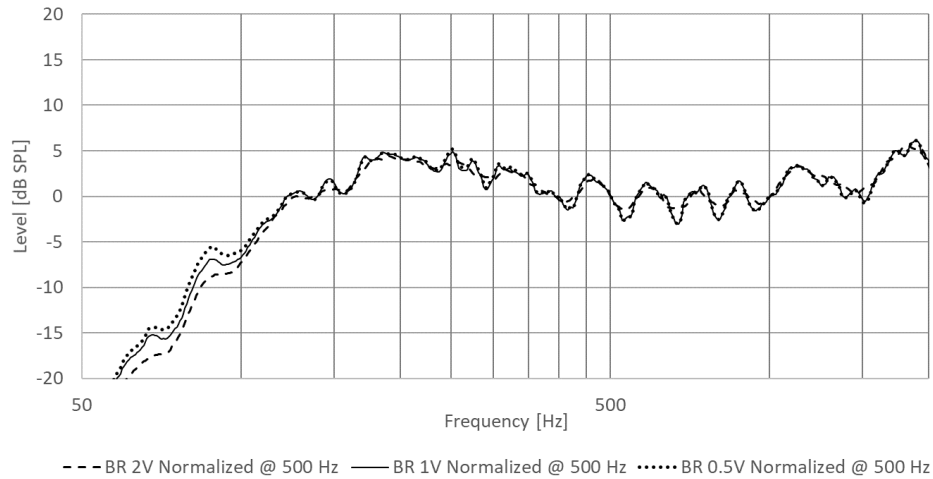


Figure 58 - BR system N ° 1 - Measured SPL comparison for the 3 voltages

Comparison of measurements against predictions

Figure 59 compares the electric impedance of the system, while Figure 60 compares the SPL for 1 u_{RMS} . As briefly discussed in the previous section, we understand both from the impedance and from the SPL that our simulated system does not predict the losses that are measured over the prototypes. Indeed, from the impedance curve we see the predicted damping for f_L being far lower than the measured one, while the predicted damping for f_H is closer to the reality. This leads to a good correlation of predicted and measured SPLs until around 120 Hz.

A way to introduce the losses in our model is to consider the resistive term R_{AP} which was intentionally neglected at a first design step (page 27). But as this term is frequency dependent, it cannot be recreated through a pure resistance component. To calculate it, we decide to rely on both the section “Intermediate-sized Tube-Mixed Mass-Resistance” from [25] and on an application note from the company Knowles regarding microphone simulation models [36]. Figure 61 on the next page illustrates only the port portion of the circuit with this term.

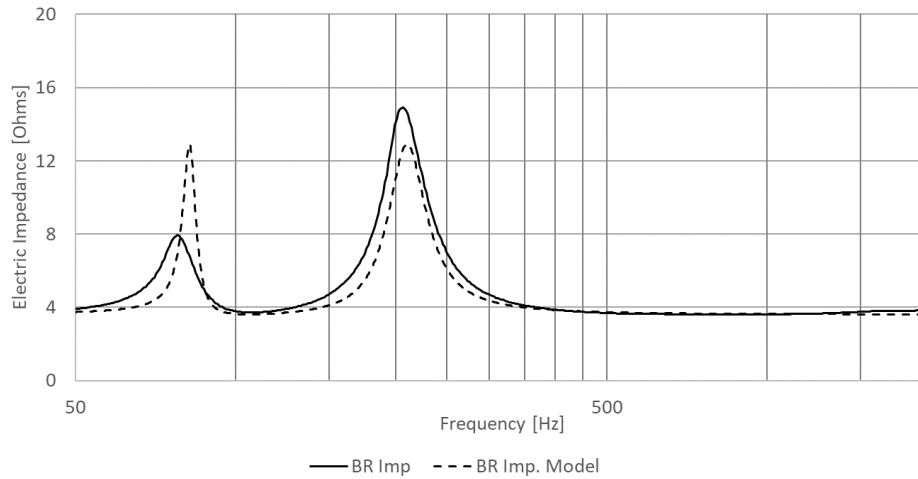


Figure 59 - BR system N ° 1 – Electric impedance comparison: Simulation / Measurement

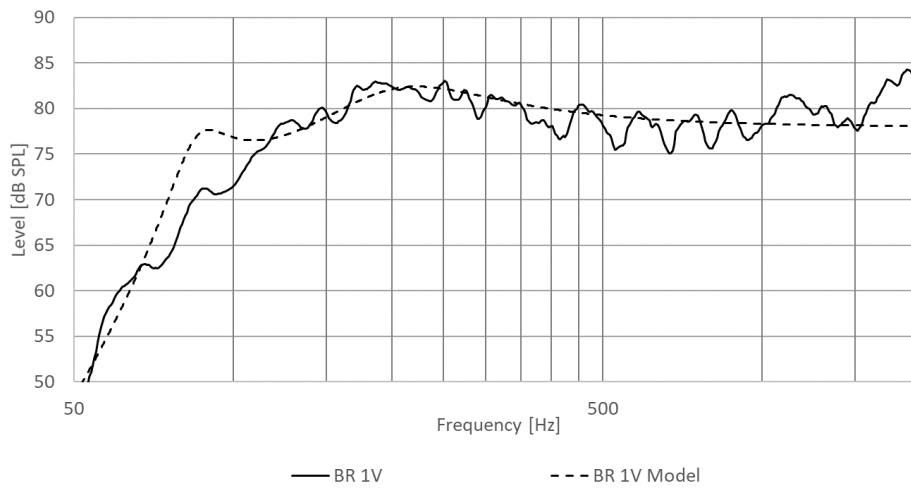


Figure 60 - BR system N ° 1 – SPL comparison: Simulation / Measurement

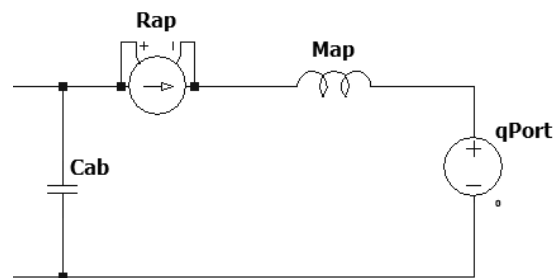


Figure 61 - BR system N ° 1 – analogous circuit for simulation of port losses

As described in [36], we create the term R_{AP} using a voltage dependent current source, into which a Laplace transform is computed as follow:

$Laplace = 1 / [(\frac{\rho_0}{\pi r^2}) \sqrt{2s\mu_0} * [(\frac{1}{r} + 2)]]$, where μ_0 is the dynamic air viscosity, and s the Laplace operator. The newly predicted electric impedance as well the SPL at 1 u_{RMS} are compared again, respectively on Figures 62 and 63. As brief comments, we observe that the impedance curve is better recreated by this new model, but on the other hand, only a small

attenuation is observed in the LFRO region with a SPL still far above what we measure over the prototype. We conclude that we face much more losses than what we can predict. And this might be a side effect of a port too narrow.

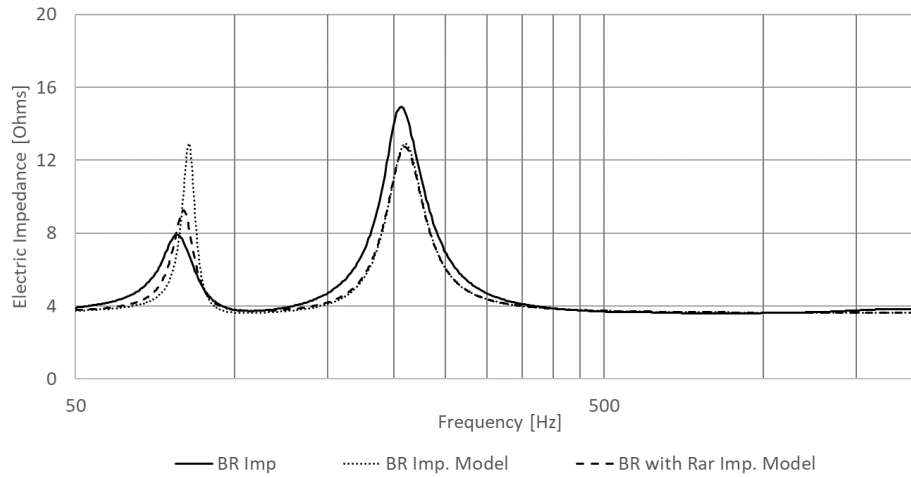


Figure 62 - BR system N ° 1 – Electric Impedance comparison: Measurement/Simulation w/ and w/o losses

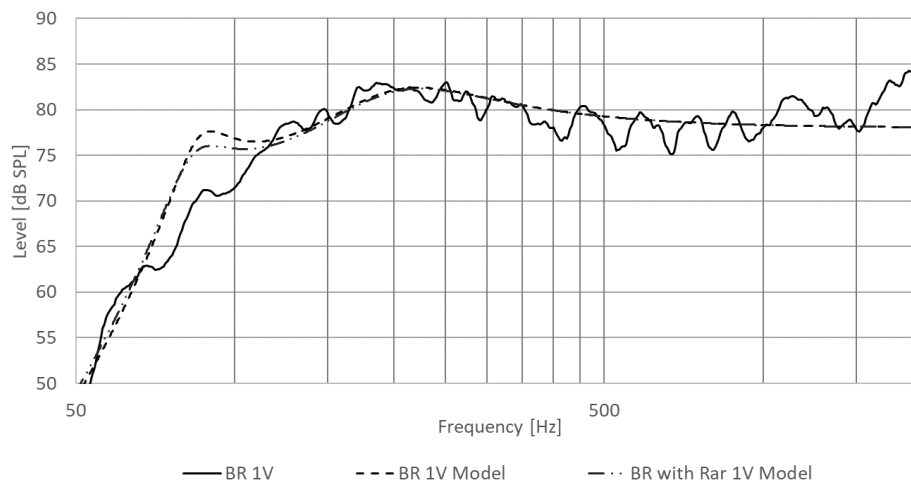


Figure 63 - BR system N ° 1 – SPL comparison: Measurement/Simulation w/ and w/o losses

Qualification of turbulences created by the original port design

As a first step, we need to confirm that both BR systems behave identically. To proceed, a measurement comparison is performed for both the electric impedance and the SPL at $1 u_{RMS}$. From the measurements reported in Appendix C, we rapidly conclude that the two systems behave identically. Only a small difference on the frequency f_L is observed, probably due to an error in adjusted length for the horn port. To quantify the aerodynamic turbulences, we rely on the work from Garcia-Alcaide et al. [37]. The procedure consists of measuring the near field response of the port (0.02 m fixed in our case), when excited by a pure sine equal to its resonance f_M . The setup for this measurement is illustrated on Figure 64, and the responses for the two BR are illustrated in the figures after.



Figure 64 - BR system N° 1 – Setup for qualification of turbulences created by ports designs

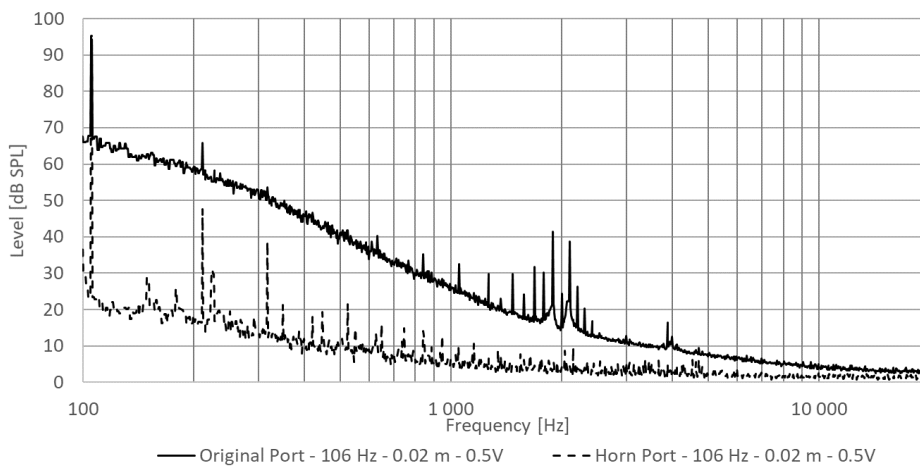


Figure 65 - BR system N° 1 – Qualification of turbulences created by ports at $0.5 u_{RMS}$

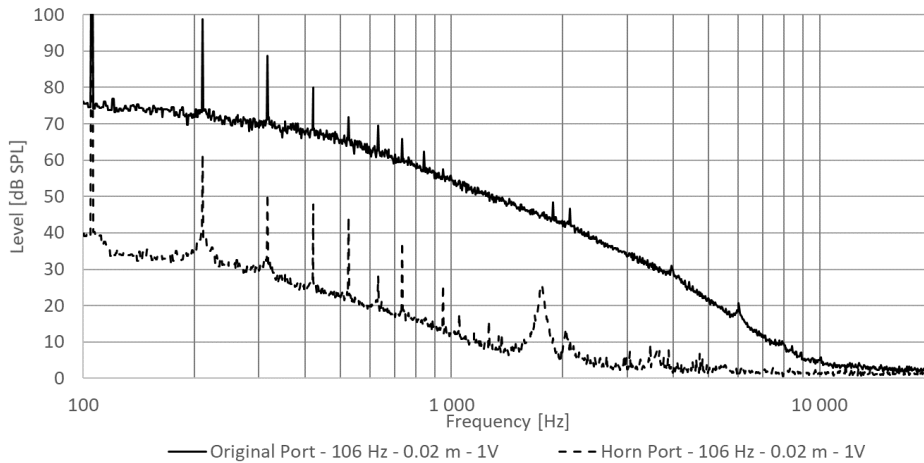


Figure 66 - BR system N° 1 – Qualification of turbulences created by ports at 1 u_{RMS}

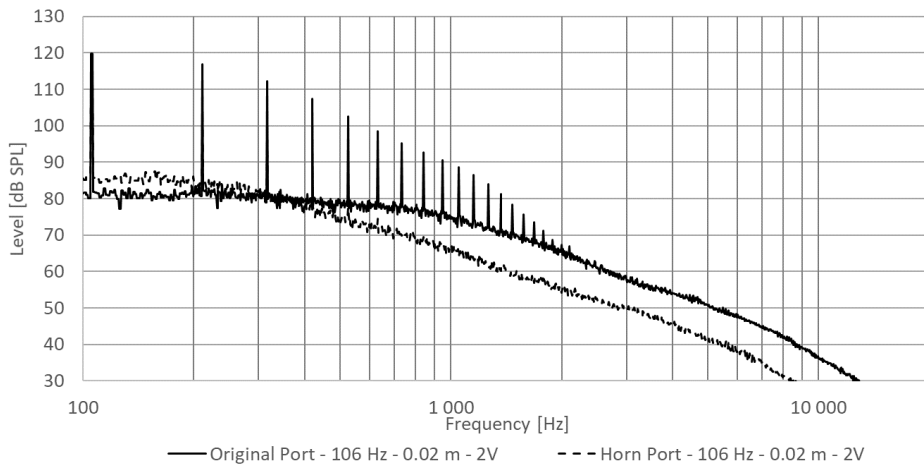


Figure 67 - BR system N° 1 – Qualification of turbulences created by ports at 2 u_{RMS}

Figures 65, 66 and 67 respectively compare the original and horn port response to a 106 Hz sine, at 0.5, 1 and 2 u_{RMS} . A first observation is that we see for almost all the configurations two types of added signal:

- a broadband noise attributed to the turbulences under study,
- but also, the first harmonics of the pure tone increasing accordingly to the voltage and for which the responsible is more probably the speaker itself than the port.

From the two first comparisons, we clearly see the benefice of using the horn port, as it transmits the tone with much less noise than the original port. On the other hand, when applying 2 u_{RMS}

the benefice of this second port is less visible. Indeed, besides still attenuating the noise above 1000 Hz by 10 dB, this port produces more turbulences in the region 100 – 200 Hz. This last observation appears in total concordance with what is commented in the part “5 Experimental investigation” of [35]: “[...] at low levels a cylindrical port with a large curvature radius produces less blowing sound than a cylindrical port with a small curvature radius, while at higher levels it is the other way around. “

By concluding that not only the turbulences are important to consider, but also the radiation efficiency and the quality factor of the port fundamental resonance (open ends tube resonance), the authors suggested a diverging geometry as per illustrated on Figure 68. But in the end, as this shape is more complex than the design we considered (compared again on Figure 69), it might be a challenge to realize it from a manufacturing and cost aspect for Seltech. In conclusion, for reasonable SPLs, we understand the port design considered in our investigations to remain a good option against a port with sharp terminations.

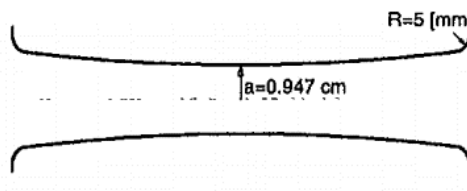


Figure 68 – BR port designs : Port E geometry [35]

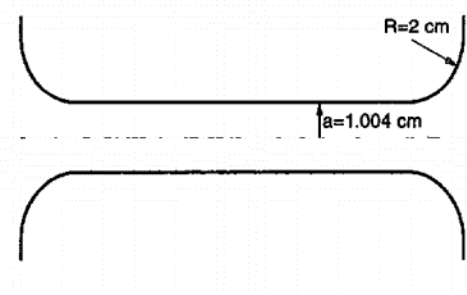


Figure 69 - BR port designs : Port C geometry [35]

Conclusion

From this first improvement method, we learned the basics of Bass-Reflex designs and how complex it can be to get a good radiating port in enclosures as small as those considered here. But even if the LF extension we get from the prototypes is smaller than what the models predict, we get a solution that amplifies the sound by around 5dB at 100Hz, and with a -3dB point extended from 150 Hz for the sealed enclosure, to about 110 Hz. In addition, for small to middle-range SPLs, a horn shape for the port terminations can significantly reduce the noise caused by aerodynamic turbulences in this type of small tube. But in the end, one could understand that this type of small port introduces heavy losses into the system, and therefore decreases the expected SPL in the LF region. A more reasonable target for f_M would allow to increase the port area again, and therefore lead to a smaller LF region, but louder and flatter.

III.II. Improvement method N ° 2 (Passive Radiator)

The investigations carried out in this section are both inspired from the work of Jiang et al. [13] and of R. H. Small [38]. Despite we understood in the part II.II of this document that a Passive Radiator (PR) system is composed both of a speaker and of a diaphragm, we do not have the measurement capabilities to properly qualify this last element. Therefore, relying on the following phrase from [38] “[...] *the passive radiator is often made from the same frame and suspension as the driver* [...]”, we decide to simply consider a secondary speaker identical to the first one, but non-wired, to design our system. For the rest of the section, this transducer will be called “passive element” (PE). Figure 70 illustrates the circuit for the PR, where:

- R_{AP} (named R_{AR} for this document) represents the losses created by the energy dissipation in the moving part of the PE,
- M_{AP} (named M_{AR} for this document) is the mass for both the moving part of the PE and the air particles around its diaphragm,
- C_{AP} (named C_{AR} for this document) represents the compliance for the moving part of the PE.

As already discussed, R_{AB} is neglected and R_{AL} is not considered in our models.

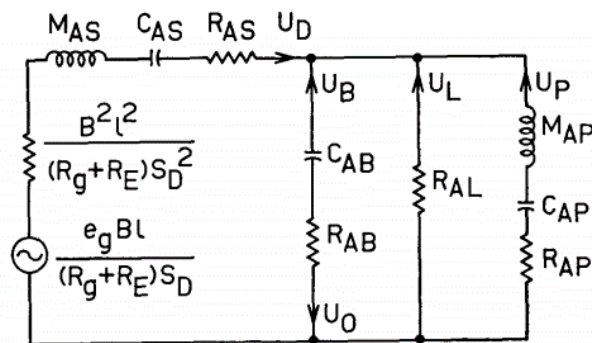


Figure 70 – Acoustical analogous circuit of a PR system [38]

From this Figure, we can observe similarities with a BR system. Indeed, the circuit is extended by an additional loop on the right of the C_{AB} term, containing so the acoustical properties of the PE (instead of the properties of a port).

Qualification of the passive element, and estimation of the shape for the extension

Applying the same method than described in the part II.III, the Table VI on the next page summarizes the measured values only for the mechanical parameters of this element. Also, proceeding as in [38], we think relevant to compare these values with the ones of the speaker. This, to assess whether the two elements will behave similarly in the design.

Table VI - PR system N ° 1 – PE qualification

Parameter	Speaker (1)	Passive element (2)	(2) – (1)	[(2) – (1)] / (1) [%]
$R_{MS/R}$ [N.s/m]	5.39e-01	5.12e-01	-2.70e-02	-5.01
$C_{MS/R}$ [m/N]	5.30e-04	4.44e-04	-8.60e-05	-16.23
$M_{MS/R}$ [kg]	1.79e-03	1.87e-03	8.00e-05	4.47

Table reports the percentage for the difference “passive element – speaker” when compared to the values of the speaker. From this comparison, we observe the parameter C_{MS} as showing the highest variation, with a value of 16.23 %. We so understand that the two elements will behave differently from each other. To further evaluate this difference, R. Small compares two compliance ratios together:

- The first one, already introduced on page 28, is the System compliance ratio (called α in [38]), and defined = $\frac{C_{AS}}{C_{AB}}$,
- The second one is the PR compliance ratio (called δ in [38]) and defined = $\frac{C_{AR}}{C_{AB}}$.

By comparing the two elements compliance to the one of the enclosure, if these two ratios are almost equals ($\delta \approx \alpha$), it signifies that the two elements should behave similarly in regards to the enclosure. In our case:

- α has already been calculated = 0.48 on page 28
- and with a term $C_{AR} = C_{MR} * S_D^2 = 4.44e-04 * (1.02e-03)^2$ for the PE, $\delta = 0.40$

With a configuration not far from $\delta \approx \alpha$, we can therefore consider the graphic illustrated on Figure 71 to estimate the shape of extension we might get in our design. Showing a normalized x-axis equivalent to $\frac{f}{f_s}$, this graphic illustrates possible alignments, according to the value of α , and for a configuration $\delta = \alpha$. With ratios values between 0.4 and 0.5, we estimate to only be able to reach non-flat alignments (depending of M_{AR} as well) close to the curve marked $\alpha = 0.6$.

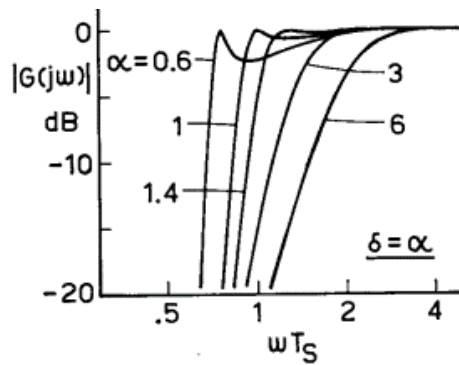


Figure 71 – “Responses obtainable from passive-radiator system for the condition $\delta = \alpha$ ” [38]

Acoustic prediction

Once the PE qualified, the circuit illustrated on Figure 72 is built with the term C_{AR} containing the previously calculated value and the terms R_{AR} and M_{AR} calculated using the formulas from the page 15.

The C_{AB} term is reduced from the volume taken by the PE in the enclosure.

At this design step, only the SPL from the system is relevant to compare with the sealed enclosure. The curves are illustrated on Figure 73 for a comparison at 0.3 m and for 1 u_{RMS} .

From this graphic, we observe that the system as it is does not improve the LF region but degrades it. In more detail, the “notch” we see on the PR curve is caused by the resonance

frequency (f_S) of the PE. As by definition $f_S = \frac{1}{2\pi} \sqrt{\frac{1}{M_{AR}C_{AR}}}$, we understand that this frequency can either be controlled by M_{AR} or C_{AR} . Therefore, if we want to decrease f_S for extending the LF response, the only change we can do on a manufactured PE is on M_{AR} . More concretely, to affect this term in the right direction, we simply need to add additional mass over the diaphragm, paying attention on keeping a good balance of it.

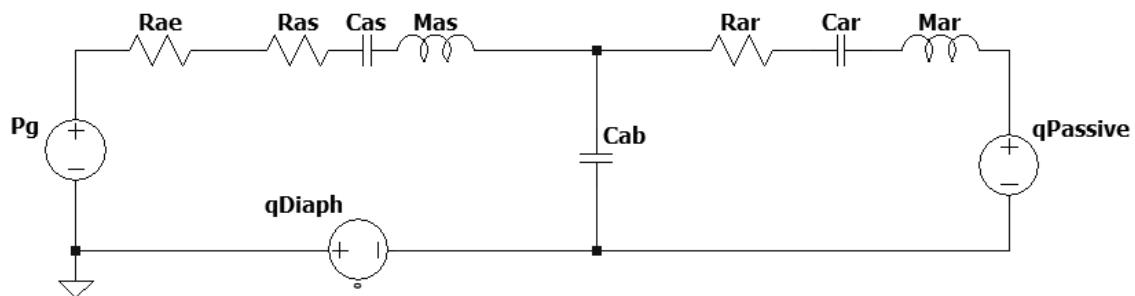


Figure 72 - Simplified acoustical circuit of a PR system

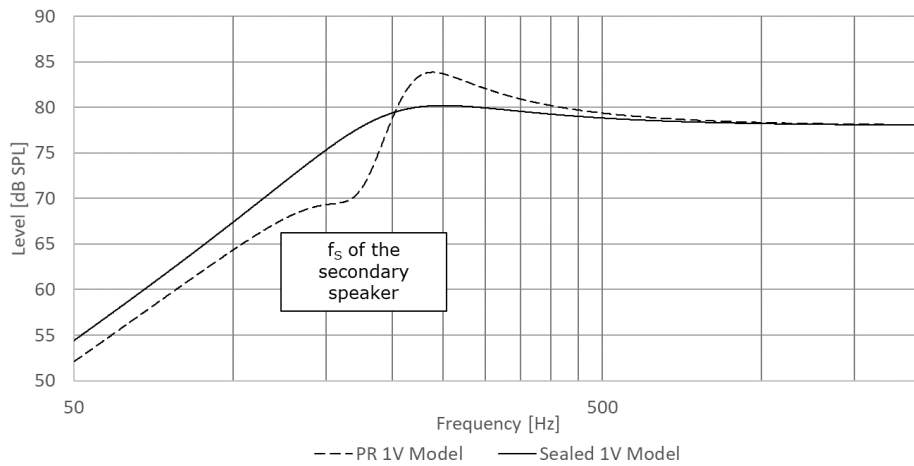


Figure 73 - PR system N° 1 – Simulated SPL comparison: PR / Sealed

Verification of the initial prediction

Prior to tune the system, it is preferable to verify the validity of our model with a brief comparison against measurements. The PR prototype is so built as per illustrated on Figures 74 and 75, simply with a second aperture for the PE, identical to the first one. The setup for the measurement is illustrated on Figure 76.



Figure 74 - PR system N° 1 – Prototype elements



Figure 75 - PR system N° 1 – Assembled prototype

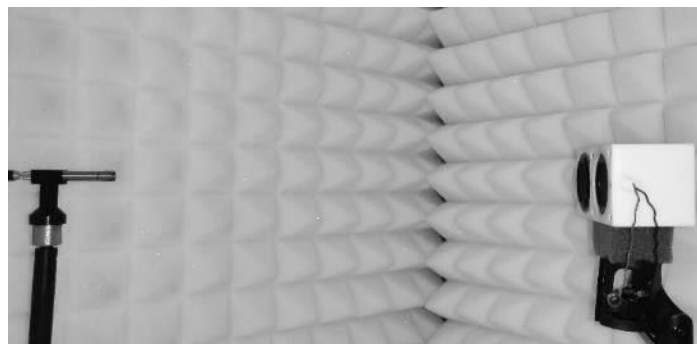


Figure 76 - PR system N° 1 – Measurement setup

On the next page, the comparison for the electric impedance is illustrated on Figure 77, and the one for the SPL at 1 u_{RMS} is illustrated on Figure 78.

From Figure 77. we see an almost perfect correlation of the curves. The different peaks are well reproduced by the model both in value and in damping. Only the minimum of impedance between the peaks is less well recreated.

From Figure 78, besides a non-perfect free field for the measurement, the curve generated by the model well follows the measurement tendency. Only the damping at the notch might have been underestimated by the model.

From these observations, we conclude on the validity of our model regarding the behavior of the prototype.

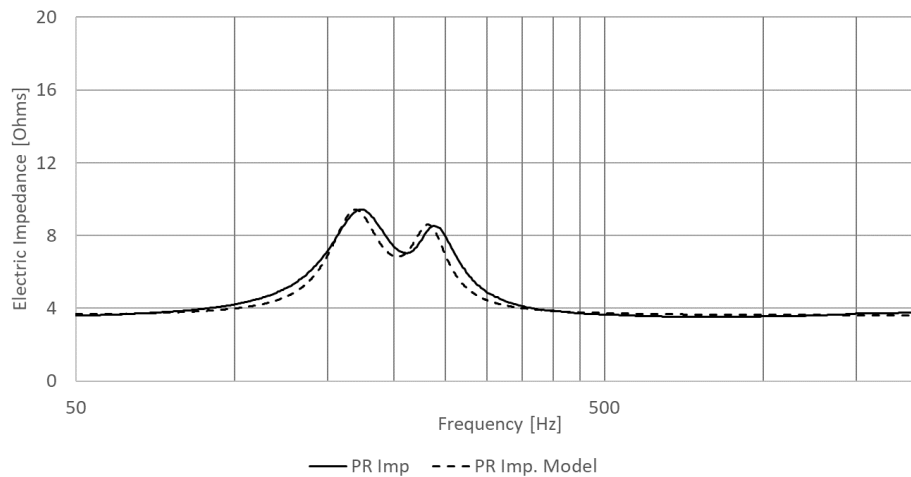


Figure 77 – PR system N ° 1 – Electric impedance comparison: Measurement / Simulation

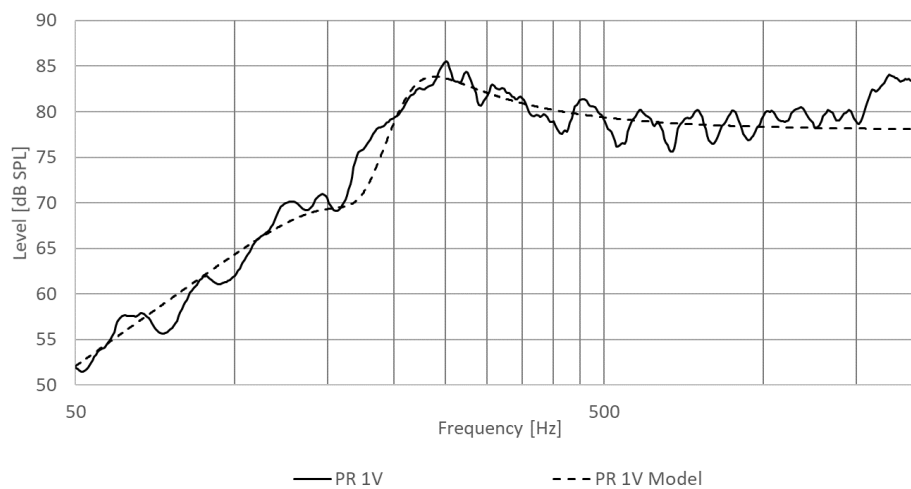


Figure 78 - PR system N ° 1 – SPL comparison: Measurement / Simulation

Tuning of the system

As previously introduced, this section will discuss the adjustment of the PE f_s , for extending the LF response. And as mentioned also, this adjustment will consist of increasing the value of Mar. But to determine the optimal value, we decide to rely on the method described in the part “4. Optimization” of [13]. The procedure described in this section consists of resolving an integral function (F) from the sealed SPL to the tuned PR SPL, and thus between two arbitrary defined frequencies. The formula for this integral is given here below:

$$F = \int_{f_1}^{f_2} [SPL_{PR}(f) - SPL_{Sealed}(f)] df$$

By then comparing the result for different M_{AR} values, we are so able to status on the optimal configuration for getting the heaviest and largest LF extension.

To proceed, the first evaluation to do is to theoretically estimate from what M_{AR} value the PR solution starts to extend the LF response, instead of degrading it.

Proceeding by step of $0.5x M_{AR}$, Figure 79 compares the simulated SPL for the sealed enclosure against different scenarios for the PR system.

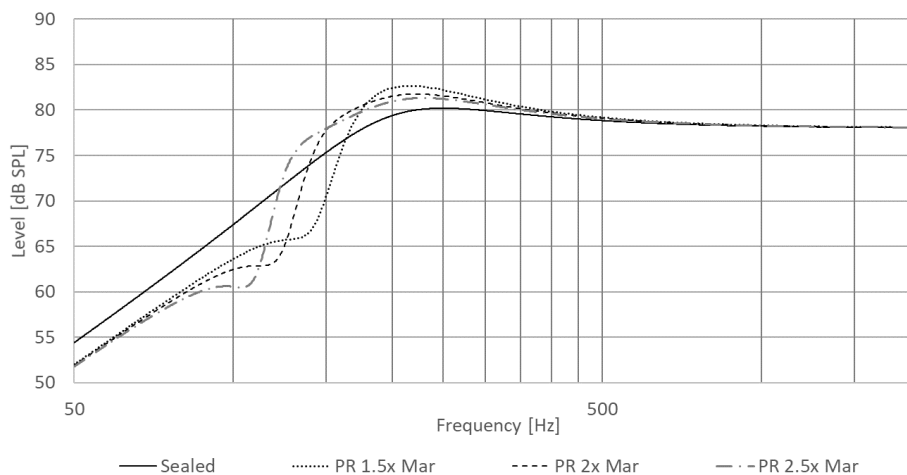


Figure 79 - PR system N° 1 – Simulated SPLs for determining the minimum mass to add

From this Figure, we define relevant to solve the integral function only from $M_{AR}' \geq 2.5x M_{AR}$. On the other hand, as predicted on page 43 we observe that the simulated extension for this value is not flat at all. Therefore, understanding that this improvement method should give a smaller LF extension than a BR system, we decide to continue our investigations by considering

a dynamic of 10 dB (instead of 3 dB for the BR) to define the two frequencies between which we intend to solve the integral function. The reason for this choice is that 10 dB corresponds to a loudness perceived as half as loud for a human.

Starting again from 1000 Hz on the sealed enclosure curve, the -10 dB point is found at about 100 Hz. Therefore, the integral will be solved for SPLs between 100 and 1000 Hz.

The Table VII and Figure 80 respectively illustrate the integral results and the curves for $2.5x M_{AR} \leq M_{AR}' \leq 4.5x M_{AR}$.

Table VII - PR system N ° 1 – F function integral result for different added masses

PR configuration	Value for the function F, with $f_1 = 100$ Hz and $f_2 = 1000$ Hz
$M_{AR}' = 2.5x M_{AR}$	257
$M_{AR}' = 3x M_{AR}$	577
$M_{AR}' = 3.5x M_{AR}$	792
$M_{AR}' = 4x M_{AR}$	775
$M_{AR}' = 4.5x M_{AR}$	667

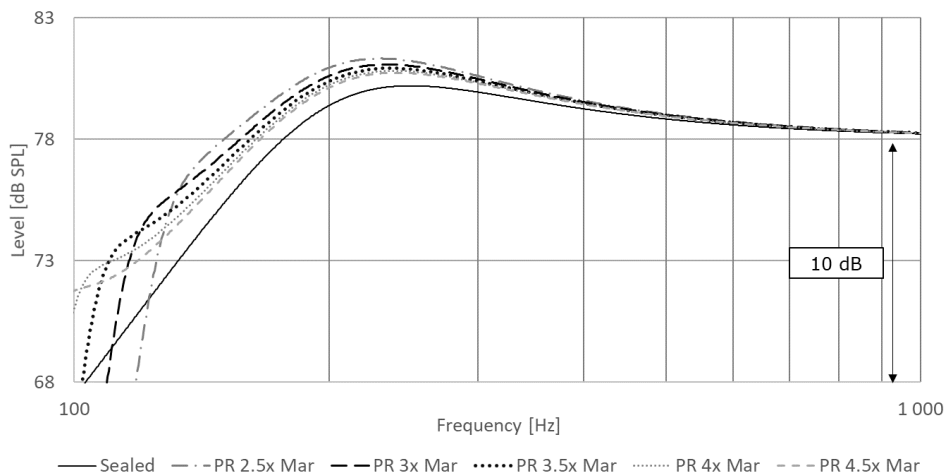


Figure 80 – PR system N ° 1 – Simulated SPLs for different added masses

After analyzing these predictions, we observe from both the results of the integrals and the shape of the curves that the optimal configuration must be given for $M_{AR}' = 3.5x M_{AR}$

Prototype customization

Now we have determined the optimal M_{AR}' term in our system, we need to find the corresponding amount of mass to add on the PE diaphragm.

From the page 15, we know that M_{AR}' is linked to M_{MR}' by the constant value of S_D^2 . To avoid calculation errors due to rounding, we directly rely on the term M_{MR} which comes from a direct measurement and transpose $M_{MR}' = 3.5x M_{MR}$.

From the page 16 we learned that the mass M_{MD}' of the moving part for the PE can be found from the formula $M_{MD}' = M_{MR}' - 2[\frac{8}{3}\rho_0 r^3]$. Following this relationship, it would give:

- $M_{MD} = 1.83$ g
- $M_{MD}' = 3.5x M_{MD} = 6.40$ g, and the mass to add = $6.40 - 1.83 = 4.57$ g
- Trying to verify this theoretical value for M_{MD} by weighing the moving part from another sample of this PE (as shown in Figure 81 and Table VIII), we found a mass approximately equal to half of the calculated value, or $M_{MD} = 1.83 / 2 = 0.915$ g

Because both the scale used is well calibrated and the above calculation remains theoretical, we therefore decide to rely on the measured value and consider the mass to add to be = 2.290 g.

Table VIII - PR system N ° 1 – M_{MD} weighing

	M_{MD} [g]
#1	0.912
#2	0,910
#3	0.908
#4	0.908
#5	0.909
Average	0.909



Figure 81 - PR system N ° 1 – PE moving mass weighing

To constitute this mass, Figures 82 and 83 illustrate that we choose to extract the diaphragm from another sample of the PE, below which we apply some mastic, both to reach the right value of mass and for being able to stick this whole additional part onto the PE.

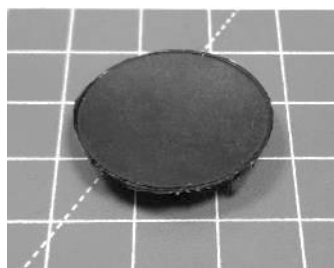


Figure 82 - PR system N ° 1 – PE additional radiating element



Figure 83 - PR system N ° 1 – PE additional radiating element weighed down

Five measurements over the scale are performed to confirm its weight (reported on Table IX), and the additional part is then mounted over the prototype as per illustrated on Figure 84

Table IX - PR system N ° 1 – additional mass weighing

	Additional Mass [g]
#1	2.287
#2	2.289
#3	2.288
#4	2.287
#5	2.290
Average	2.288



Figure 84 - PR system N ° 1 – Tuned prototype

Prototype qualification

As for the BR system, we first quantify the improvement realized by the tuned PR design prior to compare measurements against predictions. The setup for this qualification remains the same as the one for the initial system verification (Figure 65). On the next page, Figure 85 compares the SPL for the tuned design against the sealed enclosure, at 1 u_{RMS} .

A first observation is that the LF extension is much less significant than for the BR system. However, we can still quantify a frequency improvement by looking at the 75 dB SPL point: for the sealed enclosure this point is at 140 Hz, while for the PR solution it is extended to 120 Hz. From a global point of view which also takes the dB amplification into account, we doubt that this improvement can be perceived when listening to this design.

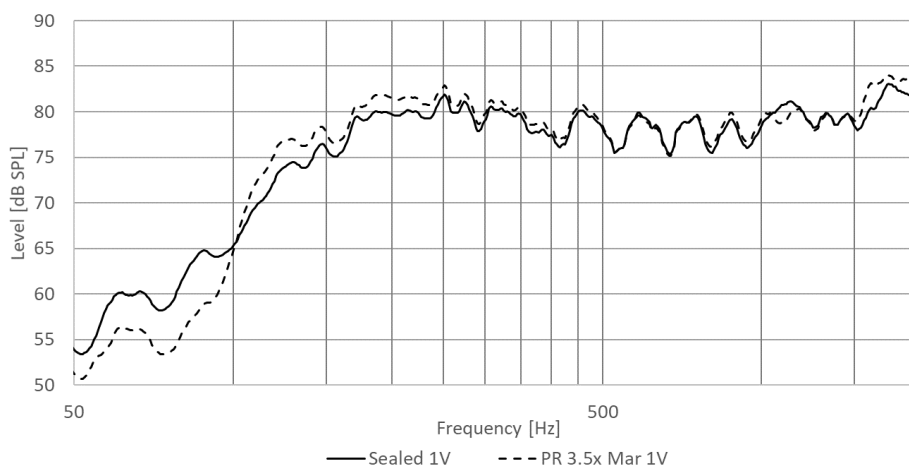


Figure 85 – Tuned PR system N ° 1 – Measured SPL comparison: PR / Sealed

Figure 86 compares the normalized SPL from the PR design at the three considered voltages. Remaining on a zoomed dynamic of -20 to $+20$ dB, we see a perfect match of the three curves, and therefore simply conclude that our system remains linear within the defined voltage range.

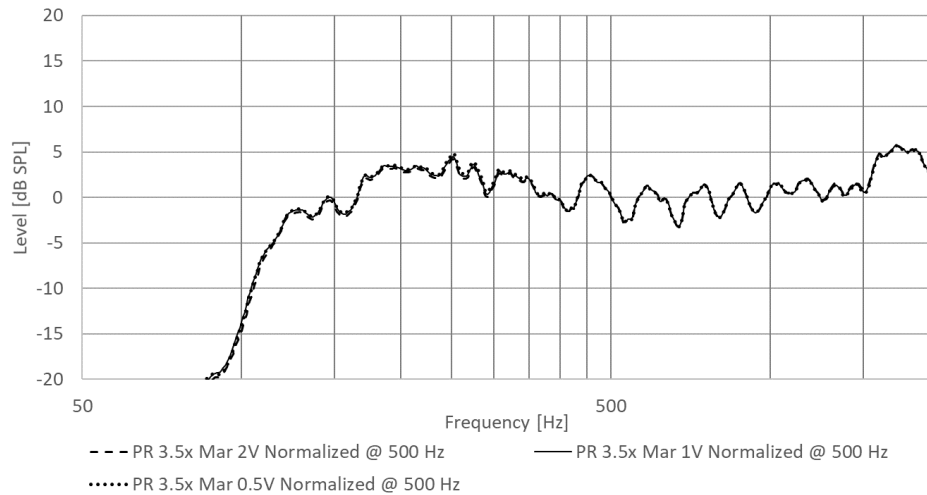


Figure 86 - Tuned PR system N° 1 – Measured SPL comparison for the 3 voltages

Comparison of measurements against predictions

Figure 87 compares the electric impedance of the system, while Figure 88 compares the SPL at $1 u_{RMS}$. As explained in [38], the form of the impedance curve is identical to the one of a Bass-Reflex system. Therefore, we expect to get on the curve the three key frequencies f_L , f_M and f_H which describe the same phenomenon than for a BR system (the mass term in the resonance f_M being the moving mass of the PE). Analyzing the curve on Figure 87, we can see a perfect match between measured and predicted values for the frequencies. Only the damping at f_L is a bit underestimated by the model. We so conclude that our model perfectly approaches mechanical behavior of the system. From the SPL curves illustrated on Figure 88 also, we see our model perfectly recreating the measurement tendency. As for the electric impedance, the damping at the notch is underestimated but we globally get a good correlation of the curves.

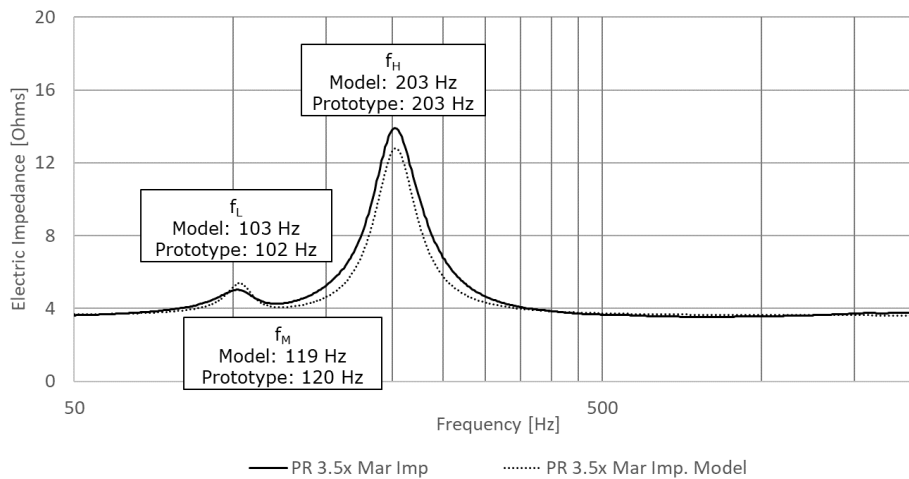


Figure 87 - Tuned PR system N° 1 – Electric impedance comparison: Measurement / Simulation

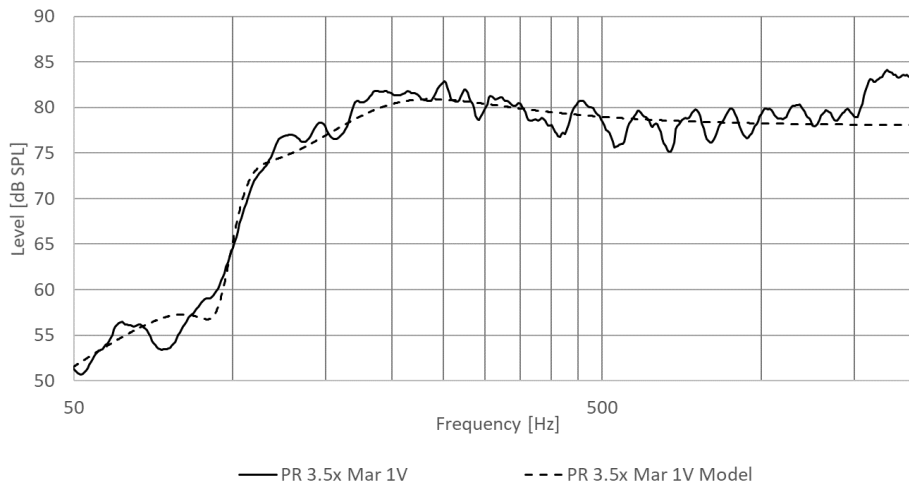


Figure 88 - Tuned PR system N° 1 – SPL comparison: Measurement / Simulation

Conclusion

Unlike the Bass-Reflex design, we conclude that we well approach the mechanical and acoustical behavior of this Passive Radiator design. However, we understand that using a speaker as passive element instead of a diaphragm is not optimized regarding the range of compliance values. Indeed, with a calculated δ ratio of 0.4, we can only achieve non-flat alignments with small extensions. In the end, even if we know that with equivalent systems, a Passive-Radiator is less efficient than a Bass-Reflex [39], we could continue the investigations by developing a PE specifically on this subject, as this design is very popular in the market. But that would require acquiring the necessary measurement capabilities, as per described in Appendix D.

III.III. Improvement method N ° 3 (Active Equalization)

As introduced in the part II.II, we intend to follow the technique used in [23], but with designing only one 2nd order active high-pass filter (HPF). However, both because we do not have the capabilities to achieve this filter in the analog domain and because we have seen from part I.II the tendency of the market to use audio processors, we intend to configure this HPF in the digital domain, on a processor as popular as those from Analog Devices.

Presentation of the audio processor

The component selected for our investigations is the codec ADAU1772 integrating an audio processing engine. Its functional diagram reported in Appendix E embeds analog-to-digital converters (and vice versa) so that users can easily deal with the analog chain of a speaker system.

This hardware solution comes with a graphical programming software called SigmaStudio. Its interface allows to connect graphics blocks together to design the signal flow and route it to the various available input and output ports. From the software libraries, the section “General 2nd Order” delivers a variety of filter algorithms among which we can find a HPF showing a transfer function identical to the elementary filters used for the network designed in [23]: $H(s) = \frac{1}{s^2 + \frac{s}{Q} + 1}$, where s is the complex frequency and Q is the filter quality factor [40].

Illustrated in Figure 89, the software menu for the settings of this HPF features:

- A field for entering the center frequency f_{HPF}
- A field for setting the quality factor Q
- A field for setting an output gain (in dB)

This last parameter acting on the global output gain (as per shown by the example in Figure 90) our intention is to let this parameter set to “0”. And so similarly to [23], we target to only amplify the signal around the center frequency by means of the Q factor.

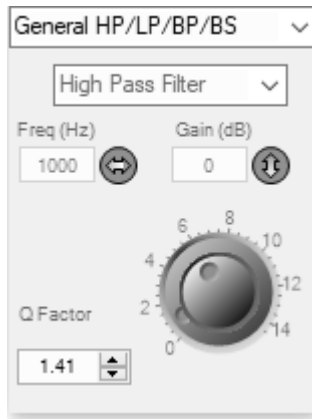


Figure 89 – Menu Settings for the SigmaStudio 2nd order HPF

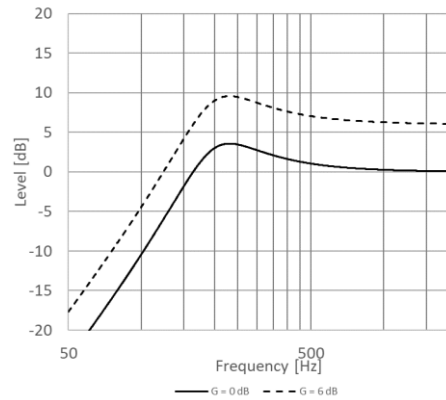


Figure 90 – Impact of the Gain parameter on the SigmaStudio HPF for $f=200$ Hz; $Q=1.41$; $G=0$ and 6 dB

Setup of the network for the prediction

As per illustrated on Figure 91, the analogous circuit used for the prediction is the one of a sealed speaker enclosure, except that we replace the voltage generator p_g by a voltage-dependent voltage source receiving the equalized signal at its input. Following a short research, we found that the elementary filter used in [23] follows the Sallen-Key topology and is composed as per illustrated on Figure 92 (with the voltage output measured between two resistors for cancelling the gain function).

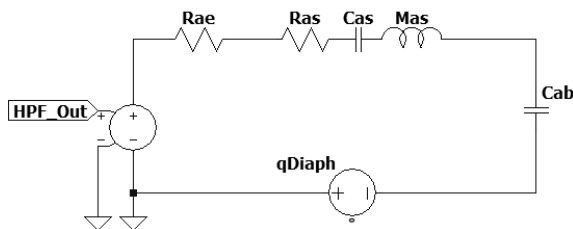


Figure 91 - Active EQ N° 1 – Analogous circuit

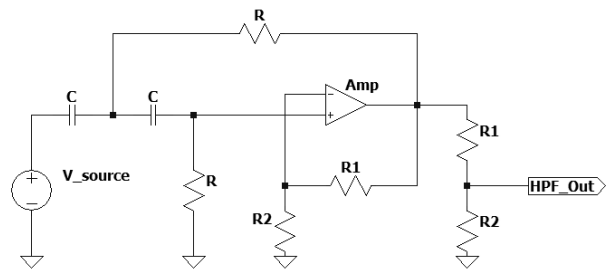


Figure 92 - Active EQ N° 1 – HPF circuit

From this last figure, the values for the components are defined as below:

- R arbitrary set to 1
- $R_2 = \frac{R}{2} = 0.5$
- $R_1 = R_2 * \left[\left(\frac{3Q-1}{Q} \right) - 1 \right]$
- $C = \frac{1}{2\pi R f_{HPF}}$

In this configuration, we can drive the network by only setting a value for value for Q and f_{HPF} .

Acoustic prediction

Without programmed function from the processor to monitor the speaker behavior and set a upper limit for Q, we propose to rely on two parameters. The first one being x_{max} , the maximum possible peak excursion for the speaker diaphragm, already mentioned = 3.5 mm on page 30. A way to predict the diaphragm displacement is to work with the original speaker model involving both the electrical and mechanical domains additionally to the acoustical one ([25]: Chapter 3: Part IX). As illustrated on Figure 93, by regenerating the predicted acoustic flow toward the mechanical domain, we can get the velocity at the diaphragm point, which once integrated through a capacitor leads to a value representative of the diaphragm displacement.

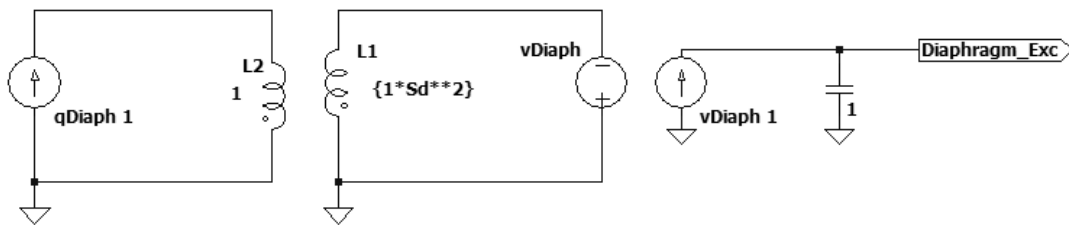


Figure 93 – Active EQ N ° 1 – Additional loop for computing the speaker diaphragm excursion

The second parameter of interest is I_{max} , the maximum peak current consumable by the speaker before damaging it. This data being unknown from the speaker manufacturer, we propose to check the theoretical fusing current of a wire identical both in diameter and in material to the one used in the speaker voice coil. Considering a copper wire of diameter = 0.13 mm, the found value is around 3.6 A.

For sure, our intention is to stay far below this theoretical limit which could (if not correctly estimated) seriously damage the speaker. To proceed, we decide to investigate this equalization solution with two parallel scenarios:

- One design in which we rule on a maximum current in the center frequency region corresponding to twice the current in the mid-frequency band,
- An alternative design in which we allow the current in the center frequency region to correspond to three times the current in the mid-frequency band.

The prediction of the current consumption is realized using the same reversed circuit than for the displacement, and by simply computing the current in the electric loop illustrated in Figure 94.

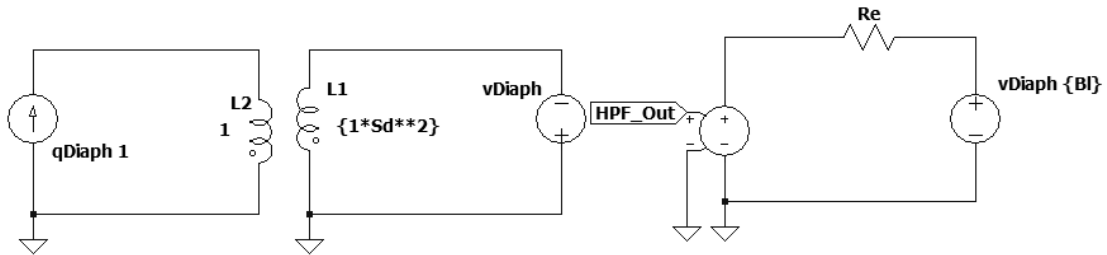


Figure 94 - Active EQ N ° 1 – Additional loop for computing the current consumption

From these defined limits, Figures 95 and 96 respectively illustrate the simulated diaphragm excursion and current consumption for $2 u_{RMS}$ input, which is the highest voltage under study, and for two proposed sets of values:

- Equalization (EQ) N ° 1: $Q = 2.2$ and $f_{HPF} = 110$ Hz (current increased by 2x at f)
- Equalization (EQ) N ° 2: $Q = 3.5$ and $f_{HPF} = 95$ Hz (current increased by 3x at f)

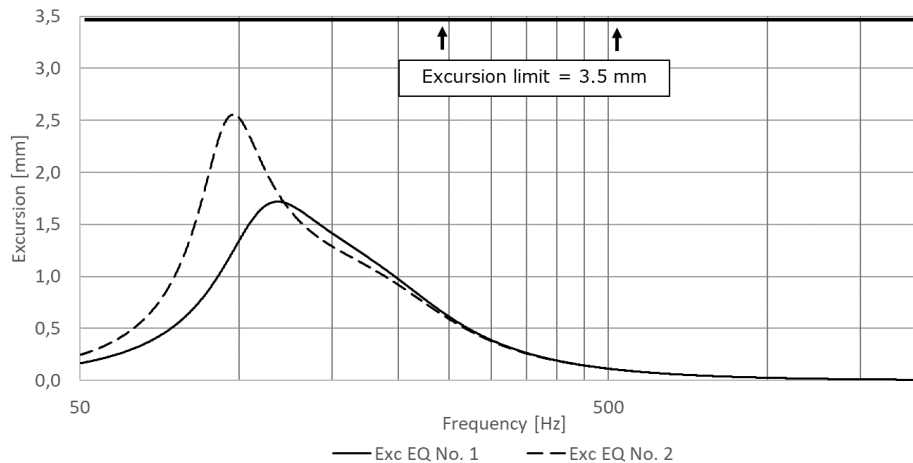


Figure 95 - Active EQ N ° 1 – simulated diaphragm excursion for EQs N ° 1 and 2

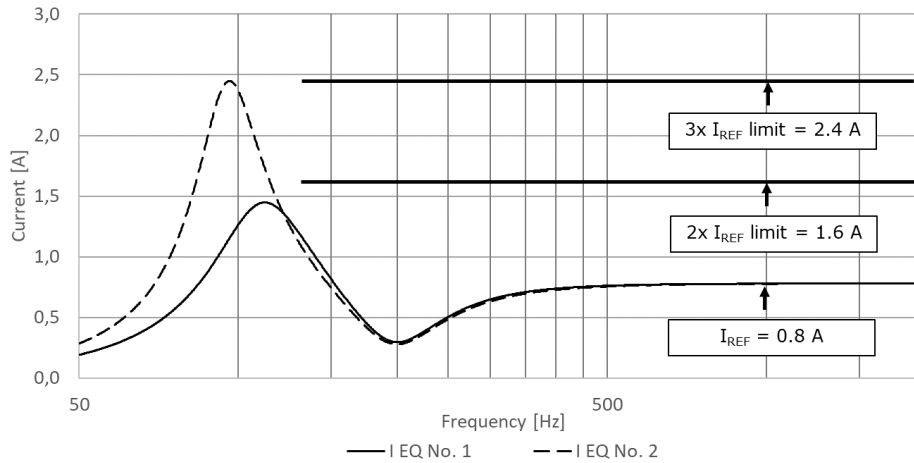


Figure 96 - Active EQ N° 1 – simulated current consumption for EQs N° 1 and 2

From the previous graphs, we confirm to remain under the excursion limit of 3.5 mm in both scenarios for which the defined current limit is reached at each of the HPF frequency. Finally, predicted SPLs at 1 u_{RMS} are compared on Figure 97 to the sealed solution. A first observation is that this EQ technique alone does not make it possible to achieve a flat extension. Also, it is not surprising to see the EQ N° 2 extending the response lower in frequencies (LFRO estimated at 75 Hz), but we observe the two scenarios to be equivalent in the range 120 – 200 Hz.

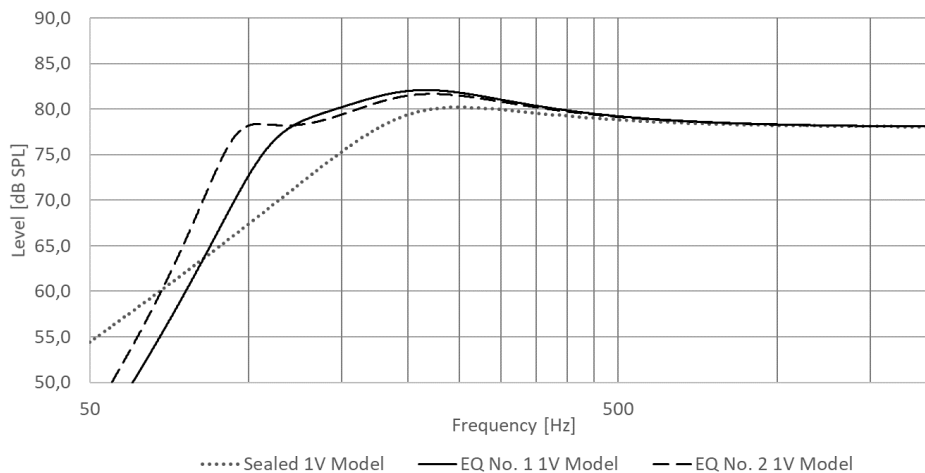


Figure 97 - Active EQ N° 1 – simulated SPL comparison: EQs N° 1 and 2 / sealed

Acoustic qualification

The audio processor comes already integrated on an evaluation board and ready to program. The audio chain for the measurement is built as per reported in Appendix F. The acoustic

environment as well as the location of the enclosure remains identical to the measurement performed in part II.

Figure 98 reports measured SPLs at 1 u_{RMS} while Figures 99 and 100 on the next page respectively summarize the SPL behavior according to the voltage input. As predicted by the models, the two solutions identically extend the LF response until about 120 Hz. Below this frequency, the EQ N ° 2 continues to amplify the sound but with a LFRO observed at 105 Hz, which is above the predicted value (75 Hz). We therefore understand that we may have reached a limit in the speaker behavior with respect to the energy injected.

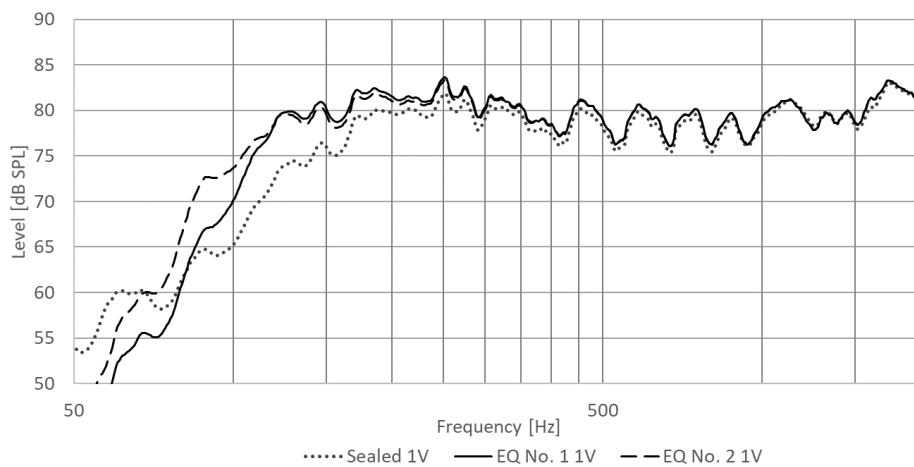


Figure 98 - Active EQ N ° 1 - Measured SPL comparison: EQs N ° 1 and 2 / sealed

When looking at the SPL behavior according to the voltage input, we observe for both solutions a decrease of SPL at 2 u_{RMS} , in the range 75-150 Hz. However, the EQ N ° 2 showing a marked variation at both at 1 and 2 u_{RMS} , we suspect this second solution to strongly behave in a nonlinear manner. A way to detect that we reach a limit of linearity in our system is by evaluating the Total amount of Harmonic Distortion (THD). This parameter, expressed in %, is defined as the ratio between all the harmonic components of a signal and the overall signal itself.

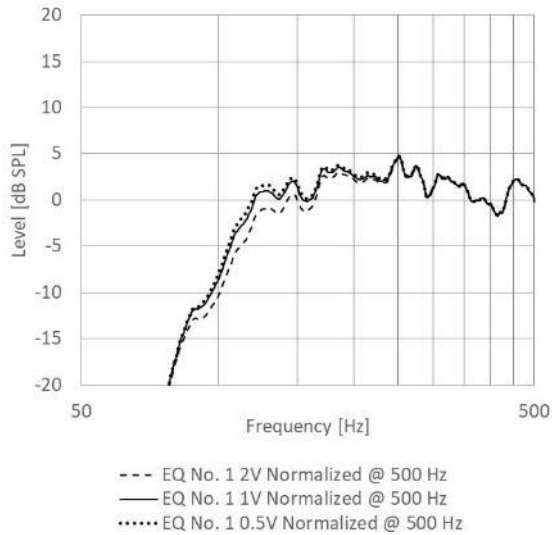


Figure 99 - Active EQ N° 1 - SPL comparison for the EQ N° 1 over the 3 voltages

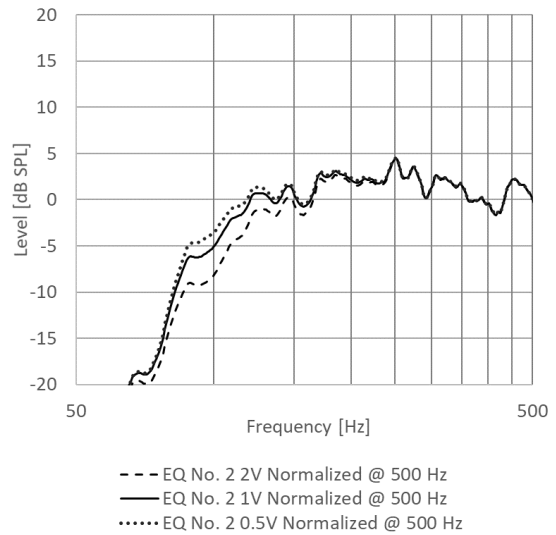


Figure 100 - Active EQ N° 1 - SPL comparison for the EQ N° 2 over the 3 voltages

Figure 101 reports this parameter for the sealed and equalized solutions as well as for the Bass-Reflex solutions in reference, all at $2 u_{RMS}$. An immediate observation is the large amount of distortion measured for the EQ N° 2, around its center frequency. Therefore, even if the distortion measured for scenario N° 1 is not negligible neither, we decide to retain only this solution for the rest of our investigations.

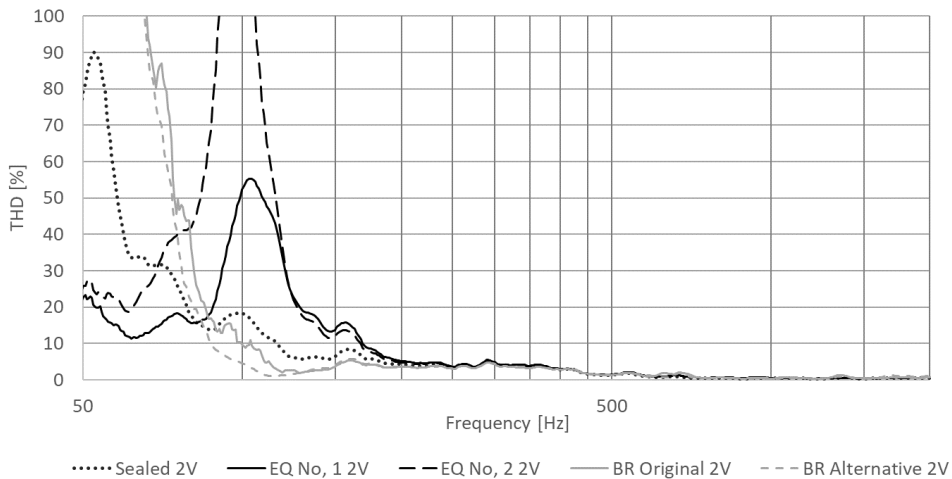


Figure 101 - Active EQ N° 1 - Measured distortion comparison at $2 u_{RMS}$: Sealed / EQs / BRs

Comparison of measurements against predictions

In accordance with our previous conclusion, Figure 102 compares predicted and measured SPLs at 1 u_{RMS} , and for the scenario N ° 1 only. From this comparison we quickly conclude on a perfect match of the curves, and that we can entirely rely on the model for designing equalizations.

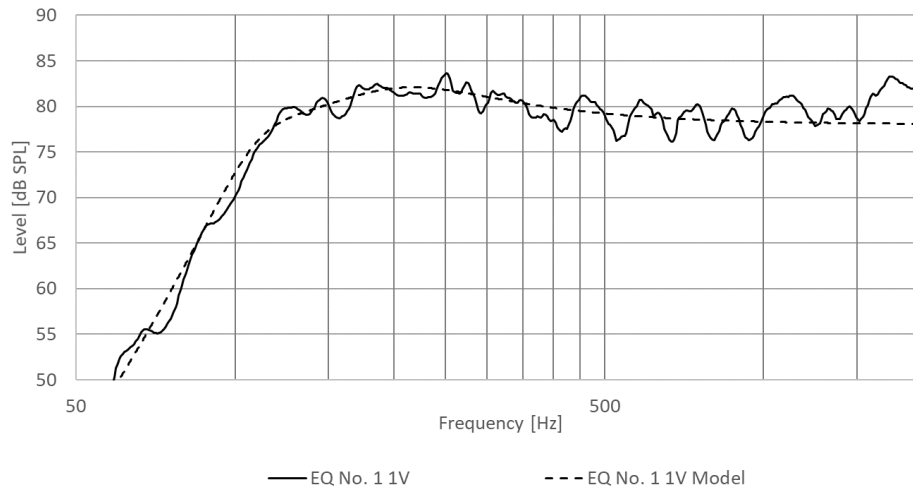


Figure 102 - Active EQ N ° 1 - SPL comparison for the EQ N ° 1: Measurement / Simulation

Figure 103 compares predicted and measured current consumptions, for the scenario N ° 1 at maximum input voltage. Besides a good correlation of the curves, we observe the prototype to consume a bit less of current than what predicted by the model. About the difference observed in high frequencies, we explain this by the fact that our model does not contain any inductance term. But about the difference on the rest of the band, we assume a phenomenon related to the increase of the voice coil resistance, with both the temperature and the energy it receives.

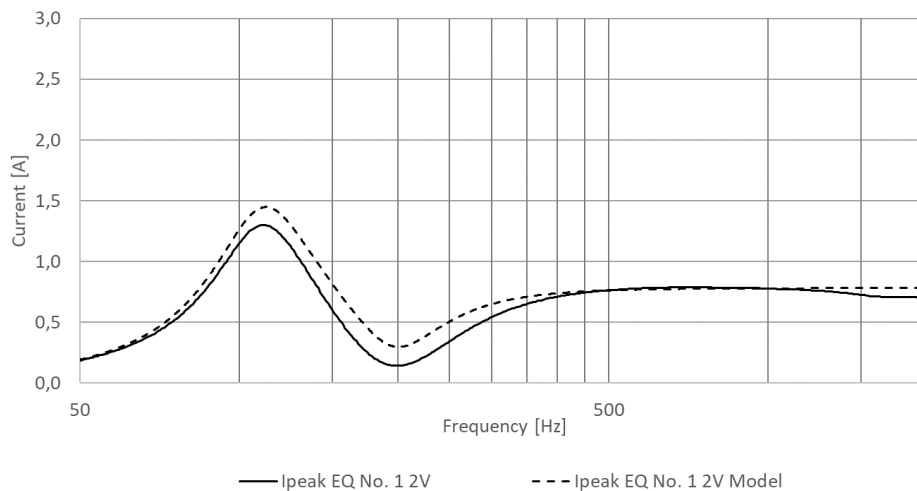


Figure 103 - Active EQ N ° 1 – Current consumption comparison for the EQ N ° 1: Measurement / Simulation

Conclusion

As for the Passive Radiator design, we conclude that we well approach the behavior of this solution. And by showing large LF extensions, this design could be a good alternative to Bass-Reflex designs. However, depending on the filter network configuration, we learned that non-linearities can quickly appear with increasing energy. This first results in a distorted sound of the solution, but also leads to a risk of damaging the speaker itself and therefore reducing its lifetime. Additionally, the increase in current consumption caused by this design remains important to consider in the context of battery-operated applications.

In the end, a solution which monitors the current consumption in real-time to activate / deactivate the equalizer according to the required energy to deliver could be a good way to deal with such a design.

III.IV. Perceptual evaluation of each of the improvement

As introduced in part II.IV, the objective of this section is to discuss the results of the listening tests carried out for each of the improvements, and thus to correlate the subjective perception of LF with the performed measurements. Also, this section intends to analyze the link between the LF sensation and the global sound preference.

However, as discussed in the PR section, although we master the system behavior, the use of a speaker as PE does not really improve the LF response. We so decided not to select this improvement for tests.

Inspired from [30], a square matrix is built (Table X) with each of the improvements to test as inputs. The different pairs come from the intersections, and a row reading determines a test direction while a column reading determines the reverse direction. In addition to these pairs, we submitted the original BR port to compare against the horn port. But for this additional test, we only asked subjects to freely speak with no questions about LF and preferences.

Finally, as described in the test protocol, the pairs order is randomly set for each subject, so that hearing fatigue does not occur at the same time.

Table X – Listening test N ° 1 – Matrix of improvements to test

	Sealed	EQ	BR (Horn port)	JBL Go 3
Sealed		X	X	X
EQ	X		X	X
BR (Horn port)	X	X		X
JBL Go 3	X	X	X	

Subjects seated at approximately 70 cm from the speaker enclosures hidden by a tissue. The SPL measured in this condition, and for a music type signal is = 70 dB SPL (global L_{eq} over 15 seconds of music extract). This value giving 77 dB SPL when recalculated at 30 cm, we understand this energy to be close to our sinusoidal measurements performed at $1 u_{RMS}$. We will therefore consider these measurements for the comparisons.

Music extracts presentation

As defined in the protocol, we played two extracts of 15 seconds each per half of combinations to be submitted. The first comes from the jazz song "It Ain't Necessarily So" by artist Jamie Cullum. The second is from the pop song "Billie Jean" by artist Michael Jackson.

Spectra of these extracts are compared in Figure 104.

A first observation is that the global energy repartition looks similar to the shape of a pink noise. Indeed, relying on articles like the one written by E. Bazil [41], mixing a song with a pink noise spectrum as target would “sounds naturally ‘balanced’.”. Also, by showing 5 dB more in LF and 10 dB more in HF, the extract from Michael Jackson seems to bring more energy overall. The two sound samples are equivalent in the mid frequency range.

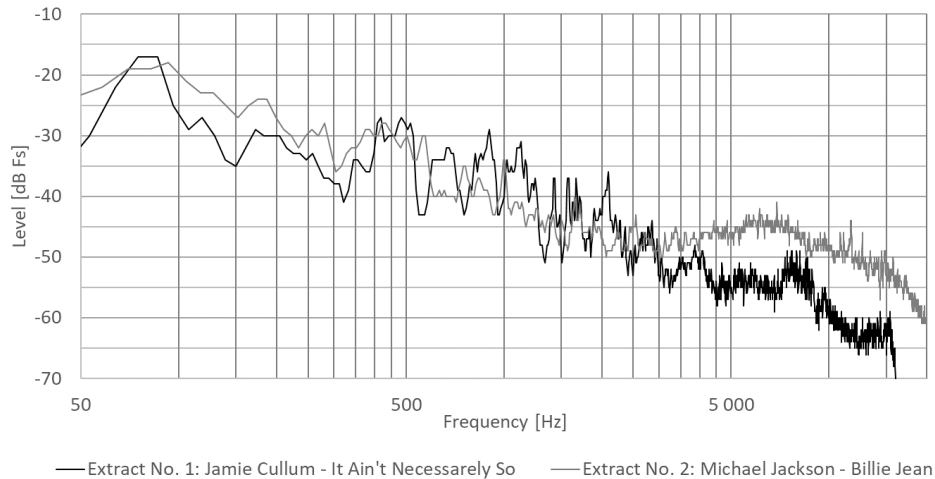


Figure 104 – Listening test N ° 1 – Music spectra comparison

Comparison of the improvements against the sealed solution

A first analysis is to compare the two improvements we selected against the performance of the original sealed enclosure. Figure 105 illustrates two curves which respectively result from the subtractions $BR_{SPL} - Sealed_{SPL}$ and $EQ_{SPL} - Sealed_{SPL}$. In this way we can better visualize the LF improvement created by each of the two systems.

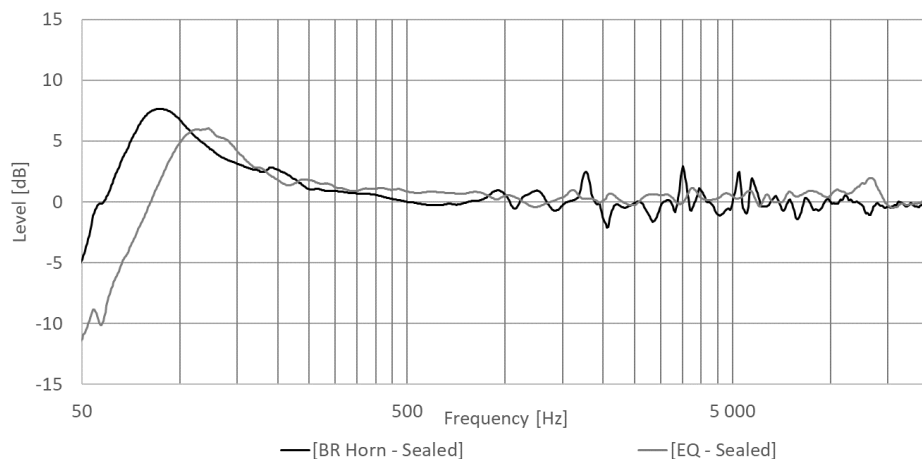


Figure 105 – Listening test N ° 1 – SPL comparison: Improvements / Sealed

The Table XI summarizes the test results (in percentage) for the questions on the LF attribution and on the preference.

Table XII reports collected words which was pronounced more than one time over all the comparisons. By looking first at the LF attribution, we remark from the averaged values that for both pairs a large majority of subjects attributed more LF to the improvements. This correlates well with what we measured and so confirm the success of our developments.

Looking then at the preferences, a large majority voted for the improvements as well. Considering so the words collected, we can verify if the reason for preference is driven by the LF extension. Table basically split in two categories: words which more refer to a positive qualification, and those which more refer to a negative qualification. Among the descriptors used, we observe that the expression “more powerful” was pronounced 7x times in regards with the BR system. However, from Figure 105, the only gain of energy we see is in the LF region. We therefore conclude on a feeling which might be related to this LF improvement.

On the EQ solution side, the positive word “wider” was pronounced 2x times against a feeling of “dry”, “closed” and “noisy” sound for the sealed solution in comparison. Here also, the word “wider” used for the EQ against the word “closed” used for the sealed solution might relates to the LF improvement from the EQ, as only this region is amplified by the solution.

Finally, for both solutions we conclude on preferences which are related to the LF extension they provide.

Table XI – Listening test N ° 1 – Comparison Improvements / Sealed: Answers to LF and preference questions

	LF Attribution			Preference		
	Sealed	EQ	No attr.	Sealed	EQ	No pref.
<i>Sealed → EQ</i>	10%	90%	0%	10%	90%	0%
<i>EQ → Sealed</i>	0%	80%	20%	10%	70%	20%
<i>(Sealed ↔ EQ) Average</i>	5%	85%	10%	10%	80%	10%
	Sealed	BR	No attr.	Sealed	BR	No pref.
<i>Sealed → BR</i>	10%	90%	0%	20%	80%	0%
<i>BR → Sealed</i>	20%	70%	10%	20%	70%	10%
<i>(Sealed ↔ BR) Average</i>	15%	80%	5%	20%	75%	5%

Table XII – Listening test N ° 1 – Comparison Improvements / Sealed: Collected words

	LF Attribution	Preference	More balanced	Wider	Clearer	More Powerful	Muffled	Dry	Closed	Noisy
<i>(Sealed ↔ EQ): Sealed</i>	5%	10%			1x			2x	1x	2x
<i>(Sealed ↔ EQ): EQ</i>	85%	80%		2x	1x	1x				
<i>(Sealed ↔ BR): Sealed</i>	15%	20%	2x				2x		2x	1x
<i>(Sealed ↔ BR): BR</i>	80%	75%	2x		1x	7x	1x			1x

Comparison between the improvements

Figure 106 illustrates the subtractions $BR_{SPL} - EQ_{SPL}$, so that we can see how much the BR solution extend the LF region compared to the EQ one.

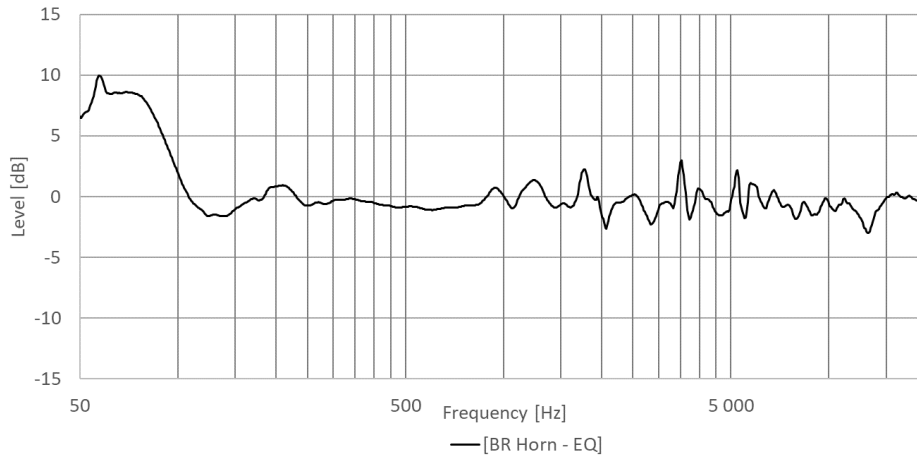


Figure 106 – Listening test N ° 1 – SPL comparison between improvements

From the Table XIII we see that the BR system is preferred at 50 % while only 30 % of the subjects attribute more LF to it. Unlike the previous comparisons, the collected words will this time help us to better understand the reason for the preference.

Table XIII – Listening test N ° 1 – Comparison between improvements: Answers to LF and preference questions

	LF Attribution			Preference		
	EQ	BR	No attr.	EQ	BR	No pref.
<i>EQ → BR</i>	30%	30%	40%	40%	50%	10%
<i>BR → EQ</i>	40%	30%	30%	30%	50%	20%
<i>Average</i>	35%	30%	35%	35%	50%	15%

Table XIV on the next page classifies the words in the same way as for the previous section. From these collected words, we notice the expression "more powerful" pronounced 4x times as well as the word "deeper" pronounced 2x times, both with respect to the BR solution. As discussed in the previous section, these feelings could relate to the LF amplification created by the BR system. However, with the expressions "more balanced" and "clearer" pronounced 4x and 2x times in favor of EQ, we understand that if the LFs are amplified too much, it can lead to a feeling of speaker system wrongly balanced.

But that does not explain why the BR system is preferred over the EQ one. An explanation for this maybe that the BR is perceived twice as "more precise". It is possible that this latter

sensation describes artifacts introduced by the processor into the EQ solution, making the sound reproduction less precise than that of the BR. But in this context, an SPL curve is not sufficient to try to explain this feeling.

Table XIV– Listening test N ° 1 – Comparison between improvements: Collected words

	LF Attribution	Preference	More accurate	More balanced	Clearer	More powerful	Deeper	Less reactive	Limited	Muffled	Distorted	Noisy
(EQ ↔ BR): EQ	35%	35%		4x	2x				1x	1x	1x	
(EQ ↔ BR): BR	30%	50%	2x	1x	1x	4x	2x	1x			1x	1x

Comparisons against a solution from the market

As both introduced in part II.IV and in the beginning of this section, the Bluetooth speaker JBL Go 3 was part of the listening tests, mainly for evaluating the improvements from this study against a solution (equivalent in size) from the market.

Figure 107 reports about normalized SPLs at 500 Hz for all the systems, while the Table XV on the next page summarizes all the answers for the LF and preference questions.

A quick observation from the SPL graph is that the LF performance of the JBL Go 3 is quite similar to the one of our improvements, except for the peak around enclosures resonance, where the JBL brings a flatter response.

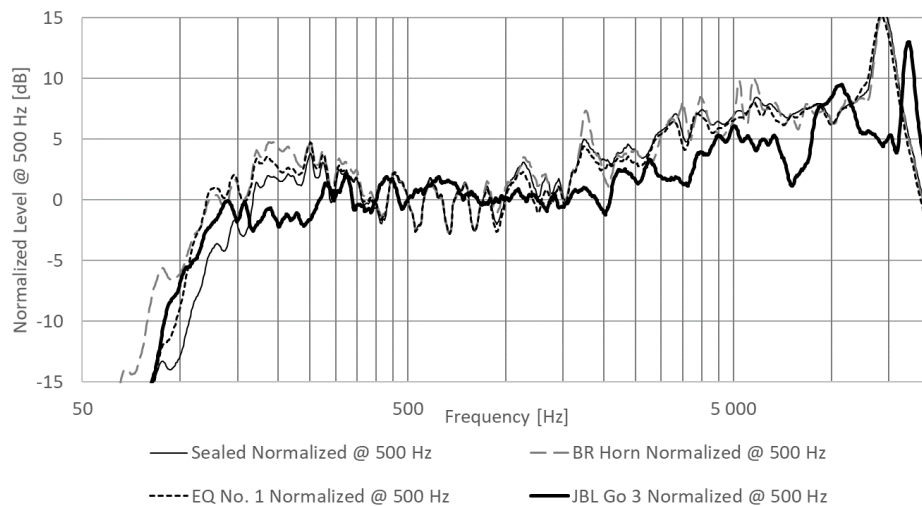


Figure 107 – Listening test N ° 1 – SPL comparison: Improvements / Sealed / JBL Go 3

By analyzing the average percentages for the LF attribution, we see that the JBL is seen to provide more bass except when compared to the BR system, for which an equality of performance is found. Looking more in detail between the two directions of test: the subjects attribute more LF to the JBL (60%) for the direction BR → JBL, while they attribute more LF to the BR (also 60%) for the other direction: JBL → BR.

Table XV – Listening test N ° 1 – Comparisons against a market solution: Answers to LF and preference questions

	LF Attribution			Preference		
	Sealed	JBL	No attr.	Sealed	JBL	No pref.
<i>Sealed → JBL</i>	10%	80%	10%	50%	50%	0%
<i>JBL → Sealed</i>	0%	90%	10%	30%	70%	0%
<i>(Sealed ↔ JBL) Average</i>	5%	85%	10%	40%	60%	0%
	EQ	JBL	No attr.	EQ	JBL	No pref.
<i>EQ → JBL</i>	30%	70%	0%	40%	60%	0%
<i>JBL → EQ</i>	50%	40%	10%	60%	40%	0%
<i>(EQ ↔ JBL) Average</i>	40%	55%	5%	50%	50%	0%
	BR	JBL	No attr.	BR	JBL	No pref.
<i>BR → JBL</i>	30%	60%	10%	90%	0%	10%
<i>JBL → BR</i>	60%	30%	10%	60%	30%	10%
<i>(BR ↔ JBL) Average</i>	45%	45%	10%	75%	15%	10%

This observation is interesting to analyze, both because the two solutions do not really perform differently in LF, and because listening to the two solutions during the test is spaced a few seconds apart, it could reveal a bias induced by the auditory memory.

One method to overcome this bias would be to immediately switch from speaker A to speaker B (and vice versa) during continuous playback.

Also, the JBL spectral response being flatter, it is possible that the overall sound balance benefits the JBL for LF attribution.

From the results on the preference, we can discuss the three cases separately. Table XIV summarizes the words collected for all comparisons.

Firstly, the JBL compared to the sealed enclosure is preferred at 60%. Considering the percentage for the LF attribution, it would make sense for the preference to correlate with this parameter. Indeed, by using the term "more powerful" again, we understand that the subjects refer to the improved LFs of this speaker system. But by expressing 3x times that the JBL is "more balanced", the preference could also be linked to the overall spectral balance of the sound, with a system amplifying less HF compared to LF.

An equality is found in the preference between the EQ solution and the JBL. However, the latter system is perceived 7x times as "muffled" against an EQ perceived 5x times as "clearer". But in the end, it seems the subjects noticed that the EQ produces some distortion. This therefore answers our question of whether the distortion measured previously was going to be perceived when listening.

Finally, when our BR solution is compared to the JBL, 75% prefer the BR system. With 4x times the word “muffled” pronounced for the JBL against the word “clearer” pronounced for the BR, it confirms that the overall sound balance counts for a lot in the preference. However, we notice here again that the expression “more powerful” is used 5x times to describe the sound signature BR.

As an aside, it is interesting to note that the JBL is perceived twice as "less reactive" than the BR system. As we know that the JBL Go 3 contains a PR system, it is possible that this feeling refers to a well-known property of PRs in the industry: a poor restitution of the transient response [39]

Table XVI – Listening test N ° 1 – Comparisons against a market solution: Collected words

	LF Attribution	Preference	More balanced	Clearer	Closer	More accurate	More powerful	Warm	Round	Realistic	Wider	Closed	Distorted	Muffled	Less Reactive	Noisy
<i>(Sealed ↔ JBL): Sealed</i>	5%	40%	2x	2x								1x	1x	2x		2x
<i>(Sealed ↔ JBL): JBL</i>	85%	60%	3x	1x			2x		1x			1x		2x		1x
<i>(EQ ↔ JBL): EQ</i>	40%	50%	2x	5x	1x	1x	2x				2x		5x			1x
<i>(EQ ↔ JBL): JBL</i>	55%	50%	1x	1x			1x	1x			1x		2x	7x		
<i>(BR ↔ JBL): BR</i>	45%	75%	1x	4x	1x	1x	5x			2x	2x					
<i>(BR ↔ JBL): JBL</i>	45%	15%	1x				1x	1x	1x		1x	1x	1x	4x	2x	

Additional comparison: original BR port against horn BR port

This additional comparison intends to determine whether the subjects perceive a difference in the sound created by the two port models.

To proceed, a third musical sample was selected from the song “Latch” by artist Disclosure. Figure in Appendix G shows the spectrum of this extract, which looks similar in all points to the other ones, apart a little more of energy in LF. Most importantly, this song contains frequent pronounced drum kicks compared to other extracts.

From Table XVII, we first see that half of the subjects did not perceive any difference between the two conceptions. For the other half, the horn design is perceived as "more powerful", while the original port produces a "more balanced" sound. The SPL of the two solutions being identical, it is not possible for us to comment on these feelings.

On the other hand, with a new feeling collected on the “attacks” of the drum kicks, it is possible that one of the two models reproduces the transients less well. One way to quantify this sensation is to measure the impulse response of each of the systems, at a distance equivalent to the listening point during the tests.

But unfortunately, having not a sufficiently low background noise to measure at this distance, Figure 108 proposes an evaluation of this response at ports output.

A brief observation of this graph is that the horn solution shows a little less damping on the time response than what the original port illustrates.

Therefore, although this measurement is not representative of what the subjects listened to, we still conclude on a new benefit of this alternative port solution, which better reproduces the transients of a sound.

Table XVII – Listening test N ° 1 – Additional comparison: collected words

	No difference	More balanced	More powerful	Bassy	Clearer	Better attacks
Original port		3x	2x	2x	1x	2x
Horn port		1x	5x		1x	2x
No difference	5x					

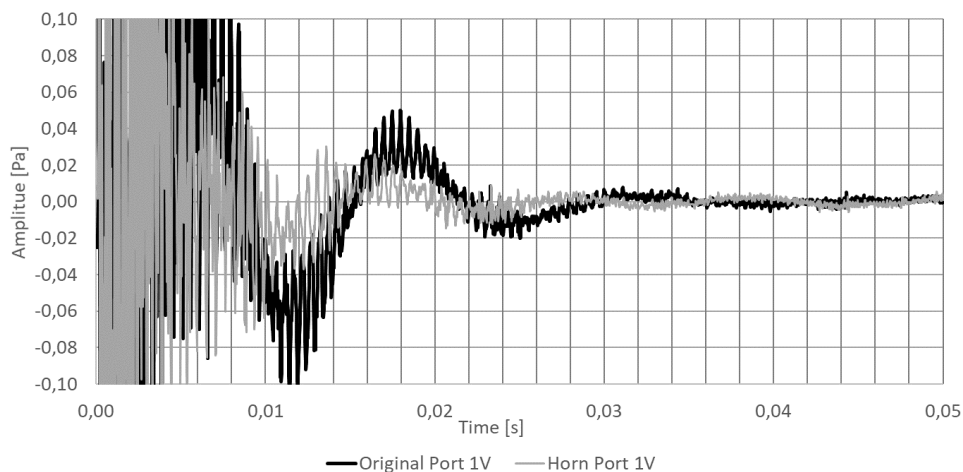


Figure 108 – Listening test N ° 1 – Impulse response comparison: Original BR port output / Horn BR port output

Conclusion

From these perceptual tests, we first learn that the improvements investigated in this study work well and are seen to provide more LF, even when this extension is not directly noticed.

Compared to the EQ solution, the BR system remains preferred and perceived to be more powerful. But from this comparison as well as comparisons with a market solution, we learn how important a sound must be well balanced to be appreciated. Indeed, although the BR and JBL solutions are judged to be almost equivalent in terms of bass, the BR remains 75% preferred for its overall sound signature. For information, by conducting these tests on a population with an age range of 20 to 55 years, we did not focus specifically on a young audience who could give more importance to the reproduction of bass.

In addition, this listening test taught us how important it is to have a good design when integrating an audio processor. Indeed, the slightest distortion resulting from too much solicitation of the speaker can be perceived by the audience, when compared to another system as efficient in LF. This reminds us of the relevance of relying on a processor allowing to monitor speaker behavior in real time, so that it remains in its linear domain.

From the side comparison performed between the two BR designs, although we cannot really conclude anything about the perceptual assessment, an additional measurement will have enabled us to learn that a horn-shaped port would help to increase system responsiveness to transients, when compared to a straight port.

Finally, we learn from this first part of investigations that a traditional Bass-Reflex design on this type of small speaker system seems to work, but also remains at today the best performance / cost ratio for Seltech, with however an attention point to be paid to potential high losses in such a small port.

Also, given the LF performance of the JBL Go 3 and market trends, we confirm the relevance for Seltech to continue developing PR solutions using a PE optimized for this purpose.

From the conclusions around this first speaker, we now propose to study again these three improvement methods around the second speaker selected in the scope of our study.

IV. Investigations around the speaker enclosure N ° 2

IV.I. Improvement method N ° 1 (Bass-Reflex)

This section follows the same method as that applied for the design around the speaker N ° 1 (part III.I). But given the small size of this second enclosure, we build a model that directly integrates potential losses into the port. The circuit for that system is illustrated on Figure 109.

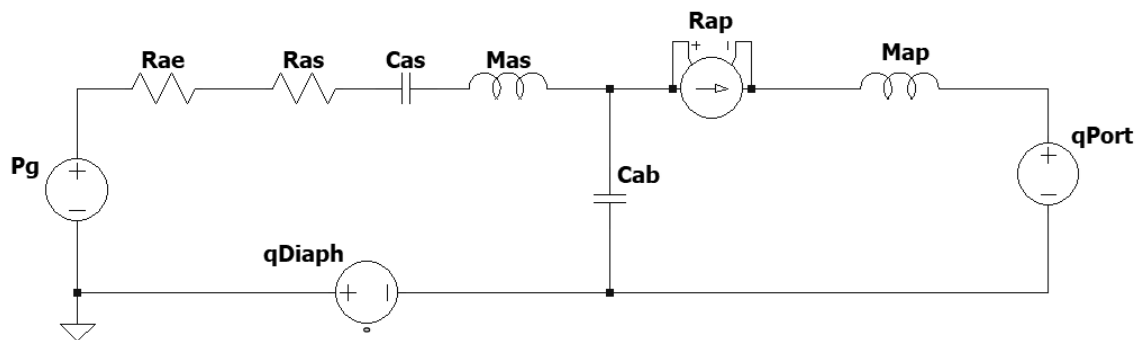


Figure 109 – Simplified acoustical circuit of a BR system

Estimation of the shape for the extension

Relying on the pages 15 and 19, we found $C_{AB} = 1.41e-11 \text{ m}^5/\text{N}$ and calculate $C_{AS} = 8.83e-12 \text{ m}^5/\text{N}$. We therefore estimate the ratio $\frac{C_{AS}}{C_{AB}} = 0.63$. Here also, the result reports an alignment close to the shape of the C_4 one (for which $\frac{C_{AS}}{C_{AB}} = 0.56$). We therefore expect to get a noticeable extension but with an irregular shape for the SPL.

Design of the port

Following the guidance in [34], and with $x_{max} = 0.25 \text{ mm}$ and a target for $f_M = 700 \text{ Hz}$ (or 50 Hz below the sealed enclosure f_B), we define the following requirements for the port:

- An area $A \geq 0.14 \text{ cm}^2$ (or a diameter $d \geq 4 \text{ mm}$)
- A length $l = 4.27 \text{ cm}$ (end corrections included)

In this design also, the proposed port respecting the condition from [34] is too long and so not technically feasible in regards with the dimensions of our system. We therefore understand that it is necessary to considerably reduce the diameter of the port for getting a reasonable length, integrable in our design. However, with a dimension range becoming noticeably small, we are reaching a technical limit about the dimensional accuracy attainable by the 3D printing technique.

To continue our investigations from this point and try to achieve a BR design for this enclosure, we decide to rely on existing tubes from the market that are manufactured using the plastic injection technique: a well-known process for mass production of plastic components, which allows great precision in view of our needs.

Figure 110 illustrates a 90-degree tube from the Aquarium market (*a tube network connector that supplies oxygen to fishes*) with an opening area $A = 0.03 \text{ cm}^2$ (2 mm of diameter) and a total length = 3.4 cm. Once shorted to 1 cm (Figure 111), the calculated resonance f_M for the tube integrated into the enclosure is = 670 Hz.

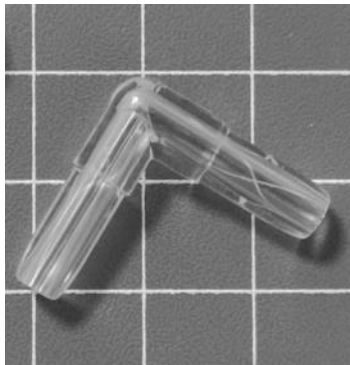


Figure 110 - BR system N ° 2 – Presentation of a tube sourced from the market

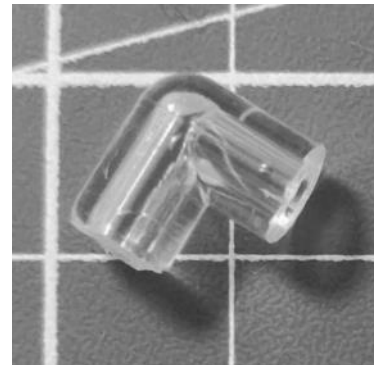


Figure 111 - BR system N ° 2 – Shortening of the tube to constitute the Port of the system

Although this extremely small port design could lead to high losses in the acoustic radiation, we decide to continue our investigation and estimate the amount of LF extension that this system could provide.

Acoustic prediction

Figure 112 on the next page illustrates the computed electric impedance for the system. From this simulation, we almost approach the previously calculated resonance by finding

$f_M = 680$ Hz. The frequency f_H is found = 960 Hz, and f_L is found = 425 Hz. We so understand that the designed system should extend the enclosure response down to about 425 Hz.

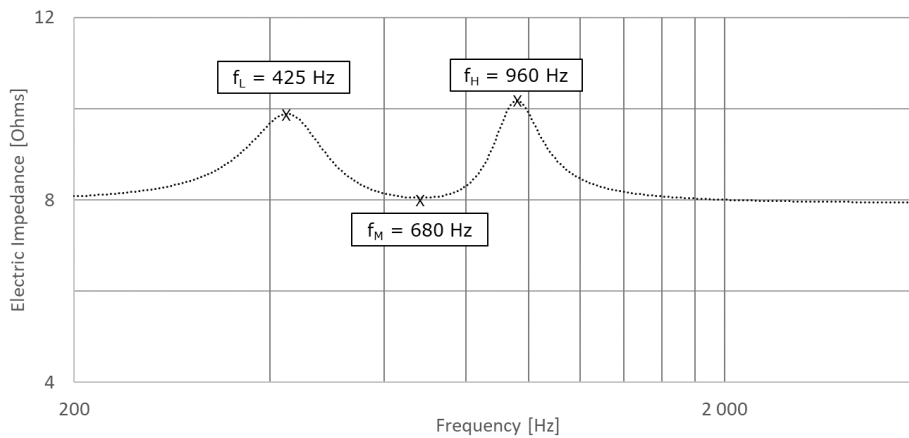


Figure 112 - BR system N ° 2 – Electric impedance simulation

Figure 113 compares simulated SPLs of the BR system against the sealed response, at 0.1 m distance and for $0.5 u_{RMS}$. While we wouldn't expect to get a flat extension, we still find a marked peak at f_H . This pronounced phenomenon is supposed to be the consequence of a very weakly damped behavior of the speaker in the enclosure. If not attenuated either by a porous material in the enclosure or by processor equalization, this peak could lead listeners to a feeling of unbalanced sound. Finally, with a LFRO around 445 Hz, we confirm the expectation of an improvement in the LF from 510 Hz to 445 Hz.

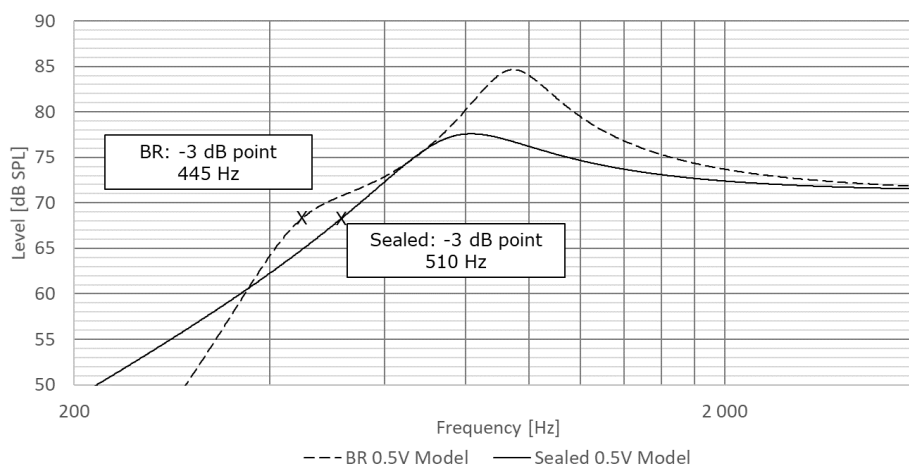


Figure 113 - BR system N ° 2 – Simulated SPL comparison: BR / Sealed

Prototype assembly and qualification

From the previous discussion, Figures 114 and 115 illustrate an enclosure identical to the sealed design, and into which a hole is drilled, and the tube is installed and fixed by means of glue.

Here also, the first step is to quantify the improvement realized by the proposed design prior to compare against prediction. The setup for the measurement is detailed on Figure 116.

Figure 117 compares the SPL for the original BR against the sealed enclosure at $0.5 u_{RMS}$. An immediate comment from the BR qualification is that we will find the predicted peak at f_H , but we do not observe any LF extension, when compared to the sealed solution.

To better understand what phenomenon is happening, we propose to compare the SPL as well as further parameters against predictions.

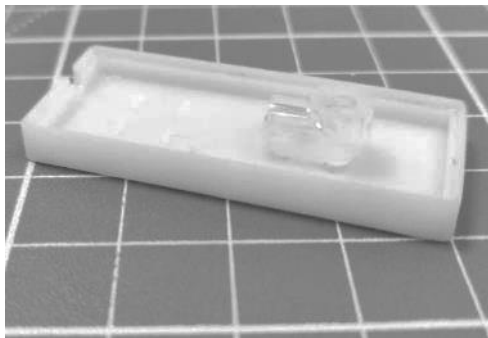


Figure 114 - BR system N ° 2 – Prototype bottom casing



Figure 115 - BR system N ° 2 – Assembled prototype

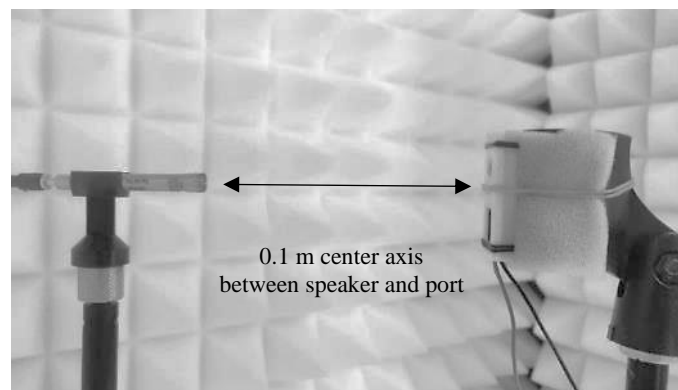


Figure 116 - BR system N ° 2 – Measurement setup

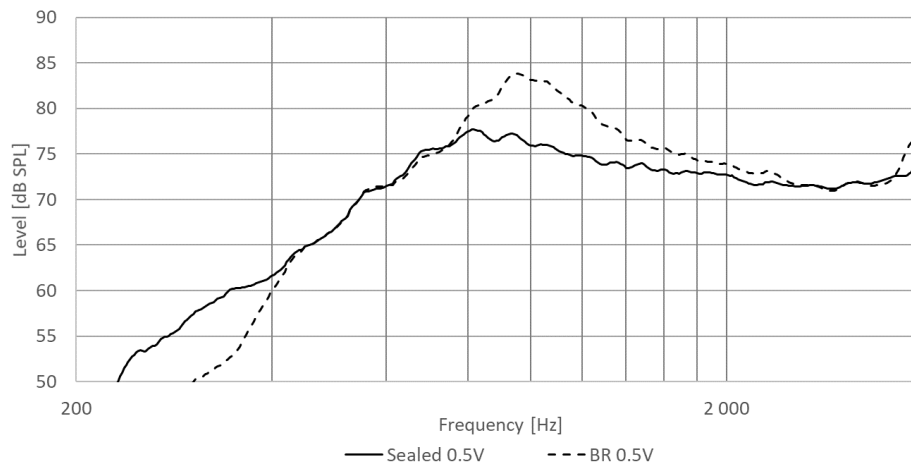


Figure 117 - BR system N ° 2 – Measured SPL comparison: BR/ Sealed

Comparison of measurements against predictions

Figures 118 and 119 respectively compare electric impedances and SPLs at 0.1 m and for 0.5 u_{RMS} . From the impedance comparison, we observe a quasi-perfect match of the curves both in values and in damping for each of the key frequencies. Only the damping at f_L is a bit underestimated by the model. However, looking at the SPL graph we first observe a small shift between predicted and measured f_H , but above all we notice that the slope below this frequency hardly changes (compared to the predicted curve), resulting in no amplification of the sound in this region. To figure out if the port radiates energy or not, an additional comparison is performed in regards with the SPL radiated at the output of the port. Figure 121 on the next page reports this comparison, with the measurement setup is illustrated on Figure 120.

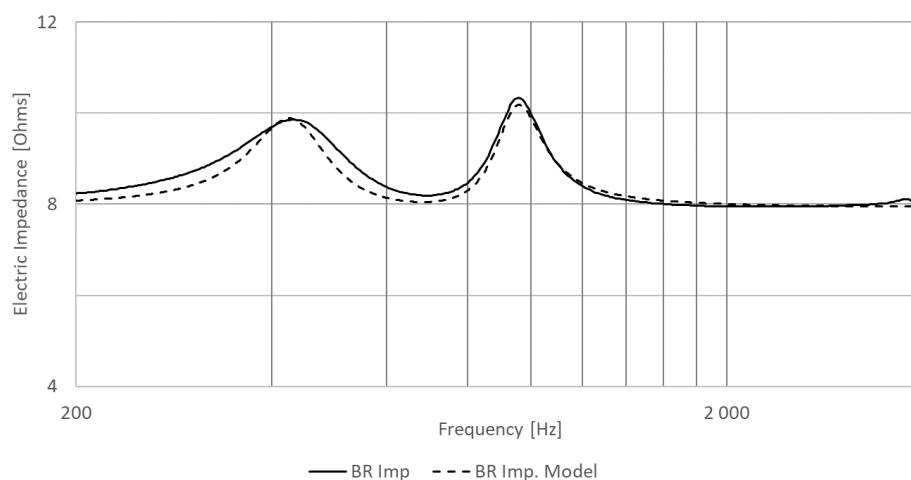


Figure 118 - BR system N ° 2 – Electric impedance comparison: Measurement / Simulation

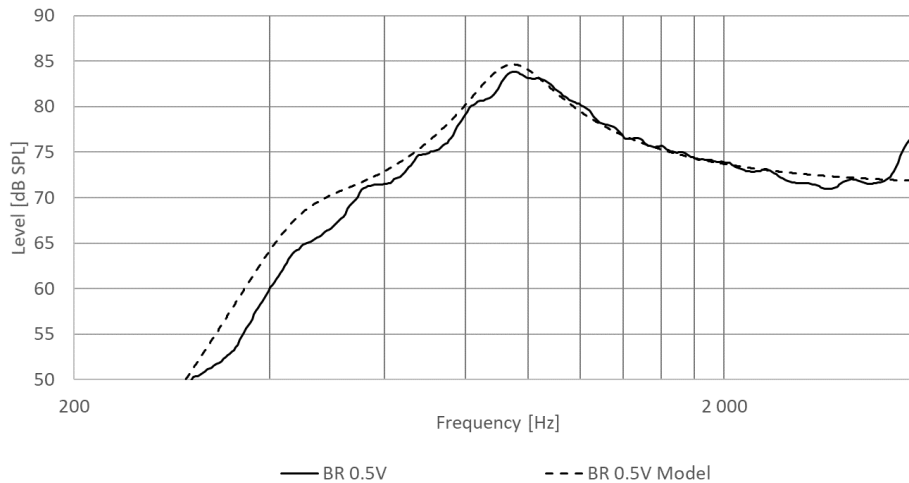


Figure 119 - BR system N ° 2 – SPL comparison: Measurement / Simulation

A first observation from the SPL graph is that the overall shape of the curve is well reproduced by the model. This confirms that the prototyped port radiates energy. But in the region around f_L , it is not surprising to observe a model that predicts a high and undamped SPL, while the measurement on the prototype shows a strongly damped curve, even causing the slope to change below f_L . From this observation, we conclude that the port seems to be functioning, but with too high losses in its acoustic radiation. The latter being probably the result of a too small opening size.



Figure 120 - BR system N ° 2 – Setup for measuring the SPL at port output

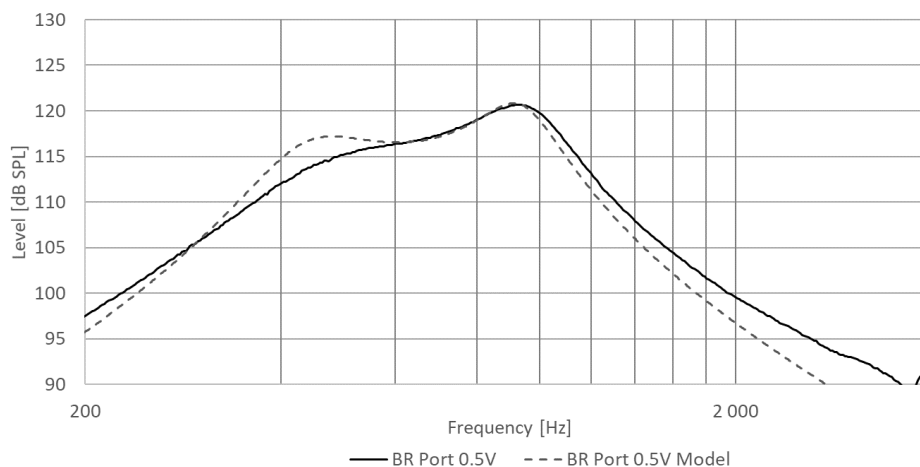


Figure 121 - BR system N ° 2 – Port output measured SPL

Conclusion

Although this first method does not bring any LF extension, we observe that we correctly approach the behavior of the system, and therefore validate a prediction method remaining valid in enclosures as small as the one considered here. In the end, as this improvement method remains very inexpensive, it could be relevant to continue our investigations but only with ports much larger than the one built here. The risk of such large ports is that it could lead to the inability to mechanically build the system. Additionally, given the low resonance damping of the enclosure, a porous material should be implemented to attenuate the peak at f_H . In the end, ratios between mechanical complexity and acoustic efficiency will have to be evaluated to decide whether this solution in such small enclosures is interesting to consider.

IV.II. Improvement method N ° 2 (Passive Radiator)

PR designs around this small enclosure are approached using the same acoustical circuit than the one built for the enclosure N ° 1. Its network reminded on Figure 122 features the three terms R_{AR} , C_{AR} , and M_{AR} that reflect the mechanical behaviour of the PE and must be properly qualified.

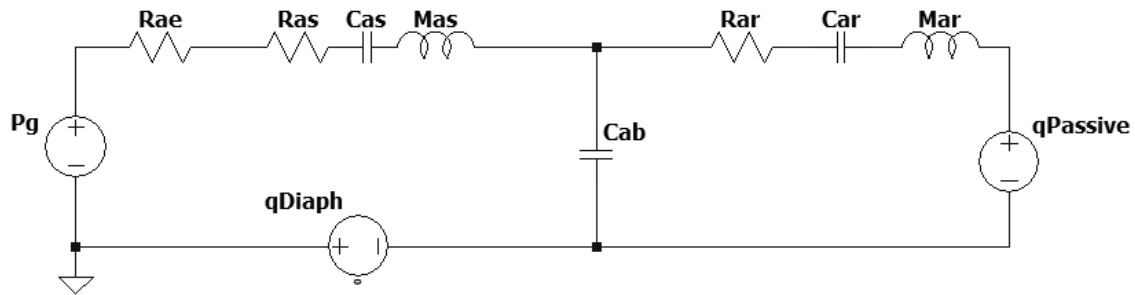


Figure 122 - PR system N ° 2 – Simplified analogous circuit for a PR system

Qualification of the passive element, and estimation of the shape for the extension

Here also, we consider a second speaker identical to the first one as PE. However, both because the related enclosure is very small and because the moving part of this type of speaker can easily be disassembled without damaging it, we decide to only integrate this last part for designing our system. Figures 123 and 124 here below illustrate the part of the speaker we consider as PE while the

Table XVIII summarizes the measured values over the transducer, prior to disassemble it.

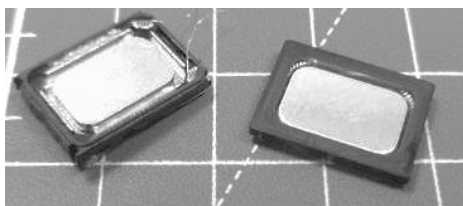


Figure 123 - PR system N ° 2 – PE presentation

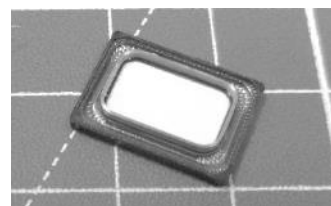


Figure 124 - PR system N ° 2 – PE bottom view

Table XVIII - PR system N ° 2 – PE qualification

Parameter	Speaker (1)	Passive element (2)	(2) – (1)	[(2) – (1)] / (1) [%]
$R_{MS/R}$ [N.s/m]	1.44e-01	1.25e-01	-1.92e-02	-13.32
$C_{MS/R}$ [m/N]	8.83e-04	1.00e-03	1.17e-04	13.20
$M_{MS/R}$ [kg]	8.04e-05	8.86e-05	8.18e-06	10.17

From the difference in percentage reported by Table, we understand the speaker used as PE to behave a bit differently (around 10 % of difference) from the original speaker, while they are supposed to be identical. This difference of behavior is assumed to reflect the variation in production of this transducer. When looking at α and δ ratios, we calculate:

$$- \quad \alpha = \frac{C_{AS}}{C_{AB}} = 0.63$$

$$- \quad \delta = \frac{C_{AR}}{C_{AB}} = 0.71$$

With almost equal ratios ($\delta \approx \alpha$), we first finally conclude on a similar behavior of the two elements when integrated into the enclosure, but we also understand that we can only achieve a non-flat and small extension.

Acoustic prediction

The circuit from Figure 122 is built, and the SPL at 0.1 m and for $0.5 u_{RMS}$ is illustrated on Figure 125. From this graphic, we observe here also that the system as it is does not improve the LF region but degrades it. As discussed in part III.II, this degradation is due to a too high PE resonance frequency.

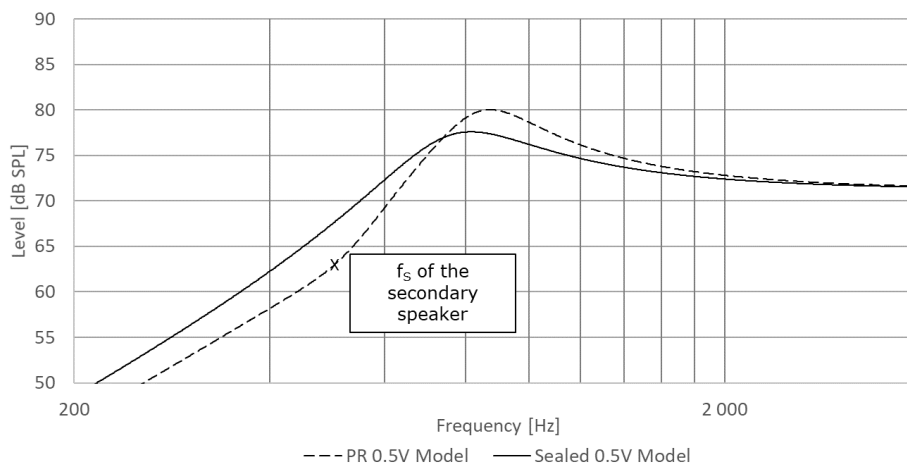


Figure 125 - PR system N ° 2 – Simulated SPL comparison: PR / Sealed

Verification of the initial prediction

The PR prototype is so built as per illustrated on Figure 126, simply with a second aperture for the PE, identical to the first one. The setup for the measurement is illustrated on Figure 127.

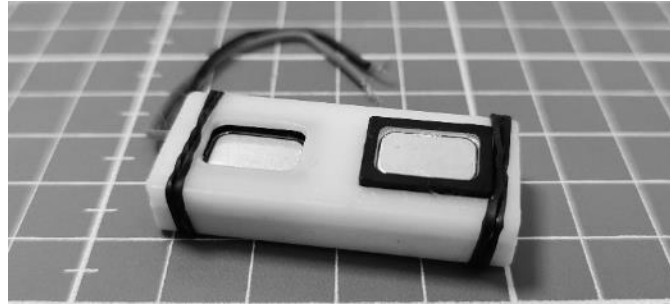


Figure 126 - PR system N ° 2 – Assembled prototype



Figure 127 - PR system N ° 2 – Measurement setup

The comparison for the electric impedance is illustrated on Figure 128, and the one for the SPL at $0.5 u_{RMS}$ is illustrated on Figure 129.

From the impedance comparison the different peaks are correctly reproduced by the model. Only a small difference on both f_L and f_H . Also, as discussed on previous cases, the global damping is a bit underestimated by the model.

We also find this underestimation on the SPL comparison: the simulated amount of energy at f_H being higher than what measured over the prototype.

Finally, we still conclude on a global validity of our model regarding the behavior of the prototype.

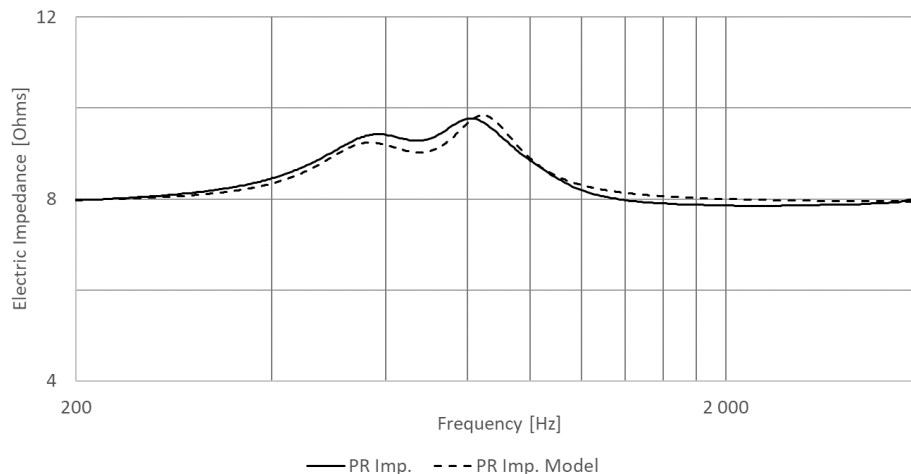


Figure 128 - PR system N ° 2 – Electric impedance comparison: Measurement / Simulation

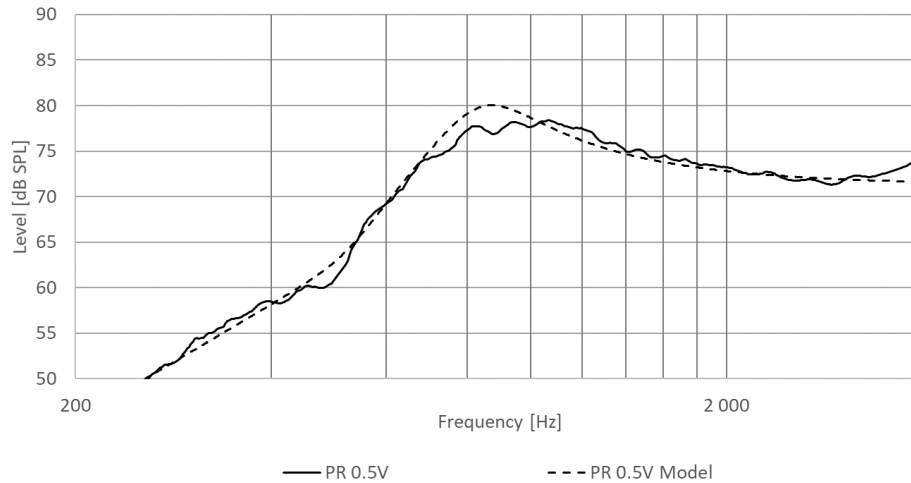


Figure 129 - PR system N ° 2 – SPL comparison: Measurement / Simulation

Tuning of the system

Still relying on the method described in [13], we intend to solve an integral function of SPLs between two defined frequencies. Starting from 4000 Hz on the sealed enclosure curve, the -10 dB point is found around 350-375 Hz. We will so solve the integral between 350 and 4000 Hz. From a first analysis, we determine $M_{AR}' \geq 2.5x M_{AR}$ for extending the LF response. The Table XIX and Figure 130 respectively report the integral results and the curves for $2.5x M_{AR} \leq M_{AR}' \leq 4x M_{AR}$.

Table XIX - PR system N ° 2 – F function integral result for different added masses

PR configuration	Value for the function F, with $f_1 = 350$ Hz and $f_2 = 4000$ Hz
$M_{AR}' = 2.5x M_{AR}$	701
$M_{AR}' = 3x M_{AR}$	835
$M_{AR}' = 3.5x M_{AR}$	794
$M_{AR}' = 4x M_{AR}$	700

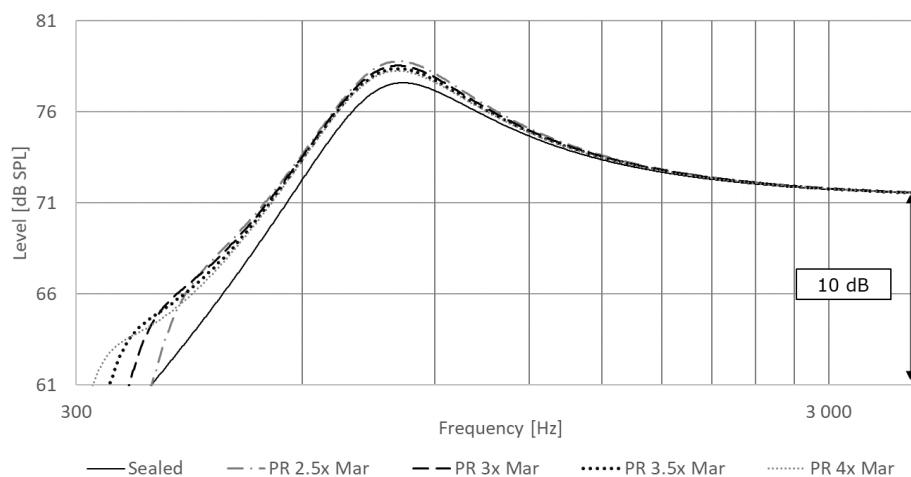


Figure 130 – PR system N ° 2 – Simulated SPLs for different added masses

From these predictions, we observe the optimal configuration to be given for $M_{AR}' = 3x M_{AR}$

Prototype customization

The procedure described on page 49 is applied to calculate M_{MD} , and the result is verified on a scale using another PE sample. After verification the considered values are:

- $M_{MD} = 87.4e-3$ g
- $M_{MD}' = 3x M_{MD} = 262.3e-3$ g, and the mass to add = approx. $175e-3$ g

To constitute this mass, Figures 131 and 132 illustrate that we choose to extract the diaphragm from another PE sample, below which we apply some mastic, both to reach the right value of mass and for being able to stick this whole additional part onto the PE.

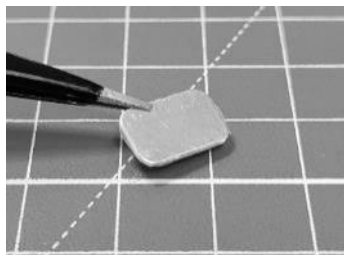


Figure 131 - PR system N ° 2 – PE additional radiating element

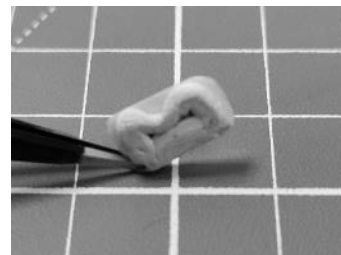


Figure 132 - PR system N ° 2 – PE additional radiating element weighed down

Five measurements over the scale are performed to confirm its weight (reported on Table XX), and the additional part is then mounted over the prototype as per illustrated on Figure 133.

Table XX - PR system N ° 2 – additional mass weighing

	Additional Mass [g]
#1	0.175
#2	0.178
#3	0.177
#4	0.178
#5	0.178
Average	0.177

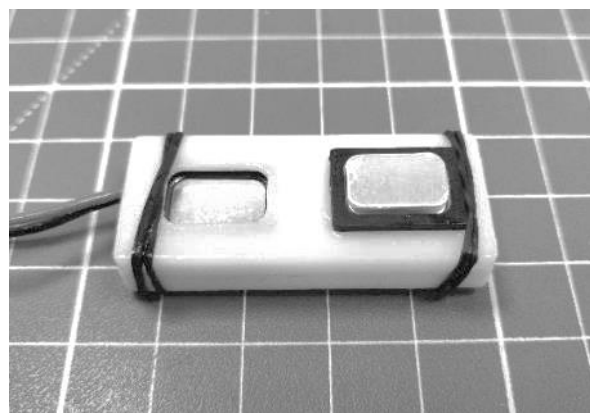


Figure 133 - PR system N ° 2 – Tuned prototype

Prototype qualification

The setup for the qualification remains the same as the one for the initial system verification (Figure 127). On the next page, Figure 134 compares the SPL for the tuned design against the sealed enclosure, at $0.5 u_{RMS}$. As discussed for the design around the speaker N ° 1, the LF extension is observed to be very small: only a few dB of amplification is seen near the 60 dB line, and in the 350-400 Hz region. Here also, the use of a speaker as PE makes it possible to study PR designs, but we doubt that this observed improvement can be perceived when listening to this solution.

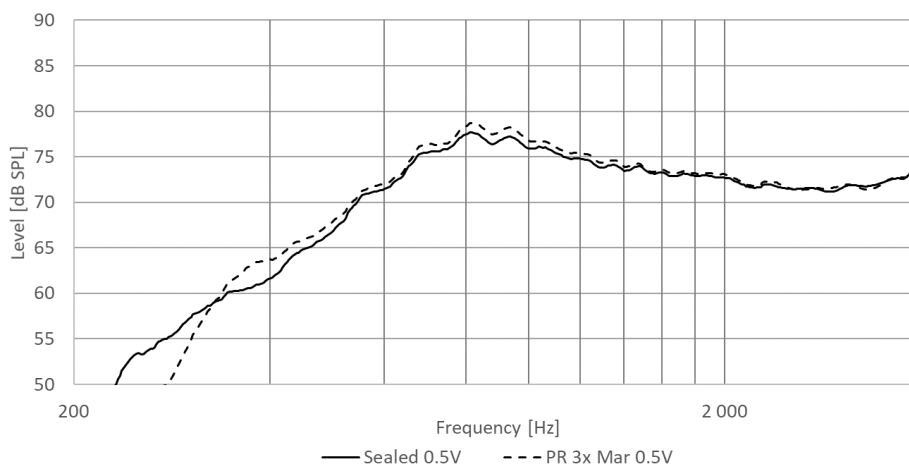


Figure 134 – Tuned PR system N ° 2 – Measured SPL comparison: PR / Sealed

Figure 135 compares the normalized SPL from the PR design at the three considered voltages. The behavior of the system remains the same except at $0.1 u_{RMS}$ input, where the radiated energy is a bit lower in the range 300-400 Hz. The comparison against predictions might help us to understand the cause of this observation.

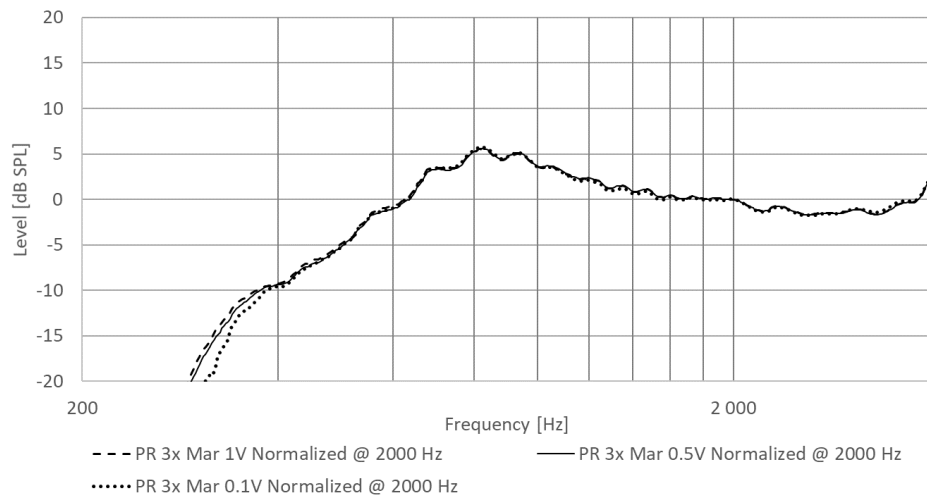


Figure 135 - Tuned PR system N ° 2 – Measured SPL comparison for the 3 voltages

Comparison of measurements against predictions

Figure 136 compares the electric impedance of the system. A first observation is that the model well recreates f_H . However, f_M is not reproduced due to an underestimation of the damping in this region, and f_L is reproduced in value only, its damping being also wrong.

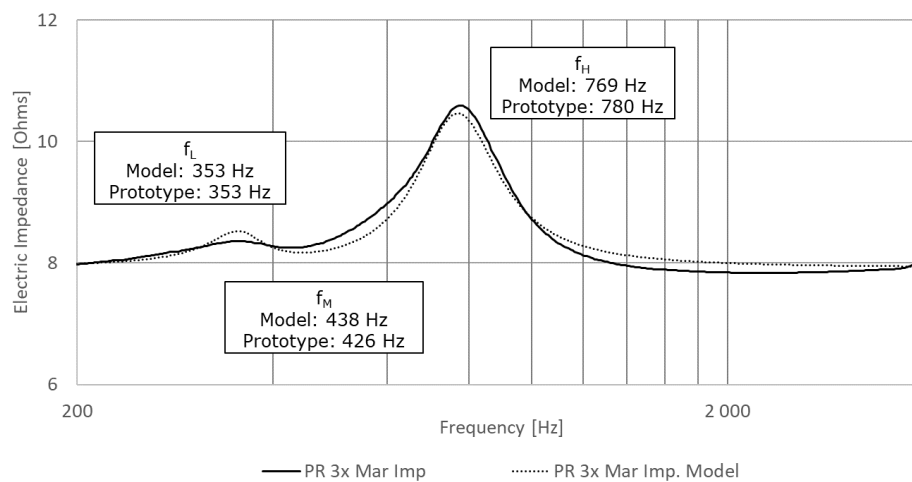


Figure 136 - Tuned PR system N ° 2 – Electric impedance comparison: Measurement / Simulation

Because of the previous observation of the non-linear behaviour over the voltage, we decide to compare the SPL both at 0.5 and 0.1 u_{RMS} . Figures 137 and 138 report these comparisons. As we see the model to better match the 0.1 u_{RMS} measurement below the LFRO region, we understand that the enclosure itself might vibrate (because of the PE motion) for voltages higher than 0.1 u_{RMS} . This observation remind us on the importance to well mechanically decouple the radiating elements from the rest of the design.

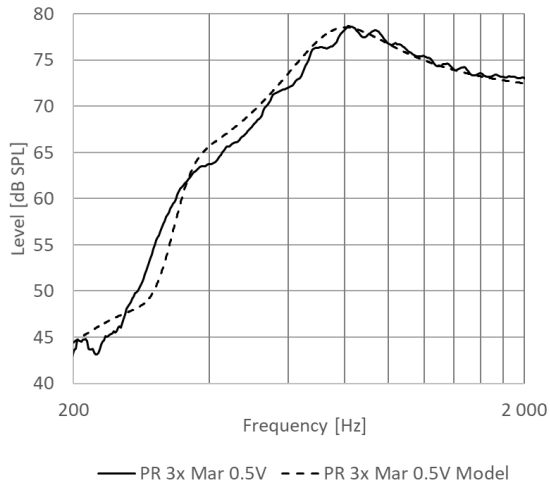


Figure 137 - Tuned PR system N ° 2 – SPL comparison at 0.5 u_{RMS} : Measurement / Simulation

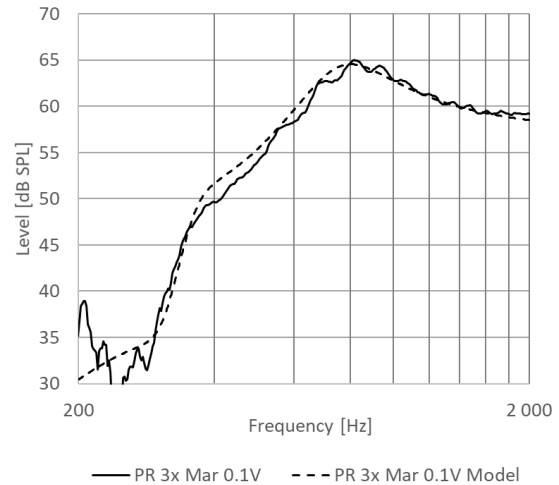


Figure 138 - Tuned PR system N ° 2 – SPL comparison at 0.1 u_{RMS} : Measurement / Simulation

Conclusion

With similar conclusions to the design around the speaker N ° 1, we confirm that we are correctly approaching the overall behavior of this Passive Radiator design. Only one point of attention is to be carried on how to integrate the PE and isolate it from the rest of the design. However, here also, using a speaker as PE instead of a diaphragm cannot lead to wide and flat LF extensions. If we want to continue our investigations around this design, we must develop a diaphragm that is both optimized in losses and in compliance. Such an element could result from joint work between Seltech and its speaker manufacturers.

IV.III. Improvement method N ° 3 (Active Equalization)

Following the technique used in [23], but with designing only one 2nd order HPF, the networks used for the prediction are respectively reminded on Figure 139 for the acoustical circuit, and on Figure 140 for the HPF. This last element is controlled by its quality factor Q and its center frequency f , as defined on page 54.

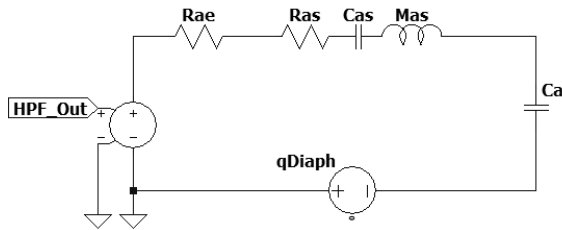


Figure 139 - Active EQ N ° 2 – Analogous circuit

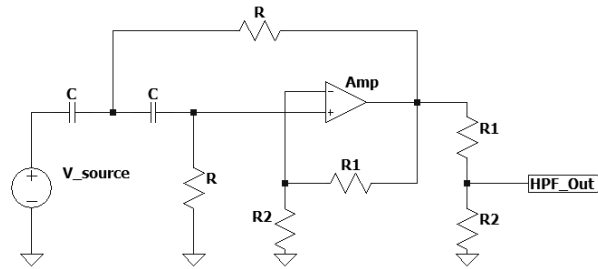


Figure 140 - Active EQ N ° 2 – HPF circuit

Acoustic prediction

The upper limit in the behavior of this second speaker is defined as follow:

- $x_{max} = 0.25 \text{ mm}$
- $I_{max} = 2x I$ in the frequency band where the HPF does not operate.

Figures 141 and 142 respectively illustrate the simulated diaphragm excursion and current consumption for 1 u_{RMS} input, which is the highest voltage under study, and for the proposed combination $Q = 2.25$ and $f_{HPF} = 400 \text{ Hz}$.

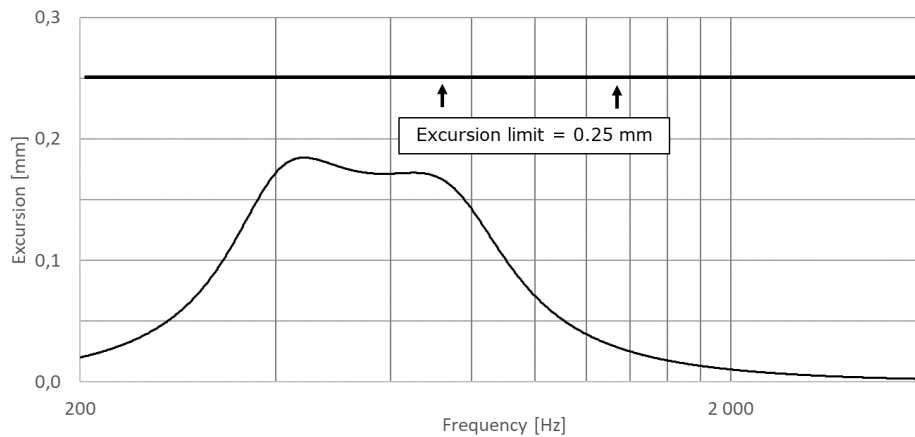


Figure 141 - Active EQ N ° 2 – simulated diaphragm excursion

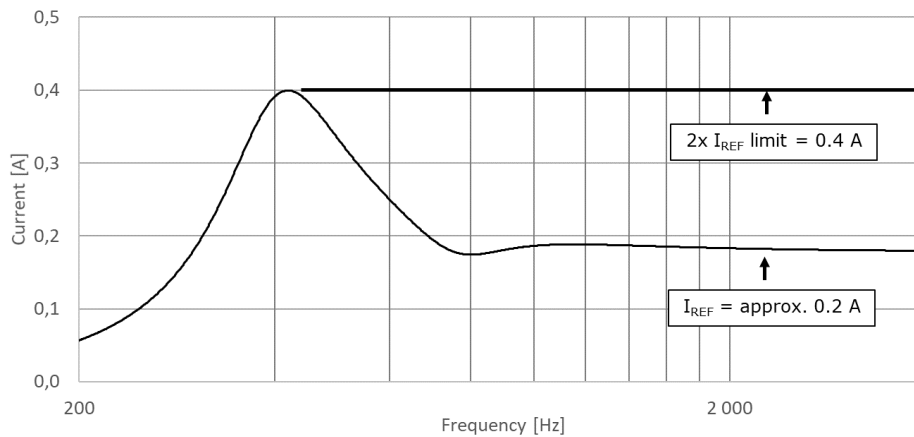


Figure 142 - Active EQ N ° 2 – simulated current consumption

From the above graphs, we confirm to remain under the excursion limit of 0.25 mm in a scenario for which the defined current limit is reached at the HPF center frequency.

The SPL predicted at $0.5 u_{RMS}$ is compared to the sealed solution on Figure 143. A quick and first observation is that the -3 dB point is extended from 515 to 390 Hz by the solution. But also, as for enclosure n ° 1 we notice that this HPF alone does not allow a flat extension to be made. The resonance peak for this second enclosure being much less damped than for the previous speaker, it may be relevant to try to attenuate it by means of a parametric equalizer available in the libraries of the processor. In this way we should learn about the possibility to achieve a flat extension.

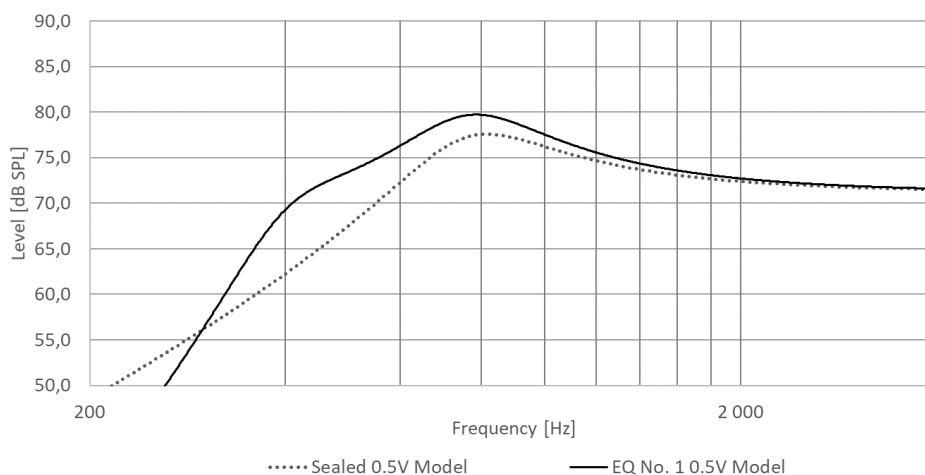


Figure 143 - Active EQ N ° 1 – simulated SPL comparison: EQ / sealed

Figure 144 illustrates the menu for the settings of the parametric equalizer available in the section “Filters” of the SigmaStudio software. From an analysis of the sealed enclosure response, we decide to configure an attenuation of 6 dB at 800 Hz, and with a quality factor

$Q = 2$. As our investigations do not integrate a model for this equalizer, we therefore intend to quantify the impact of it only from the prototype.

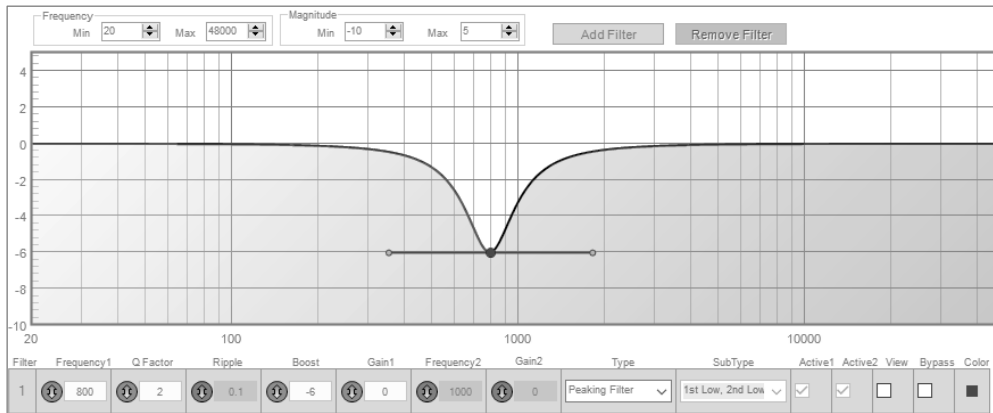


Figure 144 - Menu Settings for the SigmaStudio Parametric filter

Acoustic qualification

Figure 145 reports measured SPLs at $0.5 u_{RMS}$. Considering first the EQ solution with only the HPF, we notice a good extension with a LFRO around 390-400 Hz, as predicted by the model. By adding the parametric configured with the above values, we confirm the realization of a flat extension with a total bandwidth 400-4000 Hz contained between 70 and 75 dB SPL.

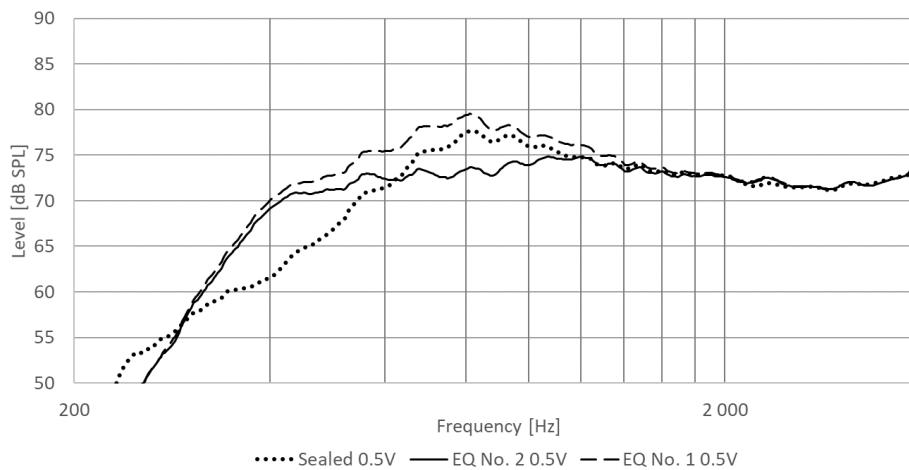


Figure 145 - Active EQ N ° 2 - Measured SPL comparison: EQs N ° 1 and 2 / sealed

Figures 146 and 147 respectively summarize the SPL behavior according to the voltage input, for the two EQ solutions. From the graphs, we see no sign of nonlinear behavior of the solutions under the voltages studied. However, from the experience gained around speaker N ° 1, we decide to still study the amount of harmonic distortion caused by these solutions.

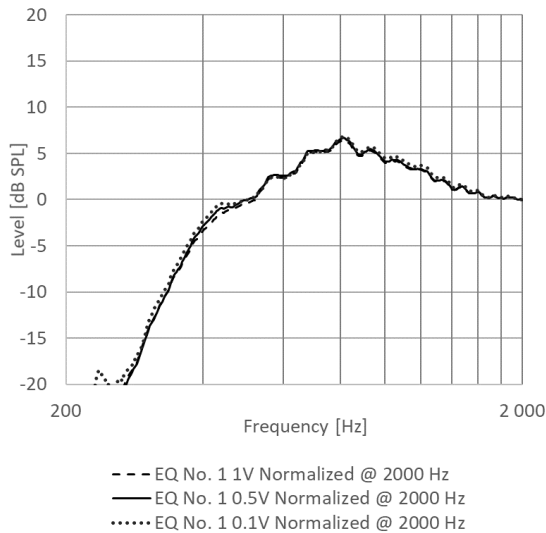


Figure 146 - Active EQ N ° 2 - SPL comparison for the EQ N ° 1 over the 3 voltages

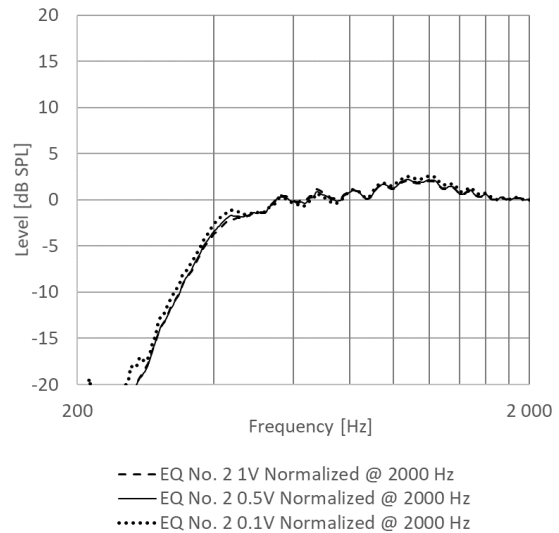


Figure 147 - Active EQ N ° 2 - SPL comparison for the EQ N ° 2 over the 3 voltages

Figure 148 reports the distortion for the sealed and equalized solutions, all at $1 u_{RMS}$. From a brief observation, EQ solutions increase the distortion at their center frequency. However, the solution combined with the parametric filter appears to produce lower distortion over the entire band. It will be interesting to see if this improvement can be detected during listening tests.

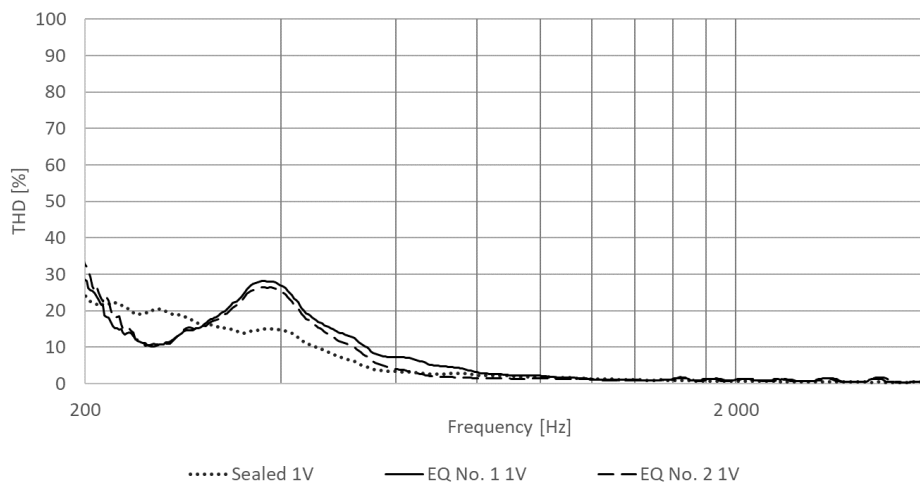


Figure 148 - Active EQ N ° 2 - Measured distortion comparison at $1 u_{RMS}$: Sealed / EQs

Comparison of measurements against predictions

Figure 149 compares predicted and measured SPLs at $0.5 u_{RMS}$. As for the design around the speaker N ° 1, we simply conclude on a perfect match of the curves, and so on a total validity of the model.

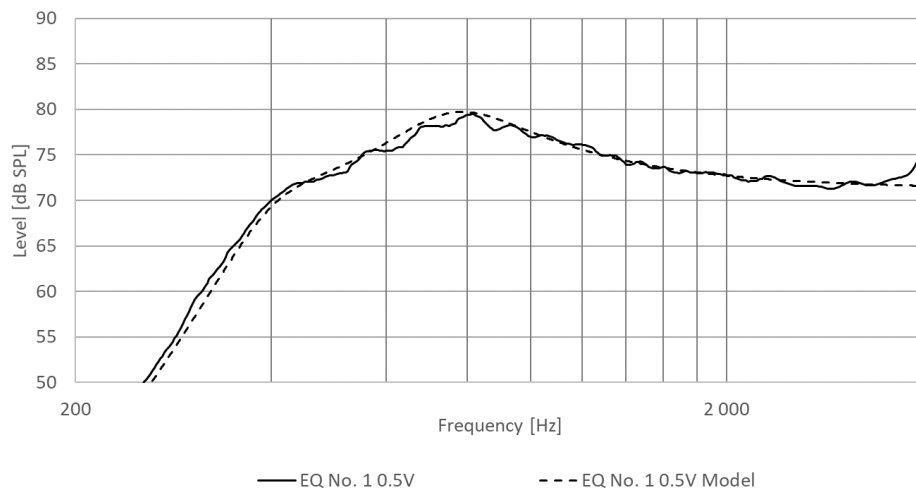


Figure 149 - Active EQ N ° 2 - SPL comparison for the EQ N ° 1: Measurement / Simulation

Finally, as for the design around the speaker N ° 1, we observe a very good correlation between predicted and measured current consumption at $1 u_{RMS}$ (Figure 150). Only a small difference in low and mid frequencies can be explained by a phenomenon related to the increase of the voice coil resistance, with both the temperature and the energy it receives.

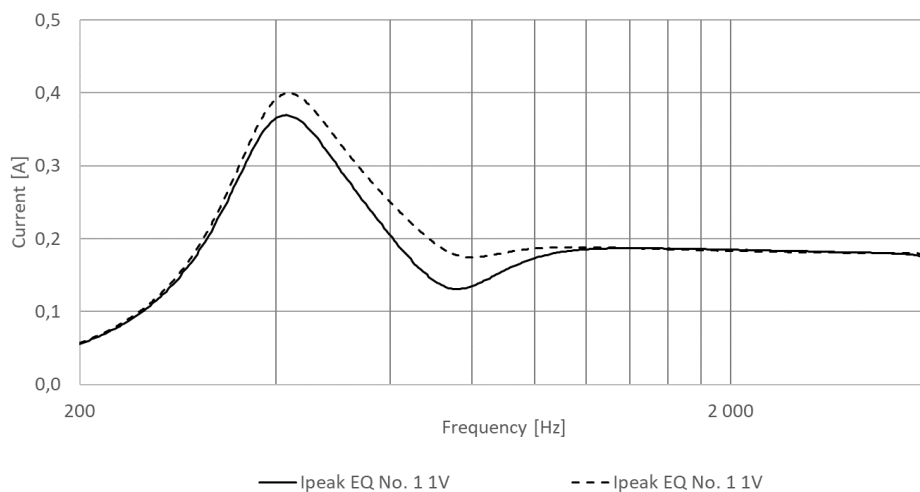


Figure 150 - Active EQ N ° 2 - Current consumption comparison for the EQ N ° 1: Measurement / Simulation

Conclusion

Unlike the first design around speaker N ° 1, we succeed here in obtaining a wide and flat LF extension compared to the sealed response. But again, this improvement comes at the cost of increased current consumption as well as the generation of additional distortion. As with the previous design, a solution that monitors power consumption in real time to turn the equalizer on / off based on output volume might be a good option to consider.

IV.IV. Perceptual evaluation of each of the improvement

As for the enclosure N ° 1, this section presents the results of listening tests performed for improvements around the second enclosure, with the same objective of correlating subjective criteria with acoustic measurements.

Here too, even if the PR system is approached well, using a speaker diaphragm as PE does not really improve the LF response. We therefore do not retain this solution for our tests.

The matrix giving the pairs to be tested is constructed in accordance with Table XXI, with some of the comparisons planned against the OnePlus 6 smartphone.

Table XXI – Listening test N ° 2 – Matrix of improvements to test

	Sealed	EQ N ° 1 (HPF)	EQ N ° 2 (HPF + Parametric)	OnePlus 6
Sealed		X	X	X
EQ N ° 1	X		X	X
EQ N ° 2	X	X		X
OnePlus 6	X	X	X	

With a measured SPL at 70 cm giving 83 dB SPL when recalculated at 10 cm, we are in higher conditions than the maximum measured over the prototypes (79 dB SPL at 2 kHz, 1 u_{RMS}). We will therefore still consider the measurements at 1 u_{RMS} for comparisons but noting that the curves may not perfectly reflect the behavior of the speakers during the tests.

Signals presentation

The first extract is from the jazz song "Whatever" by artist China Moses. The second is taken from the pop-rock song "Next to you" by artist Lake House. Spectra of these extracts are compared in Figure 151.

When analyzed between 0.2 and 20 kHz, the two songs bring similar energy despite their difference in musical style. Indeed, this type of speaker distorting quickly when excited out of its range, both songs have been chosen soft on bass and drums, explaining the similarities that we see in the LF region.

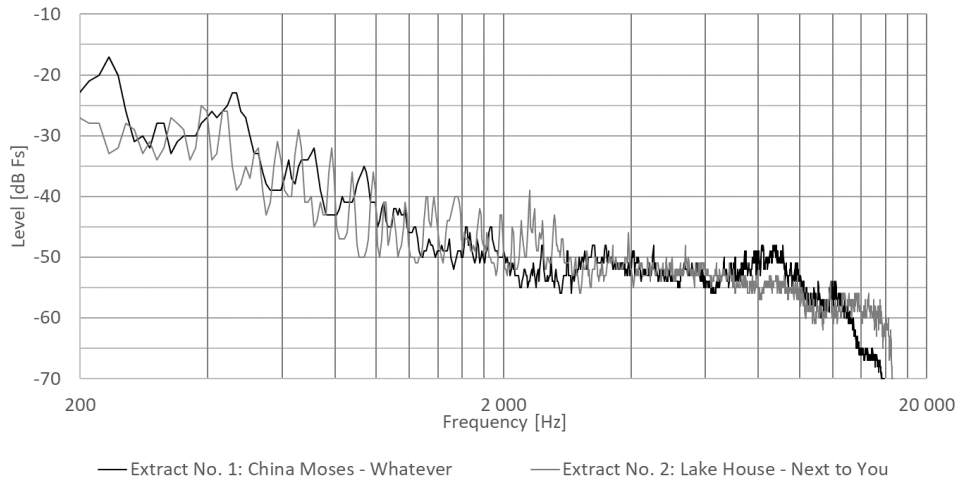


Figure 151 – Listening test N ° 2 – Music spectra comparison

Comparison of the improvements against the sealed solution

Figure 152 illustrates the subtractions of EQ curves N ° 1 and N ° 2 from the sealed response. Table XXII on the following page summarizes the results for the LF and preference questions. A first observation is that the gain in LF is much more perceived for EQ N ° 1 than for EQ N ° 2. We therefore understand that part of the LF could have been interpreted as a low medium by the subjects. Indeed, by using the word "LF" in the question instead of the word "bass", it is possible that we have biased the answers. With a preference for EQ n ° 1 (at 65%) compared to the sealed, and for the sealed (at 55%) compared to the EQ n ° 2, the words collected during the tests will help us to explain these results.

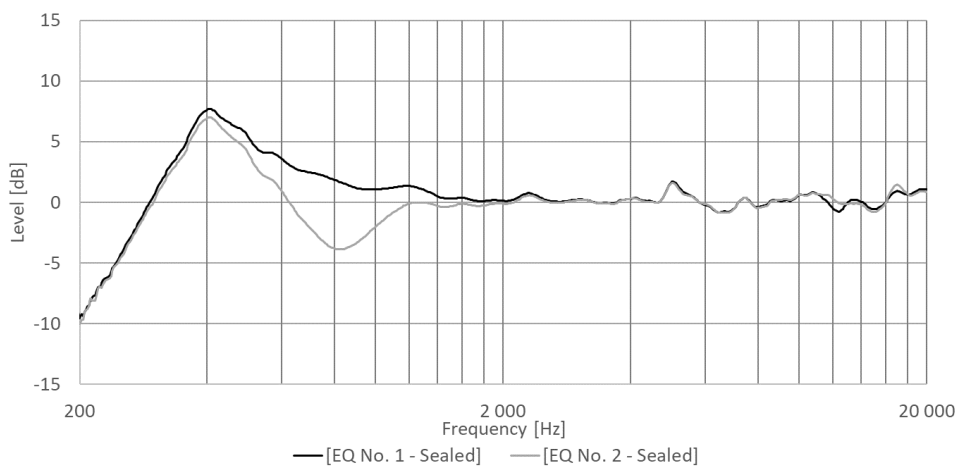


Figure 152 – Listening test N ° 2 – SPL comparison: Improvements / Sealed

From Table XXIII, we observe that EQ N ° 1 is mainly perceived as “more powerful” compared to the sealed solution, but also “closer”. As in the previous analysis, we interpret these words as being effectively related to the physical improvement of LF.

On the other hand, when EQ N ° 2 is submitted for comparison, it is a feeling of clarity in favour of the sealed solution that leads the audience (with other arguments) to prefer this solution to the EQ. Unlike the comment on the previous page, it is possible that the non-attenuation of the low mediums in the sealed solution contributes this time more to the notion of clarity instead of LF presence.

Finally, only a comparison between the two EQs should allow us to study the interest of flattening the LF extension.

Table XXII – Listening test N ° 2 – Comparison Improvements / Sealed: Answers to LF and preference questions

	LF Attribution			Preference		
	Sealed	EQ N ° 1	No attr.	Sealed	EQ N ° 1	No pref.
<i>Sealed → EQ N ° 1</i>	20%	80%	0%	20%	80%	0%
<i>EQ N ° 1 → Sealed</i>	40%	40%	20%	40%	50%	10%
<i>(Sealed ↔ EQ No. 1) Average</i>	30%	60%	10%	30%	65%	5%
	Sealed	EQ N ° 2	No attr.	Sealed	EQ N ° 2	No pref.
<i>Sealed → EQ N ° 2</i>	20%	70%	10%	30%	60%	10%
<i>EQ N ° 2 → Sealed</i>	60%	30%	10%	80%	10%	10%
<i>(Sealed ↔ EQ No. 2) Average</i>	40%	50%	10%	55%	35%	10%

Table XXIII – Listening test N ° 2 – Comparison Improvements / Sealed: Collected words

	LF Attribution	Preference	More balanced	More powerful	Better rendering	Wider	Clearer	Deeper	Closer	Round	Warmer	Distorted	Metallic	Echoes	Noisy	
<i>(Sealed ↔ EQ N ° 1): Sealed</i>	30%	30%	1x			1x	1x									1x
<i>(Sealed ↔ EQ N ° 1): EQ N ° 1</i>	60%	65%	1x	5x	1x	2x	3x	1x	3x	1x		1x	1x	1x		
<i>(Sealed ↔ EQ N ° 2): Sealed</i>	40%	55%	1x	2x			4x						2x			
<i>(Sealed ↔ EQ N ° 2): EQ N ° 2</i>	50%	35%		2x	1x	1x		1x		1x	2x	1x	1x	1x		2x

Comparison between the improvements

Figure 106 illustrates the subtraction $EQ\ No. 2_{SPL} - EQ\ No. 1_{SPL}$, in order to verify that the parametric does not create any other modification on the SPL than in the region where it is supposed to operate.

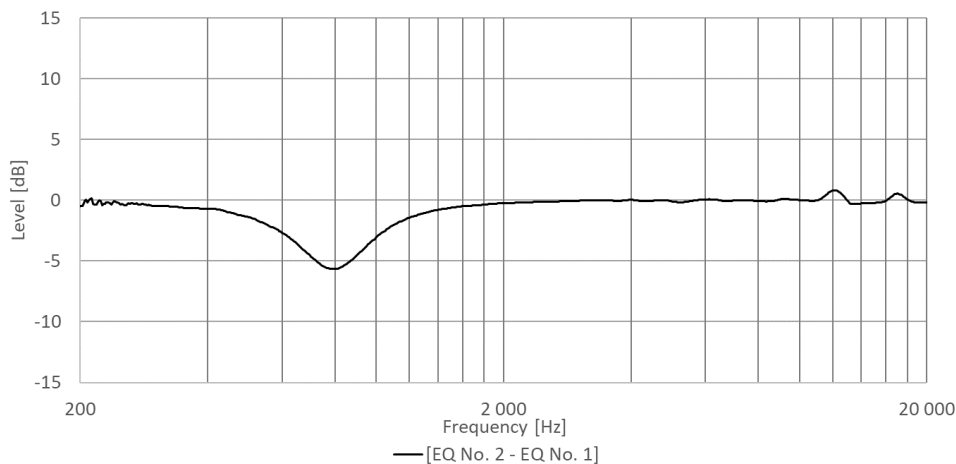


Figure 153 – Listening test N ° 2 – SPL comparison between improvements

From Table XXIV, we see most of non-response to the questions on LF and preference. We therefore fully rely on the words collected from Table XXV to try to explain this situation.

For people who noticed a difference, EQ N ° 2 was first perceived 3x times as "more balanced". Although we cannot conclude anything from a feeling expressed at 30%, we still understand that a system providing a flat sound signature can better reproduce the spectral balance of an audio mix compared to a system with a non-flat signature.

On the other hand, the EQ N ° 1 being perceived 2x as "more powerful", this may explain why this solution is preferred against the other one.

In the end, as this comparison only gives trends, it would be relevant to test this solution both on various prototypes and on a larger number of subjects, to confirm the interest in such a sound signature.

Part IV - Investigations around the speaker enclosure N ° 2: Listening test

Table XXIV – Listening test N ° 2 – Comparison between improvements: Answers to LF and preference questions

	LF Attribution			Preference		
	EQ N ° 1	EQ N ° 2	No attr.	EQ N ° 1	EQ N ° 2	No pref.
EQ N ° 1 → EQ N ° 2	20%	20%	60%	20%	20%	60%
EQ N ° 2 → EQ N ° 1	20%	30%	50%	50%	20%	30%
Average	20%	25%	55%	35%	20%	45%

Table XXV – Listening test N ° 2 – Comparison between improvements: Collected words

	LF Attribution	Preference	No difference	More balanced	More powerful	More accurate	Clearer	Warmer	Deeper	Distorted	Muffled	Aggressive
EQ N ° 1	20%	35%			2x		1x		1x	1x		1x
EQ N ° 2	25%	20%		3x		1x	1x				1x	
No difference			9x					1x				

Comparisons against a solution from the market

Figure 154 shows the SPLs normalized to 2000 Hz, both for the studied solutions and for the OnePlus 6 speaker system. Given the sound signature of the latter system, the choice of frequency for normalization can be submitted to discussion. But in the end, this way of proceeding still allows us to judge the relative presence of LF and HF compared to the energy present at 2 kHz (where this type of enclosure is supposed to behave like a perfect piston). Therefore, this graph still allows us to link the subjective perception to the measured SPLs.

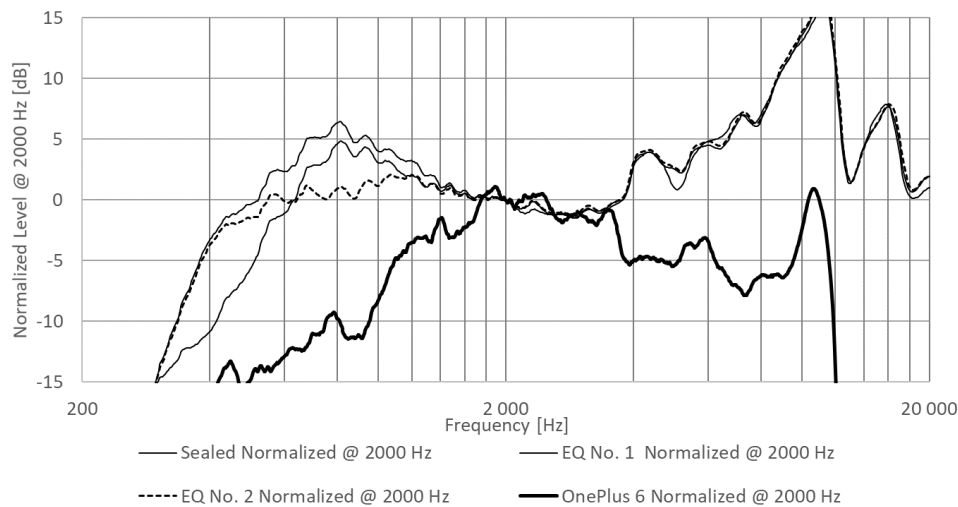


Figure 154 – Listening test N ° 2 – SPL comparison: Improvements / Sealed / OnePlus 6

Table XXVI reports the responses to the LF and preference questions. From a first analysis, our EQ solutions are both perceived as containing more bass and preferred by the subjects in front of the OnePlus smartphone. Although we are less on a one-to-one comparison than for the previous chapter, we still conclude on a successful sound signature when compared to a solution from the market similar in size.

However, when compared to the sealed enclosure, the OnePlus is generally perceived to offer more LF, although relative SPLs show the opposite. We could explain this feeling by the fact that the SPL slope of the OnePlus below 2 kHz is smoother than for the sealed solution, which increases in energy first until resonance, and then drop rapidly. It is therefore possible that the OnePlus is perceived as bringing more bass, from an overall spectral balance point of view.

But finally, when the preference is requested, the sealed solution is chosen in majority at 55%. Table XXVII of collected words on the next page could help us understand the reason for this preference.

Table XXVI – Listening test N ° 2 – Comparisons against a market solution: Answers to LF and preference questions

	LF Attribution			Preference		
	Sealed	OnePlus	No attr.	Sealed	OnePlus	No pref.
<i>Sealed</i> → <i>OnePlus</i>	30%	70%	0%	60%	40%	0%
<i>OnePlus</i> → <i>Sealed</i>	50%	50%	0%	50%	40%	10%
(Sealed ↔ OnePlus) Average	40%	60%	0%	55%	40%	5%
	EQ N ° 1	OnePlus	No attr.	EQ N ° 1	OnePlus	No pref.
<i>EQ N ° 1</i> → <i>OnePlus</i>	40%	60%	0%	80%	20%	0%
<i>OnePlus</i> → <i>EQ N ° 1</i>	70%	20%	10%	40%	50%	10%
(EQ No. 1 ↔ OnePlus) Average	55%	40%	5%	60%	35%	5%
	EQ N ° 2	OnePlus	No attr.	EQ N ° 2	OnePlus	No pref.
<i>EQ N ° 2</i> → <i>OnePlus</i>	50%	50%	0%	70%	30%	0%
<i>OnePlus</i> → <i>EQ N ° 2</i>	70%	30%	0%	80%	20%	0%
(EQ No. 2 ↔ OnePlus) Average	60%	40%	0%	75%	25%	0%

A quick observation is that in all comparisons our solutions are far seen as bringing more clarity to the sound. As a possible opposite feeling, the OnePlus is often perceived as “filtered” and “muffled”. With the word "clearer" pronounced 16x in total over the three comparisons, we understand that this feeling was very important in the choice of preference.

Looking at the other words in descending order, the expression "more powerful" appears 5x times with respect to the OnePlus when compared to the sealed solution. Considering both the shape of the SPL and the sensitivity of the human ear in mid frequencies, we understand this time that this sensation more refers to the energy present in mid frequencies than in LF. Other

sentiments collected such as the word "deeper" pronounced 3x and 2x times about EQs corroborate the choice of the LF attribution in these solutions.

Table XXVII – Listening test N ° 2 – Comparisons against a market solution: Collected words

	LF Attribution	Preference	More balanced	More powerful	More accurate	Better rendering	Wider	Clearer	Deeper	Closer	Distorted	Metallic	Closed	Muffled	Filtered	Noisy
<i>(Sealed ↔ OnePlus): Sealed</i>	40%	55%	1x		1x		1x	6x					2x	2x		
<i>(Sealed ↔ OnePlus): OnePlus</i>	60%	40%		5x	1x		2x			1x	1x	1x	1x	1x	2x	1x
<i>(EQ N ° 1 ↔ OnePlus): EQ N ° 1</i>	55%	60%	1x		1x	1x	2x	6x	3x	1x	2x			2x	1x	1x
<i>(EQ N ° 1 ↔ OnePlus): OnePlus</i>	40%	35%	2x	1x	1x	1x	1x	2x			1x	2x		5x	1x	1x
<i>(EQ N ° 2 ↔ OnePlus): EQ N ° 2</i>	60%	75%	1x	1x				4x	2x	1x	1x		2x	3x		
<i>(EQ N ° 2 ↔ OnePlus): OnePlus</i>	40%	25%	2x	2x			2x	3x			2x		1x	2x	2x	3x

Conclusion

At the end of this second listening test, we confirm the good functioning of our improvements which are distinctly noticed when listening to them. However, we cannot confirm the interest of designing a flat LF extension. Indeed, when the two EQ solutions are compared with each other, most of the audience does not notice any difference. As commented during this comparison, it would be relevant to conduct another measurement campaign on both diverse prototypes and a larger number of subjects, to confirm or not the interest in such a design.

Finally, when we compare our solutions to a similar sized product from the market, these firsts are initially perceived to be stronger in bass, but above all we understand that the preferences towards these solutions are mainly driven by their HF signature.

One thing that we must consider about this last property, is that our devices radiate directly into space while the speaker system built into the OnePlus first radiates into a front volume (made of a tubing network) to then lead to the outside.

We therefore conclude without surprise from this last observation that the way of integrating a speaker system into a product is at least as important as the design of the system itself.

V. Summary of the investigations and conclusion

V.I. Synthesis

Reviewing the methods considered in this study, we understand that a traditional Bass-Reflex design remains the most efficient at low frequency, both in terms of measurement and perception. Also, by not involving anything other than a plastic tube, this system remains the simplest to design against the other two methods. However, from these investigations we will also have learned to what extent a small port size can cause large losses in the radiation, thus leading our models to overestimate the performances.

On the other hand, further investigation has taught us that a port with horn terminations can help reduce noise from aerodynamic turbulence, but also potentially increase the responsiveness of the system to transients.

Then, providing as much LF as a Bass-Reflex, but being totally possible to design in both speaker systems, the Active Equalization technique is still a method that Seltech does not know much about. And although our models perfectly approximate the performance of this solution, we will have come up against non-linearities that both appear and are perceived as a function of the requested input energy.

By relying on processors to program such a type of EQ, we realized how easy it is to tune a wide and flat extension over the original system response. But when we asked our test subjects to compare this flat extension against a non-flat design, we could not confirm the benefits of designing such a shape of sound signature.

Finally, even if not retained for our listening tests, the investigations around Passive Radiators will have made it possible to understand the behavior of systems very popular on the market. Indeed, by integrating a speaker as passive element, we have been then able to fully model the solution and confirm that we can predict its performance well.

On the other hand, as we know that the use of a speaker like PE is not suitable for this kind of design, we were only able to obtain non-flat and narrow extensions.

In the end, whatever the extension method considered, we will also have learned from this study, that within a population aged from 20 to 55 years, the LF presence in a sound is appreciated, but the overall spectral balance of this sound is even more so.

V.II. Industrial feasibility and cost point of view

Under the assumption that the three improvements give comparable performances, this study will have proved to us the potential difficulties for the integration of a BR port in a system as compact as those we considered. Indeed, when these ports are designed curved, this can sometimes lead to an impossibility of manufacturing the solution as it has been imagined in regards with constraints of mass production processes such as plastic injection.

On the other hand, when compared to the other two solutions, a Bass-Reflex design remains by far the cheapest, and this cost aspect is important to consider for applications where the budget of the audio function is not a priority. In the end about this method, as soon as the space available for the audio part of a device becomes drastically small, it will be relevant to set up evaluation indicators such as ratios between mechanical complexity and expected acoustic efficiency, to be able to decide whether to opt for this solution or not.

Otherwise, we will have fully understood that a Passive Radiator system can replace a Bass-Reflex when the enclosure becomes too small. However, this system using a diaphragm instead of a port, it is first a more expensive solution but also a more sensitive one to performances variation within production. Indeed, where a Bass-Reflex just needs to be controlled on its port dimensions, a diaphragm must be controlled on its three mechanical parameters R_{MR} , C_{MR} and M_{MR} . In addition, by adding a secondary vibrating element to the system, there will be a point of attention to be paid on both a good insulation from vibrations and a good overall balance of the system. Finally, active equalization could appear as the simplest design to handle, in front of a Bass-Reflex. But that is without count on the fact that this design involves a processor as well as an amplifier in the audio chain. If not a problem for the industrial side, it could be an issue for the cost aspect. Indeed, apart relying on customer capabilities, this solution would require Seltech to develop and supply all the electronics around the speaker enclosure. In addition, apart from the risk of not being competitive in terms of cost in this second scenario, this design consumes energy compared to the other two. And this remains important to consider in the context of battery-operated applications.

Ultimately, since all the methods reviewed in this document modify the behavior of the speaker itself, it may be necessary to requalify its power supply capability each time a LF extension is designed. This qualification being done both in regards with the maximum possible excursion for the diaphragm and the current consumption capacity.

V.III. Future work proposals

As this document only reflects one year of investigations, it cannot cover all the ideas and open questions around the reviewed methods. In this context, the aim of this section is to offer some open ideas for further work following this study.

A first obvious proposal is to equip ourselves with a diaphragm measurement equipment, as described in Appendix D. Indeed, from our investigations around Passive Radiators designs, we understood how important it is to master the behavior of a PE to properly adjust its resonant frequency, and thus achieve the targeted extension.

However, knowing the properties of a diaphragm is not the only aspect to consider in PR designs. Indeed, although we can act on the moving mass of this element to adjust our alignment, we can in no way modify the loss and compliance properties of an already manufactured object.

Therefore, given the competition of PR designs in the market, only joint work between Seltech and its manufacturing partners could lead to competitive membranes giving wide and flat extensions.

As for Bass-Reflex designs, as the listening tests carried out have led us to conclude that a big bass peak is not necessarily what the public prefers, faced with a feeling of global spectral balance, we could launch new investigations on larger ports with a more reasonable target for the Helmholtz frequency, thus leading to a smaller, but flatter LF region.

An additional idea to help flatten the SPL at the speaker resonance would be to add a piece of porous material into the enclosure.

Finally, we could as well design an EQ alone, as combine it with BR / PR systems (to correct the artifacts of such systems), but in the end we will have to improve our knowledge on a solution to monitor the current consumption in real time in the speaker. Thus, to automatically activate / deactivate the equalizer, or even to modify its properties according to the required input energy.

All the above ideas remain purely proposals, in a constantly evolving market with recurring innovations.

Bibliography

- [1] B. Kinsella, "Streaming Music, Questions, Weather, Timers and Alarms Remain Smart Speaker Killer Apps, Third-Party Voice App Usage Not Growing," 3 May 2020. [Online]. Available: <https://voicebot.ai/2020/05/03/streaming-music-questions-weather-timers-and-alarms-remain-smart-speaker-killer-apps-third-party-voice-app-usage-not-growing/>. [Accessed 6 July 2021].
- [2] M. G. De Hillerin, "Audio matters in smartphones and here's why," 15 September 2020. [Online]. Available: <https://www.dxomark.com/audio-matters-in-smartphones-and-heres-why/>. [Accessed 5 July 2021].
- [3] M. G. De Hillerin, "2000 to 2021: The evolution of smartphone audio playback," 18 May 2021. [Online]. Available: <https://www.dxomark.com/evolution-of-smartphone-audio-playback/>. [Accessed 5 July 2021].
- [4] M. G. De Hillerin, "Test Enceinte Go 2 : JBL améliore son best-seller ultra-nomade," 10 July 2018. [Online]. Available: <https://www.lesnumeriques.com/enceintes-portables/jbl-go-2-p42613/test.html>. [Accessed 5 July 2021].
- [5] L. Paillat, "Test Enceinte ultra-portable JBL Go 3 : une brique de savon aux performances sonores étonnantes," 30 April 2021. [Online]. Available: <https://www.lesnumeriques.com/enceintes-portables/jbl-go-3-p59571/test.html>. [Accessed 5 July 2021].
- [6] Audio Video Unlimited, "What Are Passive Radiators In Speakers?," [Online]. Available: <https://www.avu.ca/audio/what-are-passive-radiators-in-speakers/>. [Accessed 05 September 2021].
- [7] L. Renouard and R. Bertrand, "Test: Ultimate Ears Wonderboom 2, la petite enceinte étanche qui flotte," 19 July 2019. [Online]. Available: <https://www.ledauphine.com/magazine-lifestyle/2019/07/19/test-ultimate-ears-wonderboom-2-la-petite-enceinte-etanche-qui-flotte>. [Accessed 04 September 2021].
- [8] J. Martins, "The First Smart Speaker from Apple: A Strong Design and How It Is Perceived," 15 October 2020. [Online]. Available: <https://audioxpress.com/article/the-first-smart-speaker-from-apple-a-strong-design-and-how-it-is-perceived>. [Accessed 04 September 2021].
- [9] L'Audiophile Débutant , "Xiaomi Smart Speaker | Test De L'Enceinte Ok Google," 4 March 2021. [Online]. Available: <https://www.audiophiledebutant.fr/audio/xiaomi-smart-speaker-test-de-lenceinte-ok-google/>. [Accessed 04 September 2021].
- [10] Anker, *Rave portable speaker: production description* (<https://www.anker.com/products/variant/rave/A3391Z11>).
- [11] P. Stemmelin, "Harman/Kardon Aura : enceinte transparente sans-fil qui a du coffre," 13 December 2013. [Online]. Available: <https://www.lesnumeriques.com/platine-musicale-serveur-audio/harmankardon-aura-p17996/harmankardon-aura-enceinte-transparente-sans-fil-qui-a-coffre-n32211.html>. [Accessed 04 September 2021].
- [12] Soomal, "JBL GO Smart Portable Speaker: Tear Down," [Online]. Available: <http://eng.soomal.com/edoc/10100000068.htm>. [Accessed 04 September 2021].
- [13] Y.-W. Jiang, J.-H. Kwon, H.-K. Kim and S.-M. Hwang, "Analysis and Optimization of Micro Speaker-Box Using a Passive Radiator in portable Device," *Archive of Acoustics*, Vol. 42, No. 4, pp. 753-760, 2017.

- [14] C. Patil, "Smart Speakers With Smart Processors," 25 November 2018. [Online]. Available: <https://www.chetanpatil.in/smart-speakers-with-smart-processors/>. [Accessed 04 September 2021].
- [15] J. Young, "Dedicated Audio Processors at the Edge are the Future. Here are the Reasons Why," 1 June 2019. [Online]. Available: <https://voicebot.ai/2019/06/01/dedicated-audio-processors-at-the-edge-are-the-future-here-are-the-reasons-why/>. [Accessed 4 September 2021].
- [16] H. Teutsch, "Audio and Acoustic Signal Processing's Major Impact on Smartphones," 28 October 2016. [Online]. Available: <https://signalprocessingsociety.org/publications-resources/blog/audio-and-acoustic-signal-processing%E2%80%99s-major-impact-smartphones>. [Accessed 4 September 2021].
- [17] Android Authority, "Smartphone audio is important, and here's what it takes to build the best," 26 January 2021. [Online]. Available: <https://www.androidauthority.com/cirrus-logic-amplifiers-1193093/>. [Accessed 04 September 2021].
- [18] M. Arora, H. Moon and S. Jang, "Low Complexity Virtual Bass Enhancement Algorithm," in *AES 29th International Conference*, Seoul, Korea, 2006.
- [19] H. Moon, M. Arora, C. Chung and S. Jang, "Enhanced Bass Reinforcement Algorithm for small-sized Transducer," in *AES 122th Convention*, Vienna, Austria, 2007.
- [20] A. L. Thuras, "Sound Translating Device". Patent 1869178, 26th July 1932.
- [21] H. F. Olson, "Loudspeaker and method of propagating sound". Patent 1988250, 15th January 1935.
- [22] V. Välimäki and J. D. Reiss, "All About Audio Equalization: Solutions," *Applied Sciences*, June 2016.
- [23] W. Marshall Leach, JR., "Active Equalization of closed box loudspeaker systems," *Journal of the Audio Engineering Society, Volume 29*, pp. 405 - 407, June 1981.
- [24] C. W. Rice and E. W. Kellogg, "Notes on the Development of a New Type of Hornless Loud Speaker," *Transactions A.I.E.E.*, 1925, Vol. XLIV.
- [25] L. L. Beranek, *Acoustics*, Massachusetts: Institute of Technology, 1954.
- [26] L. L. Beranek and T. Mellow, *Acoustics: Sound fields, Transducers and Vibration (Second Edition)*, Academic Press, 2019.
- [27] R. Elliott, "Measuring Loudspeaker Parameters," June 2018. [Online]. Available: <https://sound-au.com/tsp.htm#s2>. [Accessed 1 02 2021].
- [28] A. N. Thiele, "Loudspeakers in Vented Boxes: Parts I and II," *Journal of the Audio Engineering Society*, pp. 382-392 and 471-483, May and June 1971.
- [29] D. Ponteggia, *Audiomatica AN-003 - Single Pass Measurement Of Thiele And Small Parameters Using A Laser Transducer*, 2012.
- [30] E. Parizet and V. Nosulenko, "Multi-dimensional listening test: selection of sound descriptors and design of the experiment," *Noise Control Eng. J*, 08 July 1999.

- [31] E. Parizet, N. Hamzaoui and G. Sabatie, "Comparison of some listening test methods : a case study," *Acta Acustica united with Acustica*, pp. 356-364, 2005.
- [32] G. Lorho, "Perceptual Evaluation of Mobile Multimedia Loudspeakers," in *Audio Engineering Society, Convention Paper 7050*, Vienna, Austria, 2007.
- [33] Z. Liu, Y. Shen, P. Yu and H. Yin, "Evaluation of Portable Loudspeakers Using Virtual Listening Test," in *Audio Engineering Society, Convention e-Brief 284*, Los Angeles, CA, USA, 2016.
- [34] R. H. Small, "Vented-Box Loudspeaker Systems Part I: Small-Signal Analysis, and Part II: Large-Signal Analysis," *Journal of the Audio Engineering Society*, pp. 316-235 and 326-332, June 1973.
- [35] N. B. Roozen, J. E. M. Vael and J. A. M. Nieuwendijk, "Reduction of bass-reflex port nonlinearities by optimizing the port geometry," in *The 104th convention of AES*, Amsterdam, 1998.
- [36] Knowles, *Application Note 20: Getting started with Knowles Sisonic simulation models*, Itasca, 2018.
- [37] V. M. Garcia-Alcaide, S. Palleja-Cabre, R. Castilla, P. J. Gamez-Montero, J. Romeu, T. Pamies, J. Amate and N. Milan, "The aerodynamics phenomena of a particular bass-reflex port," in *AES 140th Convention*, Paris, 2016.
- [38] R. H. Small, "Passive-Radiator Loudspeaker systems, Part I: Analysis and Part II: Synthesis," *Journal of the Audio Engineering Society*, pp. 592-601 and 683-689, October and November 1974.
- [39] M. Tanasescu, "Passive radiator speaker design – Box calculation example," 13 June 2016. [Online]. Available: <https://audiojudgement.com/passive-radiator-speaker-design/>. [Accessed 19 August 2021].
- [40] Analog Devices, "General Filters," 23 June 2020. [Online]. Available: <https://wiki.analog.com/resources/tools-software/sigmastudio/toolbox/filters/general2ndorder>. [Accessed 20 August 2021].
- [41] E. Bazil, "Mixing To A Pink Noise Reference," December 2014. [Online]. Available: <https://www.soundonsound.com/techniques/mixing-pink-noise-reference>. [Accessed 04 September 2021].
- [42] Analog Devices, *ADAU1772 Datasheet Rev. C*, 2012 - 2014.

List of Figures

Figure 1 – “Smart speaker use case frequency. January 2020” [1].....	1
Figure 2 - “What do you use your smartphone for?” September 2020 [2]	1
Figure 3 - SPL comparison: Nokia N95 / Xiaomi Black Shark 4. Graph recreated from [3]	2
Figure 4 - SPL comparison: JBL Go 2 / JBL Go 3. Graph recreated from [4] and [5]	2
Figure 5 – Apple HomePod mini split view [8].....	3
Figure 6 – Anker Rave split view [10]	3
Figure 7 – Micro Passive Radiator prototypes [6].....	3
Figure 8 - Pitch perception of a complex tone (Missing fundamental effect) [15]	4
Figure 9 – Geographical distribution of Seltech offices	5
Figure 10 – Speaker N ° 1 - Detailed composition	6
Figure 11 – Sealed enclosure N ° 1 - Assembly elements	7
Figure 12 - Sealed enclosure N ° 1 - Assembled system	7
Figure 13 – Sealed enclosure N ° 1 - Measurement setup	7
Figure 14 – Sealed enclosure N ° 1 - Typical electric impedance	8
Figure 15 – Sealed enclosure N ° 1 - Typical SPL at 0.3 m, normalized at 500 Hz	8
Figure 16 – Speaker N ° 2 - Detailed description	8
Figure 17 – Sealed enclosure N ° 2 - Assembly elements	9
Figure 18 – Sealed enclosure N ° 2 - Assembled system.....	9
Figure 19 – Sealed enclosure N ° 2 - Measurement setup	9
Figure 20 – Sealed enclosure N ° 2 - Typical electric impedance	10
Figure 21 – Sealed enclosure N ° 2 - Typical SPL at 0.1 m, normalized at 2000 H	10
Figure 22 – Bass-Reflex principle drawing [20]	11
Figure 23 – Bass-Reflex response against sealed enclosure response [20].....	11
Figure 24 – Passive Radiator principle drawing [21]	12
Figure 25 – Passive Radiator response against sealed enclosure response [21].....	12
Figure 26 – “ Possible three-operational-amplifier realization of the active equalizer” [23].....	13
Figure 27 – (a) system before equalization; (b) system after equalization; (c) equalizer [23]	13
Figure 28 - Acoustical analogous circuit for a sealed enclosure system [25]	14
Figure 29 – Simplified analogous circuit for a sealed enclosure	15
Figure 30 – Speaker N ° 1 – Diameter considered for the calculation of S_D	16
Figure 31 – Speaker N ° 1 – Parameters measurements 1/2	17
Figure 32 - Speaker N ° 1 – Parameters measurements 2/2.....	17
Figure 33 - Speaker N ° 2 – Dimensions considered for the calculation of S_D	18

Figure 34 - Speaker N ° 2 – Parameters measurements 1/2.....	18
Figure 35 - Speaker N ° 2 – Parameters measurements 2/2.....	18
Figure 36 – Additional electric network for the SPL calculation	19
Figure 37 - Sealed enclosure N ° 1 – Model / Measurement electric impedance comparison	20
Figure 38 - Sealed enclosure N ° 1 – Model / Measurement SPL comparison	21
Figure 39 – Sealed enclosure N ° 1 – SPL behavior over the voltage	21
Figure 40 - Sealed enclosure N ° 2 – Model / Measurement electric impedance comparison	22
Figure 41 - Sealed enclosure N ° 2 – Model / Measurement SPL comparison	23
Figure 42 - Sealed enclosure N ° 2 – SPL behavior over the voltage	23
Figure 43 – Listening tests environment	25
Figure 44 – Acoustical analogous circuit of a BR system [34].....	27
Figure 45 – Illustration of alignments C ₄ , B ₄ , and QB ₃ (n ° 8, 5, and 3) [28]	28
Figure 46 – Typical electric impedance of a BR system [34].....	29
Figure 47 – BR system N ° 1 – Prototype drawings	30
Figure 48 – BR system N ° 1 – Horn port prototype drawings.....	31
Figure 49 – Simplified acoustical circuit of a BR system (lossless).....	31
Figure 50 – Electric network for the SPL calculation of a BR system	32
Figure 51 – BR system N ° 1 – Simulated electric impedance	32
Figure 52 - BR system N ° 1 – Simulated SPL comparison: BR / Sealed	33
Figure 53 - BR system N ° 1 – Original prototype	33
Figure 54 - BR system N ° 1 – Horn port prototype.....	33
Figure 55 - BR system N ° 1 – Assembled prototype.....	34
Figure 56 - BR system N ° 1 – Measurement setup.....	34
Figure 57 - BR system N ° 1 – Measured SPL comparison: BR / Sealed.....	34
Figure 58 - BR system N ° 1 - Measured SPL comparison for the 3 voltages.....	35
Figure 59 - BR system N ° 1 – Electric impedance comparison: Simulation / Measurement.....	36
Figure 60 - BR system N ° 1 – SPL comparison: Simulation / Measurement	36
Figure 61 - BR system N ° 1 – analogous circuit for simulation of port losses	36
Figure 62 - BR system N ° 1 – Electric Impedance comparison: Measurement/Simulation w/ and w/o losses	37
Figure 63 - BR system N ° 1 – SPL comparison: Measurement/Simulation w/ and w/o losses	37
Figure 64 - BR system N ° 1 – Setup for qualification of turbulences created by ports designs	38
Figure 65 - BR system N ° 1 – Qualification of turbulences created by ports at 0.5 u _{RMS}	38
Figure 66 - BR system N ° 1 – Qualification of turbulences created by ports at 1 u _{RMS}	39
Figure 67 - BR system N ° 1 – Qualification of turbulences created by ports at 2 u _{RMS}	39
Figure 68 – BR port designs : Port E geometry [35]	40

Figure 69 - BR port designs : Port C geometry [35].....	40
Figure 70 – Acoustical analogous circuit of a PR system [38].....	42
Figure 71 – “Responses obtainable from passive-radiator system for the condition $\delta = \alpha$ ” [38].....	44
Figure 72 - Simplified acoustical circuit of a PR system.....	44
Figure 73 - PR system N ° 1 – Simulated SPL comparison: PR / Sealed.....	45
Figure 74 - PR system N ° 1 – Prototype elements	45
Figure 75 - PR system N ° 1 – Assembled prototype	45
Figure 76 - PR system N ° 1 – Measurement setup	45
Figure 77 – PR system N ° 1 – Electric impedance comparison: Measurement / Simulation	46
Figure 78 - PR system N ° 1 – SPL comparison: Measurement / Simulation.....	46
Figure 79 - PR system N ° 1 – Simulated SPLs for determining the minimum mass to add	47
Figure 80 – PR system N ° 1 – Simulated SPLs for different added masses	48
Figure 81 - PR system N ° 1 – PE moving mass weighing.....	49
Figure 82 - PR system N ° 1 – PE additional radiating element	49
Figure 83 - PR system N ° 1 – PE additional radiating element weighed down.....	49
Figure 84 - PR system N ° 1 – Tuned prototype.....	50
Figure 85 – Tuned PR system N ° 1 – Measured SPL comparison: PR / Sealed.....	50
Figure 86 - Tuned PR system N ° 1 – Measured SPL comparison for the 3 voltages.....	51
Figure 87 - Tuned PR system N ° 1 – Electric impedance comparison: Measurement / Simulation	52
Figure 88 - Tuned PR system N ° 1 – SPL comparison: Measurement / Simulation.....	52
Figure 89 – Menu Settings for the SigmaStudio 2 nd order HPF	54
Figure 90 – Impact of the Gain parameter on the SigmaStudio HPF for $f = 200$ Hz; $Q = 1.41$; $G = 0$ and 6 dB.....	54
Figure 91 - Active EQ N ° 1 – Analogous circuit.....	54
Figure 92 - Active EQ N ° 1 – HPF circuit.....	54
Figure 93 – Active EQ N ° 1 – Additional loop for computing the speaker diaphragm excursion.....	55
Figure 94 - Active EQ N ° 1 – Additional loop for computing the current consumption	56
Figure 95 - Active EQ N ° 1 – simulated diaphragm excursion for EQs N ° 1 and 2.....	56
Figure 96 - Active EQ N ° 1 – simulated current consumption for EQs N ° 1 and 2.....	57
Figure 97 - Active EQ N ° 1 – simulated SPL comparison: EQs N ° 1 and 2 / sealed	57
Figure 98 - Active EQ N ° 1 - Measured SPL comparison: EQs N ° 1 and 2 / sealed	58
Figure 99 - Active EQ N ° 1 - SPL comparison for the EQ N ° 1 over the 3 voltages	59
Figure 100 - Active EQ N ° 1 - SPL comparison for the EQ N ° 2 over the 3 voltages	59
Figure 101 - Active EQ N ° 1 - Measured distortion comparison at $2 u_{RMS}$: Sealed / EQs / BRs.....	59
Figure 102 - Active EQ N ° 1 - SPL comparison for the EQ N ° 1: Measurement / Simulation	60
Figure 103 - Active EQ N ° 1 – Current consumption comparison for the EQ N ° 1: Measurement / Simulation	60

Figure 104 – Listening test N ° 1 – Music spectra comparison	63
Figure 105 – Listening test N ° 1 – SPL comparison: Improvements / Sealed.....	63
Figure 106 – Listening test N ° 1 – SPL comparison between improvements.....	65
Figure 107 – Listening test N ° 1 – SPL comparison: Improvements / Sealed / JBL Go 3	66
Figure 108 – Listening test N ° 1 – Impulse response comparison: Original BR port output / Horn BR port output	69
Figure 109 – Simplified acoustical circuit of a BR system.....	71
Figure 110 - BR system N ° 2 – Presentation of a tube sourced from the market	72
Figure 111 - BR system N ° 2 – Shortening of the tube to constitute the Port of the system	72
Figure 112 - BR system N ° 2 – Electric impedance simulation	73
Figure 113 - BR system N ° 2 – Simulated SPL comparison: BR / Sealed	73
Figure 114 - BR system N ° 2 – Prototype bottom casing.....	74
Figure 115 - BR system N ° 2 – Assembled prototype.....	74
Figure 116 - BR system N ° 2 – Measurement setup.....	74
Figure 117 - BR system N ° 2 – Measured SPL comparison: BR / Sealed.....	75
Figure 118 - BR system N ° 2 – Electric impedance comparison: Measurement / Simulation	75
Figure 119 - BR system N ° 2 – SPL comparison: Measurement / Simulation	76
Figure 120 - BR system N ° 2 – Setup for measuring the SPL at port output.....	76
Figure 121 - BR system N ° 2 – Port output measured SPL.....	76
Figure 122 - PR system N ° 2 – Simplified analogous circuit for a PR system	78
Figure 123 - PR system N ° 2 – PE presentation	78
Figure 124 - PR system N ° 2 – PE bottom view	78
Figure 125 - PR system N ° 2 – Simulated SPL comparison: PR / Sealed	79
Figure 126 - PR system N ° 2 – Assembled prototype	80
Figure 127 - PR system N ° 2 – Measurement setup	80
Figure 128 - PR system N ° 2 – Electric impedance comparison: Measurement / Simulation	80
Figure 129 - PR system N ° 2 – SPL comparison: Measurement / Simulation.....	81
Figure 130 – PR system N ° 2 – Simulated SPLs for different added masses	81
Figure 131 - PR system N ° 2 – PE additional radiating element.....	82
Figure 132 - PR system N ° 2 – PE additional radiating element weighed down.....	82
Figure 133 - PR system N ° 2 – Tuned prototype.....	82
Figure 134 – Tuned PR system N ° 2 – Measured SPL comparison: PR / Sealed.....	83
Figure 135 - Tuned PR system N ° 2 – Measured SPL comparison for the 3 voltages.....	84
Figure 136 - Tuned PR system N ° 2 – Electric impedance comparison: Measurement / Simulation	84
Figure 137 - Tuned PR system N ° 2 – SPL comparison at 0.5 u_{RMS} : Measurement / Simulation	85
Figure 138 - Tuned PR system N ° 2 – SPL comparison at 0.1 u_{RMS} : Measurement / Simulation	85

Figure 139 - Active EQ N ° 2 – Analogous circuit.....	86
Figure 140 - Active EQ N ° 2 – HPF circuit.....	86
Figure 141 - Active EQ N ° 2 – simulated diaphragm excursion	86
Figure 142 - Active EQ N ° 2 – simulated current consumption	87
Figure 143 - Active EQ N ° 1 – simulated SPL comparison: EQ / sealed	87
Figure 144 - Menu Settings for the SigmaStudio Parametric filter.....	88
Figure 145 - Active EQ N ° 2 - Measured SPL comparison: EQs N ° 1 and 2 / sealed	88
Figure 146 - Active EQ N ° 2 - SPL comparison for the EQ N ° 1 over the 3 voltages	89
Figure 147 - Active EQ N ° 2 - SPL comparison for the EQ N ° 2 over the 3 voltages	89
Figure 148 - Active EQ N ° 2 - Measured distortion comparison at 1 u _{RMS} : Sealed / EQs.....	89
Figure 149 - Active EQ N ° 2 - SPL comparison for the EQ N ° 1: Measurement / Simulation	90
Figure 150 - Active EQ N ° 2 – Current consumption comparison for the EQ N ° 1: Measurement / Simulation	90
Figure 151 – Listening test N ° 2 – Music spectra comparison	92
Figure 152 – Listening test N ° 2 – SPL comparison: Improvements / Sealed	92
Figure 153 – Listening test N ° 2 – SPL comparison between improvements.....	94
Figure 154 – Listening test N ° 2 – SPL comparison: Improvements / Sealed / OnePlus 6.....	95

List of Tables

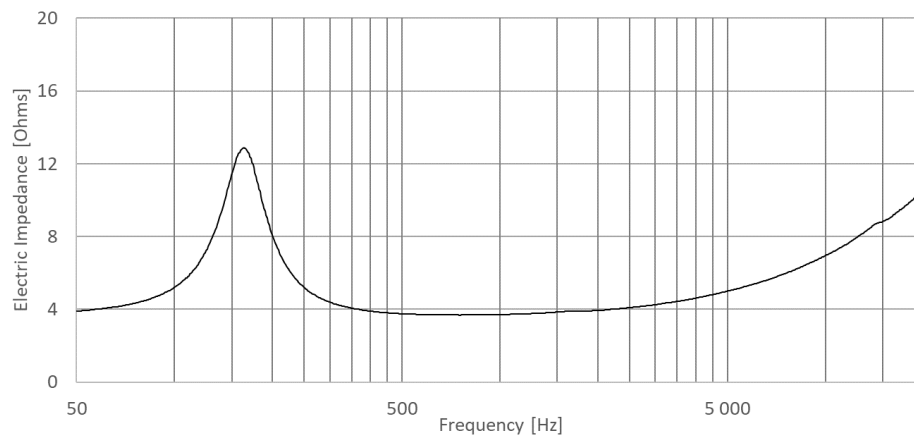
Table I – Speaker N ° 1 - Main characteristics	7
Table II – Speaker N ° 2 – Main characteristics	9
Table III – Speaker N ° 1 – Measurements of the fundamental parameters	17
Table IV – Speaker N ° 2 - Measurements of the fundamental parameters	19
Table V - BR alignments: corresponding compliance ratios [28].....	28
Table VI - PR system N ° 1 – PE qualification	43
Table VII - PR system N ° 1 – F function integral result for different added masses	48
Table VIII - PR system N ° 1 – M _{MD} weighing	49
Table IX - PR system N ° 1 – additional mass weighing.....	50
Table X – Listening test N ° 1 – Matrix of improvements to test.....	62
Table XI – Listening test N ° 1 – Comparison Improvements / Sealed: Answers to LF and preference questions	64
Table XII – Listening test N ° 1 – Comparison Improvements / Sealed: Collected words.....	64
Table XIII – Listening test N ° 1 – Comparison between improvements: Answers to LF and preference questions	65
Table XIV – Listening test N ° 1 – Comparison between improvements: Collected words	66
Table XV – Listening test N ° 1 – Comparisons against a market solution: Answers to LF and preference questions	67
Table XVI – Listening test N ° 1 – Comparisons against a market solution: Collected words.....	68
Table XVII – Listening test N ° 1 – Additional comparison: collected words	69
Table XVIII - PR system N ° 2 – PE qualification	78
Table XIX - PR system N ° 2 – F function integral result for different added masses	81
Table XX - PR system N ° 2 – additional mass weighing	82
Table XXI – Listening test N ° 2 – Matrix of improvements to test.....	91
Table XXII – Listening test N ° 2 – Comparison Improvements / Sealed: Answers to LF and preference questions	93
Table XXIII – Listening test N ° 2 – Comparison Improvements / Sealed: Collected words.....	93
Table XXIV – Listening test N ° 2 – Comparison between improvements: Answers to LF and preference questions	95
Table XXV – Listening test N ° 2 – Comparison between improvements: Collected words	95
Table XXVI – Listening test N ° 2 – Comparisons against a market solution: Answers to LF and preference questions.....	96
Table XXVII – Listening test N ° 2 – Comparisons against a market solution: Collected words	97

Appendix A: Speaker N ° 1:

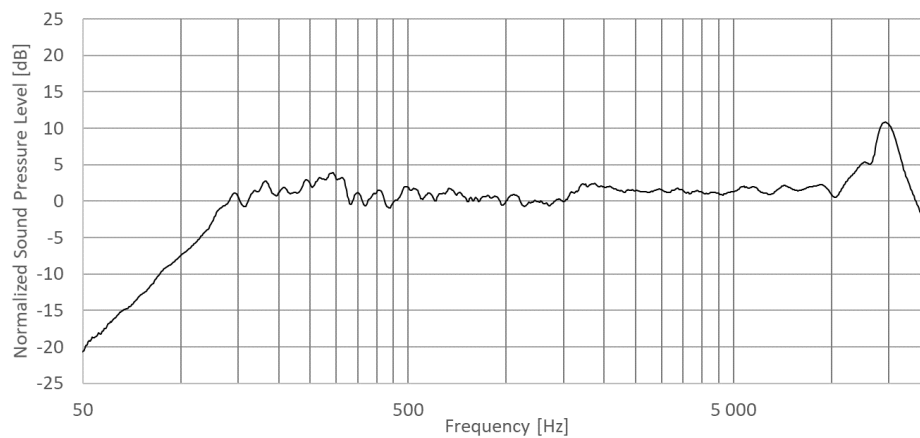
Typical Impedance and baffled SPL at 0.1 m



Environment setup



Electrical Input Impedance



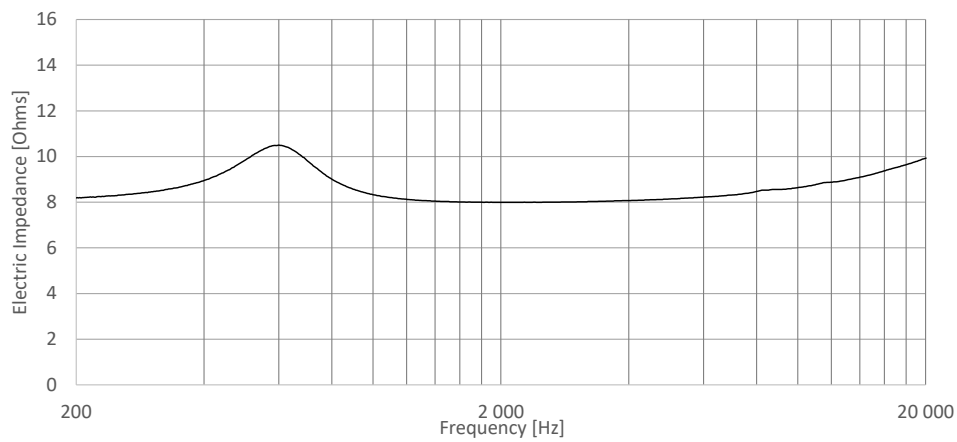
Sound Pressure Level. Normalized @ 1000 Hz

Appendix A: Speaker N ° 2:

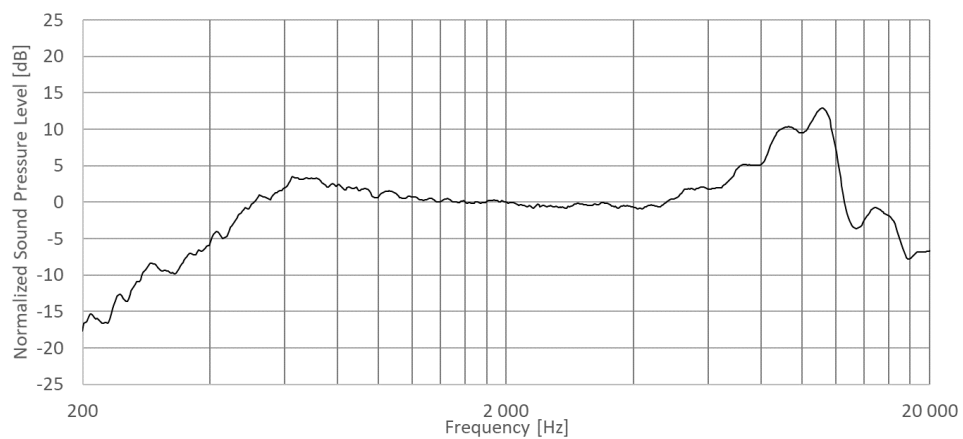
Typical Impedance and baffled SPL at 0.1 m



Environment setup



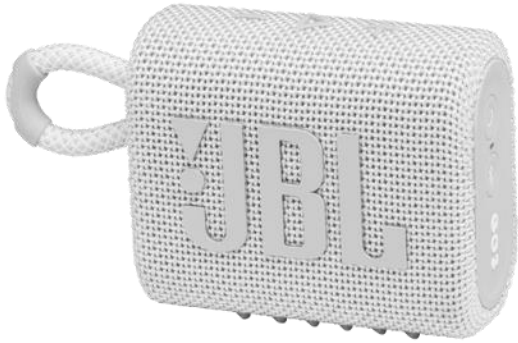
Electrical Input Impedance



Sound Pressure Level. Normalized @ 2000 Hz.

Appendix B: Bluetooth speaker JBL Go 3

Free field SPL at 0.1 m



Product illustration

(Source: <https://fr.jbl.com/enceinte-bluetooth/GO+3-.html>)

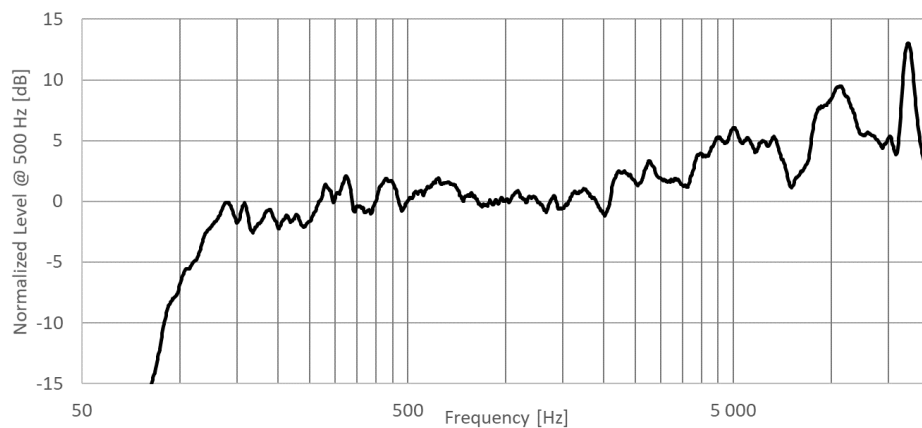
Main characteristics

(Source: <https://fr.jbl.com/enceinte-bluetooth/GO+3-.html>)

Dimensions (cm)	8.6 x 6.9 x 4.0
Electric Power (W)	4.2
Frequency response (Hz)	110 - 20000
Bluetooth version	5.1



Environment setup



Sound Pressure Level. Normalized @ 500 Hz

Appendix B: Smartphone OnePlus 6

Free field SPL at 0.1 m



Product illustration

(Source: <https://www.lesnumeriques.com/telephone-portable/oneplus-6-p43783/test.html>)

Main characteristics

Sources:

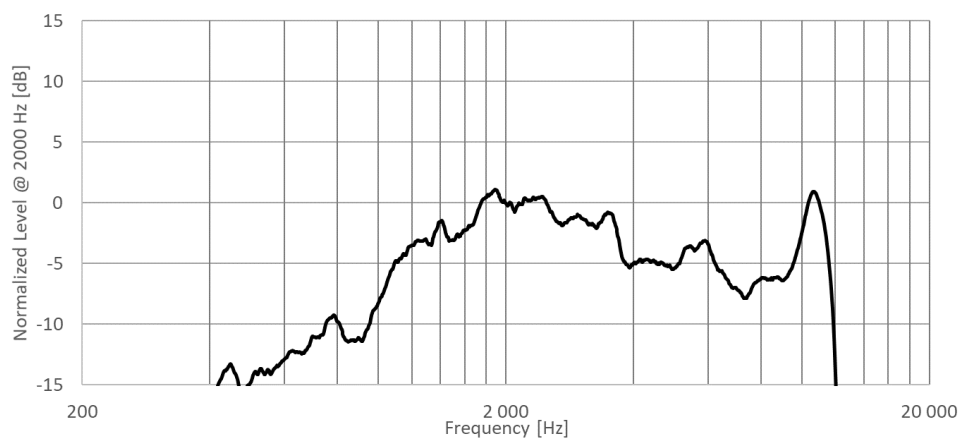
<https://www.lesnumeriques.com/telephone-portable/oneplus-6-p43783/test.html>

https://www.theregister.com/2018/05/30/oneplus_6_perfect_porridge/

Dimensions (cm)	155.7 x 75.4 x 7.8
Speaker location	Bottom side: left
Bottom side illustration :	



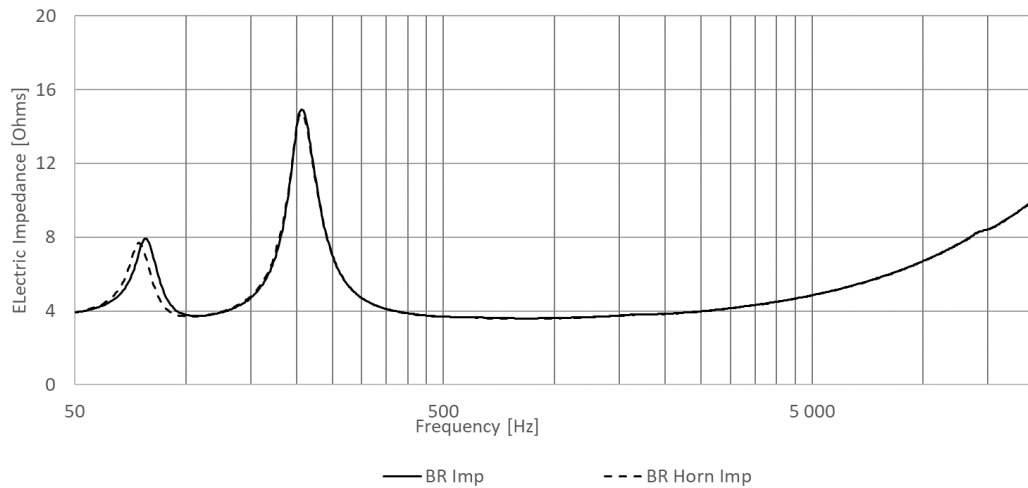
Environment setup



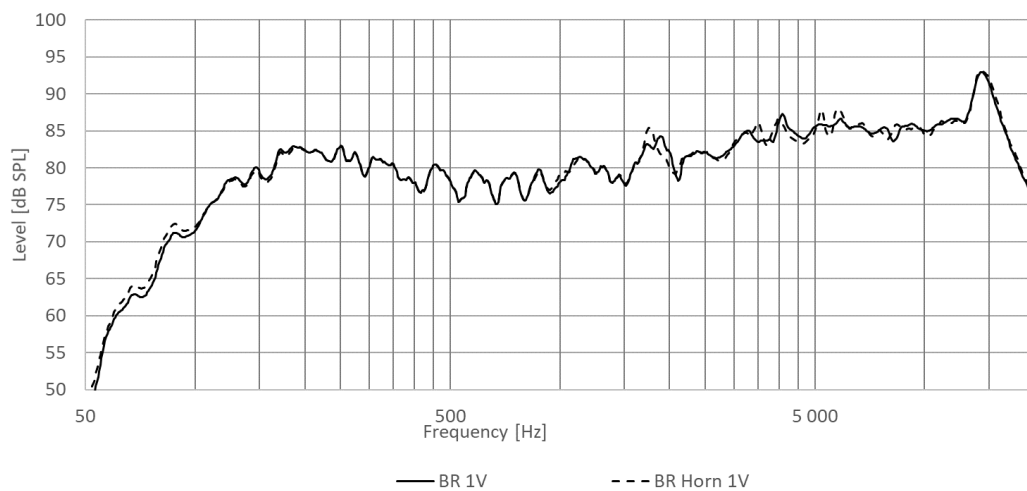
Sound Pressure Level. Normalized @ 500 Hz

Appendix C: Investigations around the speaker enclosure N ° 1

Bass-Reflex: Original and Horn ports comparison



Electrical Input Impedance comparison



Sound Pressure Level comparison at 0.3 m, and for 1 URMS

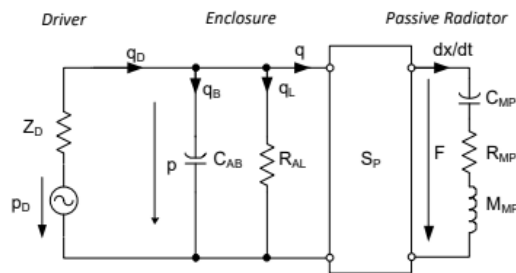
Appendix D: Klippel Application Note 57

Parameter Measurement of Passive Radiators (Revision 1.0, from July 6, 2020)

Extract: Theory part, page 2

Theory

At low frequencies and small amplitudes a passive radiator system can be modeled by linear lumped parameters as shown in the right picture. Driver and enclosure are modeled by an acoustic network and the passive radiator is represented by the lumped elements mechanical mass M_{MP} , mechanical compliance C_{MP} and mechanical resistance R_{MP} .



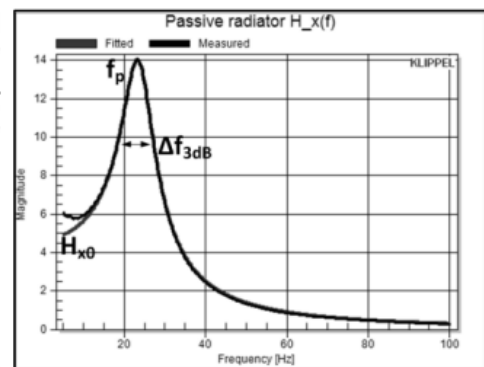
The stimulating driver acts as a sound pressure source which is exciting the passive radiator with the force $F = pS_P$, with S_P being the effective cone area of the passive radiator and p being the sound pressure in the enclosure. From this circuit, the linear transfer function between displacement and sound pressure can be obtained.

$$H_x(j\omega) = \frac{x(j\omega)}{p(j\omega)} = \frac{C_{MP}S_P}{j\omega R_{MP}C_{MP} - \omega^2 M_{MP}C_{MP} + 1}$$

Using easy interpretable derived parameters like f_p (resonance frequency of the passive radiator) and $Q_{MP} = \frac{f_p}{\Delta f_{3dB}}$ the magnitude response is modeled by this equation:

$$H_x(f) = \left| \frac{H_{x0}}{\frac{jf}{Q_{MP}} - \frac{f^2}{f_p^2} + 1} \right|$$

The picture on the right shows a fitted response based on this model and the actually measured transfer function.



Appendix D: Klippel Application Note 57

Parameter Measurement of Passive Radiators (Revision 1.0, from July 6, 2020)

Extract: Measurement Principle part, page 3

Measurement Principle

Measuring the Transfer Functions:

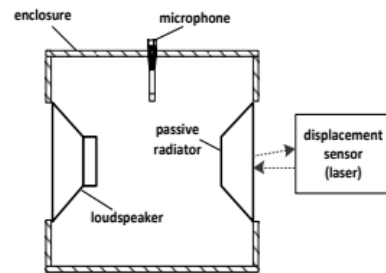
The tools for obtaining the transfer function are provided by the KLIPPEL TRF module [1]. The TRF stimulates the loudspeaker with a frequency sweep so that the passive radiator gets pneumatically excited. The transfer function $H_x(j\omega)$ is derived from the measured sound pressure in the test box and the passive radiator deflection which is measured by a triangulation laser sensor.

After attaching the additional mass the *Added Mass Method*, the TRF operation has to be performed twice.

Calculating the parameters:

The linear parameters are determined by the CAL operation *Calc Parameters*. This operation computes the Q-factor Q_{MP} and resonance frequency f_p by employing a fitting algorithm. The mechanical compliance and resistance are calculated from the resonance frequency, Q-factor and moving mass.

Measurement Setup:



Measurement procedure:

1. Mounting the DUT (Device Under Test)
2. Setting up the stimulus
3. Performing a TRF measurement
4. Adding mass to the DUT
5. Performing another TRF measurement
6. Passing the TRF results to a CAL operation
7. Running the CAL operation

Appendix E: Analog Devices ADAU1772 Datasheet (Rev. A)

Extract: first page



Evaluation Board User Guide UG-477

One Technology Way • P.O. Box 9106 • Norwood, MA 02062-9106, U.S.A. • Tel: 781.329.4700 • Fax: 781.461.3113 • www.analog.com

Evaluating the ADAU1772 Four ADC, Two DAC Low Power Codec with Audio Processor

EVAL-ADAU1772Z PACKAGE CONTENTS

EVAL-ADAU1772Z evaluation board
EVAL-ADUSB2EBZ (USB) communications adapter
USB cable with Mini-B plug
Evaluation board/software quick start guide

DOCUMENTS NEEDED

ADAU1772 data sheet
AN-1006 Applications Note, *Using the EVAL-ADUSB2EBZ*

GENERAL DESCRIPTION

This user guide explains the design and setup of the EVAL-ADAU1772Z evaluation board.

This evaluation board provides full access to all analog and digital I/Os on the ADAU1772. The ADAU1772 core is controlled by Analog Devices, Inc., SigmaStudio™ software, which interfaces to the board via a USB connection. The EVAL-ADAU1772Z can be powered by a single AAA battery, by the USB bus, or by a single 3.8 V to 6 V supply; any of these are regulated to the voltages required on the board. The printed circuit board (PCB) is a 4-layer design, with a single ground plane and a single power plane on the inner layers. The board contains connectors for external microphones and speakers. The master clock can be provided externally or by the on-board 12.288 MHz passive crystal.

EVAL-ADAU1772Z EVALUATION BOARD TOP SIDE AND BOTTOM SIDE

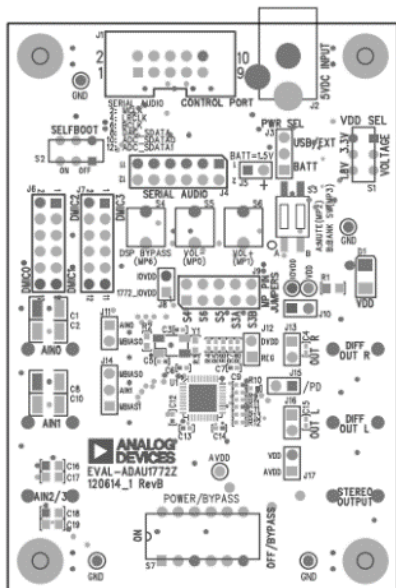


Figure 1. EVAL-ADAU1772Z Evaluation Board Top Side

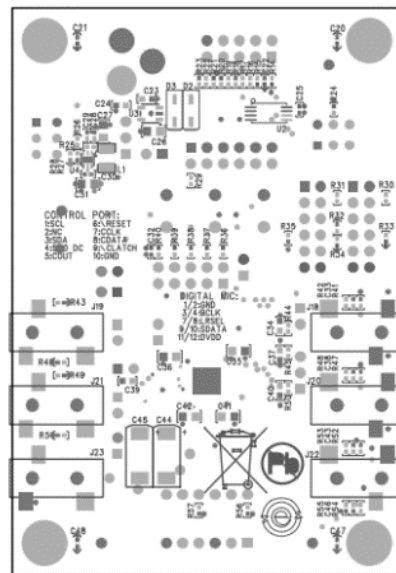
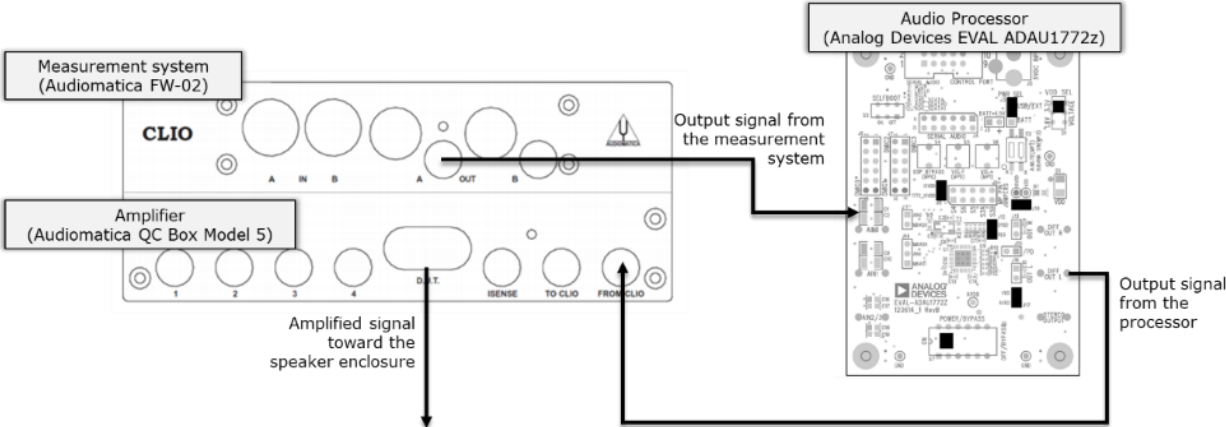


Figure 2. EVAL-ADAU1772Z Evaluation Board Bottom Side

Appendix F: Investigations around the speaker enclosure N ° 1

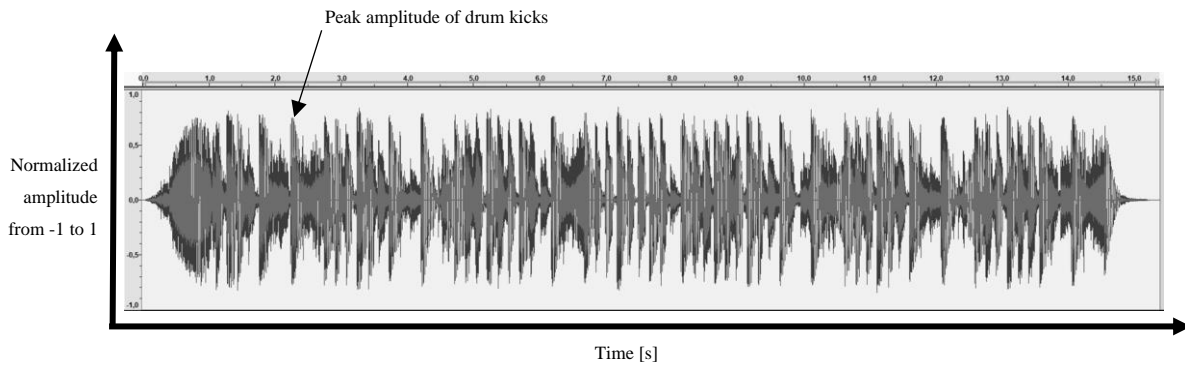
Active Equalization: Audio chain description



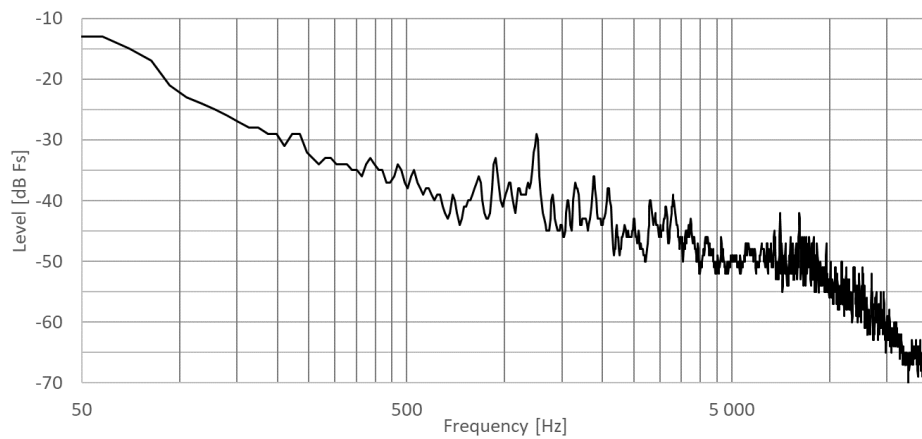
Appendix G: Investigations around the speaker enclosure N ° 1

Listening tests: 3rd musical extract for BR ports comparisons

15 seconds extract from the song “Latch” by artist Disclosure



Time waveform analysis



Spectrum analysis

RÉSUMÉ

Les enceintes acoustiques conçues par la société Seltech sont destinées à un marché électronique où des appareils polyvalents sont de plus en plus utilisés à l'écoute de la musique. Comprenant ainsi la reproduction des basses fréquences, par des objets compacts, comme un fort intérêt pour les acteurs de ce marché, ce document passe brièvement en revue les tendances technologiques, puis étudie trois méthodes connues de l'industrie pour améliorer les basses que sont : le Bass-Reflex, le Radiateur Passif et l'Egalisation Active programmée sur processeur.

Aussi, comme le mot « amélioration » conduit souvent à différentes interprétations, ce document propose des bases pour une évaluation perceptive des prototypes issus des méthodes étudiées, et tente ainsi de relier les appréciations subjectives aux mesures acoustiques.

SUMMARY

Speaker enclosures designed by the company Seltech are operated in an electronic market where versatile devices are increasingly used in listening to music. Understanding the bass reproduction from compact sized objects to be a wide interest to players in this market, this document briefly reviews technological trends, and studies three known methods to improve the basses that are: the Bass-Reflex, the Passive Radiator and the Active Equalization programmed on a processor.

Also, as the word “improvement” often leads to different interpretations, this document proposes bases for a perceptual evaluation of the prototypes resulting from the studied methods, and thus attempts to relate subjective appreciations to acoustical measurements.

Keywords: Speaker enclosures, Speaker systems, Speaker boxes, Low frequencies improvement, LF Improvement, Bass, Bass-Reflex, BR, Passive-Radiator, PR, Active Equalization, EQ, High-Pass Filter, HPF, Acoustic circuits, Listening Test, Spectral Balance,